Western University

### Scholarship@Western

Electronic Thesis and Dissertation Repository

8-17-2020 1:00 PM

# The Role of V-ATPase in Regulating pH in the Digestive Tract of Tetranychus urticae Koch

Zoran Culo, *The University of Western Ontario*

Supervisor: Vojislava Grbić, *The University of Western Ontario*
A thesis submitted in partial fulfillment of the requirements for the Master of Science degree in Biology
© Zoran Culo 2020

Follow this and additional works at: https://ir.lib.uwo.ca/etd

# Abstract

The phytophagous two-spotted spider mite, *Tetranychus urticae* (Koch), is a major global pest to agriculture and other plant-production industries. Digestive tract pH is a key factor in regulating the enzymatic activity that facilitates digestion and detoxification of ingested plant cell contents and in my thesis I used various pH indicator dyes to determine the pH of regions of the digestive tract in *T. urticae*, *in vivo*. Digital colour values of stained specimen images were cross-referenced with the colour values from images of each dye taken at different pH values to determine the digestive tract pH in non-fed, fed and dsRNA-treated fed mites. The pH of vesicles in early-stage, free-floating midgut cells remained stable regardless of treatments whereas gut lumen pH showed slight changes as a result of feeding and when the expression of the gene *tetur09g04140*, which codes for V-ATPase subunit a, was downregulated. The identification of pH in the digestive tract of *T. urticae* can be used to better understand the localization of enzymatic activities responsible for digestive and detoxification processes.

**Keywords:** *Tetranychus urticae*, pH, digestive tract, enzymes, V-ATPase, detoxification, indicator dyes, midgut, vesicles, digestive cells

# Summary for Lay Audience

Spider mites are versatile pests that can adapt to feed on many different types of plants and quickly develop resistance to toxic chemicals from both plants and pesticides. Thus, they are serious pests in agriculture and other plant-growing industries. The processing of ingested plant material and harmful chemicals is predicted to take place in the mite's digestive system by a variety of enzymes. Factors such as pH affect the ability of enzymes to perform. In this study I documented the pH in the digestive system of the two-spotted spider mite, *Tetranychus urticae*, using indicator dyes which show different colours depending on the pH of the substance they are dissolved in. These dyes were fed or injected in normal mites and mites with the gene coding for V-ATPase (a protein complex that regulates pH) was targeted by genetic silencing. The data suggest pH in cells were stable whereas pH in gut compartments showed slight change when the mites were fed and when the production of V-ATPase was interfered with. These results provide information that can be used in future research to find out which enzymes are operating in the mite's digestive system as well as how active they are.

# Acknowledgements

The goal of my thesis was pretty straightforward: determine the pH of digestive tract compartments in spider mites. However, completing it quickly turned into a seemingly insurmountable task! The people who I have encountered during my thesis project have given me outstanding motivation to strive towards success. This thesis would not have been possible without the support provided by family, friends and professional associates.

I would first like to thank Vojislava Grbić (aka Vava) for being not only my supervisor but also my friend. Vava has consistently motivated me to get the job done and to become a better scientist. Thank you for all our helpful meetings, friendly conversations and fun times we shared.

Vladimir Zhurov, our research associate, provided valuable contributions for my thesis. Vlad's used his analytical skills to process the data and editing skills to organize the results in a comprehensive manner. I always enjoy listening to him explain science stuff with that awesome Russian accent!

The numerous obstacles I have encountered throughout the process of developing the thesis were overcome by a combination of patience, creativity and comradery by everyone who is or was part of the Grbić lab. I would like to extend my thanks to: Akanchha Shukla, David Letwin, Emilie Widemann, Golnaz Salehipourshirazi, Hanna Varonina, Jeremy Spenler, Julien Le Roy, Kristie Adriana Bruinsma, Michele Antonacci, Miodrag Grbić, Nicolas Bensoussan, Nivitha Bhaskar, Repon Saha, Sameer Dixit, Sean Hoang Pham and Zhaoji Dai. No matter where we end up, we will always be a team!

Special thanks to the Grbić lab's retired lab technician Biljana Popović. Biljana gave me valuable guidance on relevant protocols and laboratory procedures. Biljana was very professional and friendly from the day I met her to the day she left for Montenegro. Živeli!

Special thanks to the members of my Advisory Committee: Jeremy McNeil and Richard Gardiner. Our meetings were very helpful and enjoyable. Hope to see you both some more in the future!

I would also like to extend my thanks to the students and faculty of the Biology Department who I have encountered during my time at Western. Each has contributed to shaping my journey. Fantastic community!

My family is my life's foundation and the biggest influence in shaping me into the person I am today. Their love and support carried me through this project and will continue to carry me into the future. I look forward to growing closer and stronger with my father Nenad, my mother Neda, my sister Diana and my brother Dino.

Finally, none of this would have been made possible if it were not for my best friend, my stuffed penguin Peanut, who was with me every step of the way.

"Peep peep!"

# List of Tables

# List of Figures

# List of Abbreviations

| | |
|---|---|
| **BB** | Bromophenol blue |
| **CR** | Chlorophenol red |
| **F3R3** | Mites treated with dsRNA targeting an intergenic region as a negative control |
| **IG** | Indole glucosinolates |
| **MC** | Midgut caeca |
| **MV** | Midgut ventriculus |
| **PM** | Posterior midgut |
| **PR** | Phenol red |
| **TB** | Thymol blue |
| **TSSM** | Two-spotted spider mite |
| **VATP** | Mites treated with dsRNA targeting the *tetur09g04140* gene |

# Table of Contents

# 1  Introduction

## 1.1  Herbivorous arthropods

Herbivorous arthropods have evolved diverse strategies to counter plant defenses for successful herbivory (Howe and Jander 2008; Krantz and Lindquist 1979; Mello and Silva-Filho 2002; Rioja et al. 2017; Stahl et al. 2017). The development of strategies adapted for countering plant defenses is an integral component to the evolutionary success of herbivorous arthropods (Després et al. 2007; Jongsma and Bolter 1997) and their proliferation throughout the world wherever plants are present. Plants, in turn, have evolved diverse defensive strategies to deter, inhibit or entirely negate predation by herbivores (Fürstenberg-Hägg et al. 2013; Hickler and Meiners 2009; Howe and Jander 2008; Mello and Silva-Filho 2002). This "arms race" of herbivore-plant adaptations and herbivore counter-adaptations has contributed to the diversification of plant and herbivorous arthropod species (Després et al. 2007; Howe and Jander 2008; Mitchell et al. 2016) over millions of years (Fürstenberg-Hägg et al. 2013).

The diverse community of herbivorous arthropods can be classified based on the size of their host range, from specialists that feed on a single or a few plant species to generalists capable of feeding on many plant species from different families (Ali and Agrawal 2012; Howe and Jander 2008). The number of plant species that herbivorous arthropods can successfully feed on is determined by their ability to evade or overcome the defensive strategies of their plant hosts (Ali and Agrawal 2012; Howe and Jander 2008; Mello and Silva-Filho 2002; Stahl et al. 2017). Specialists such as monarch butterflies feed on milkweed leaves whereas generalists such as grasshoppers can feed on the foliage of multiple plant species. Larvae of the monarch butterfly *Danaus plexippus* L. are specialized for feeding on the leaves of *Asclepias spp* and have adapted to sequester ingested defensive compounds, thus becoming

toxic to potential predators (Malcom and Zalucki 1996). The intimate specialization would consequently render *D. plexipus* vulnerable if milkweed is unavailable.

Such is not the case for a generalist like the grasshopper *Chorthippus parallelus*, which can overcome nutritional deficiencies and defensive strategies by feeding on a variety of available plants (mostly grasses) rather than focusing on a single food source (Franzke et al. 2010). The trade-off for the generalist feeding behaviour of *C. parallelus* is a higher vulnerability to the variety of defenses in the different plant hosts, which can be circumvented by modifying the composition of plant species in the diet (Franzke et al. 2010). In theory, there is no limit to the range of plant species a generalist herbivore can target, so long as the defensive strategies of its hosts are successfully avoided or countered. Extreme generalist species have the remarkable ability to successfully target many plant species regardless of how varied their inherent defensive strategies or phylogenies are. My thesis focuses on the extreme generalist mite *Tetranychus urticae* (Koch).

## 1.2   The Two-Spotted Spider Mite *Tetranychus urticae*

*Tetranychus urticae* is a phytophagous mite species (order Acari) and member of the Tetranychidae family. The life cycle of *T. urticae* consists of an egg stage, a larval stage, two instars and sexually dimorphic adults (**Figure 1**). The mites become quiescent as chrysalids when moulting from larvae to protonymphs (protochrysalids), proto- to deutonymphs (deutochrysalids) and deutonymphs to adults (teleiochrysalids) (Ikagemi et al. 2000). Adult females have a maximum body size of 0.5 mm in length and a lifespan of 2-4 weeks under ideal conditions. *Tetranychus urticae* is commonly referred to as two-spotted spider mites (TSSMs) for the two distinctive dark spots on the sides of its body.  TSSMs have been used as
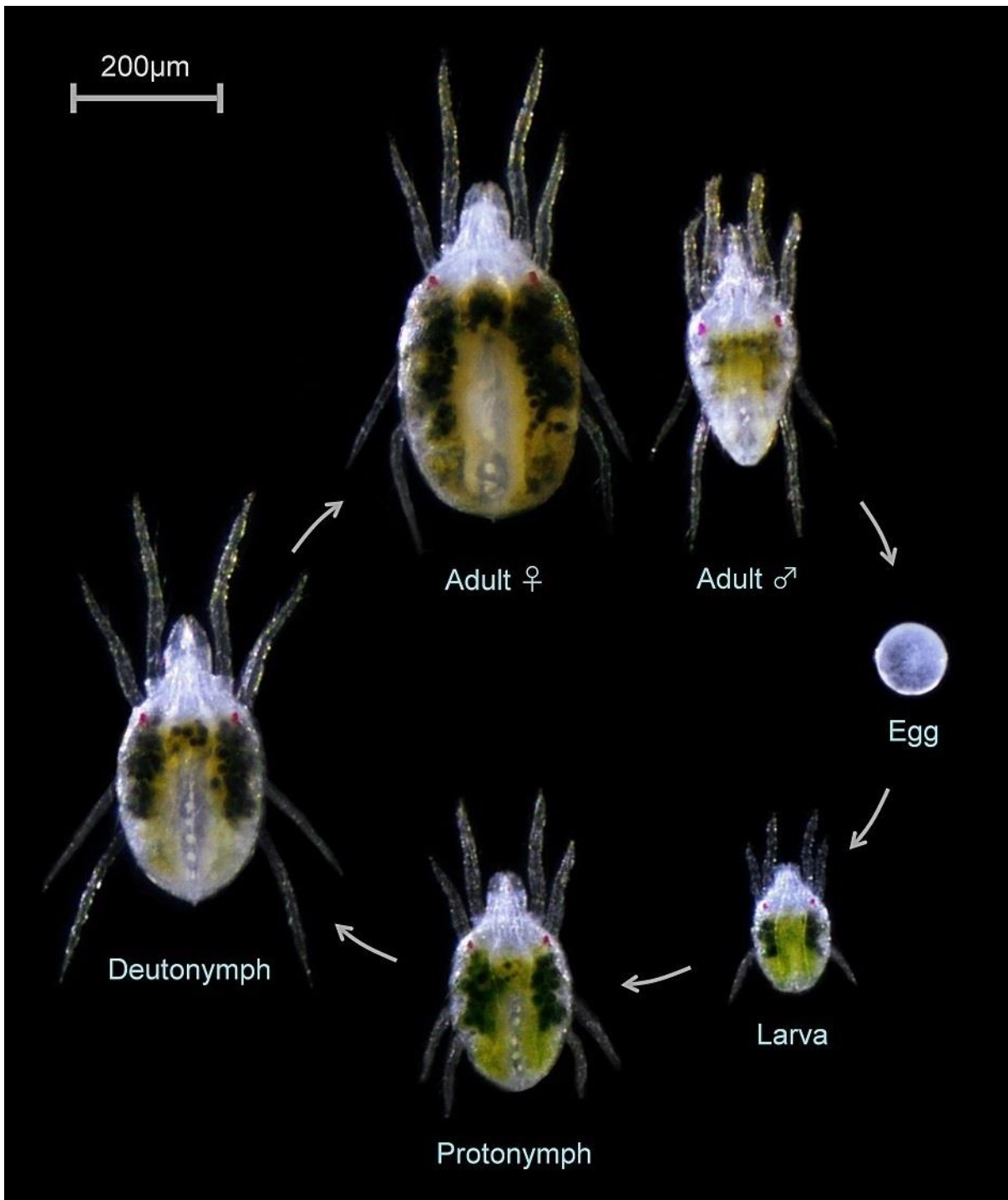
**Figure 1. Life cycle of *Tetranychus urticae*.**
The larval stage is distinguished by having only three pairs of legs. A fourth pair is grown when moulting into the protonymph stage. The protonymph moults into a larger deutonymph and then into adults. Adult females are large and round whereas males are relatively smaller with posterior-pointed bodies.

model organisms in genetics-based research due to the availability of its fully sequenced

genome (Grbić et al. 2011).

### 1.2.1  Impact of and treatment against TSSM infestations

TSSMs are phytophagous mites with an extremely vast host range of over 1,100 host plant species belonging to more than 140 families (Migeon and Dorkfeld 2010). TSSMs are also a major problem for plant production and agricultural industries as they are pests to over 150 crop species, with infestations resulting in significant financial losses due to reduced crop yield and the cost of chemical control. The cost of synthetic acaricides used to treat spider mite damage in the European Union is estimated at over $1 billion USD annually (Attia et al. 2013). Xenobiotic compounds from both plant defenses and pesticides often lose their potency as spider mites quickly develop resistance against novel toxic compounds (Rioja et al. 2017; Stahl et al. 2017).

Pesticides also present a threat to off-target species, which has prompted the need for safer methods including biological controls and genetics-based treatments designed to specifically target TSSM species. Biological controls involve the use of organisms to target and reduce the population of a specific pest species. Predatory mites that feed on *T. urticae*, such as *Phytoseiulus persimilis* and *Neoseiulus californicus,* have been used individually or in combination (Rhodes et al. 2006). Predatory mites can also be accompanied by pathogens such as parasitic fungi to increase *T. urticae* mortality. Dogan et al. (2017) demonstrated 60% and 80% increase in mortality for *T. urticae* in leaf and Petri dish mite populations, respectively, when a virulent strain of *Metarhizium brunneum* infected them. Alternatively, genetics-based solutions coding for specific genes in a target species would eliminate substantial risks to non-target species.

RNA interference (RNAi) is a genetics-based process that can be used to trigger fatal responses in organisms, which was previously demonstrated in several pest insect species

(Huvenne and Smagghe 2010). An RNAi response is facilitated by the uptake of dsRNA that has compatibility with a target sequence and binds to compatible mRNA, therefore negating the translation process. Multiple methods can be used to deliver dsRNA into pest species, including sprays and transgenic plants, though practical results have been highly variable in previous research (Lin et al. 2016; Song et al. 2018; Suzuki et al. 2017b). The availability of a fully sequenced genome for *T. urticae* (Grbić et al. 2011) allows researchers to describe specific genes and determine effective targets for genetics-based pesticides. My thesis focuses on quantifying the pH in the digestive tract of *T. urticae* and the possibility of using RNAi to negatively affect resource acquisition as a consequence of tampering with pH regulation.

## 1.3   Digestive anatomy of *T. urticae*

The digestive system of *T. urticae* (**Figure 2**) follows an anterior-posterior organization defined by three distinctive regions: foregut, midgut and hindgut (Alberti and Crooker 1985; Erban and Hubert 2012; Hughes 1950; Mothes and Seitz 1981; Terra and Ferreira 1994). In adult females, the digestive system can occupy an estimated 40-50% of the body while feeding. TSSMs feed on host plants by penetrating leaves with a stylet to inject a cocktail of hydrolyzing enzymes (Jonckheer et al. 2016) and extract liquefied contents from individual mesophyll cells (Andre and Remacle 1984; Bensoussan et al. 2016). The contents are received through the oral groove (mouth) and moved through the oesophagus by a pharyngeal pump (Andre and Remacle 1984; Mothes and Seitz 1981). The ingested plant cell content enters the central ventriculus of the horseshoe-shaped midgut and is distributed throughout the caeca. Free-floating cells bud off from epithelial generative cells and densely populate the midgut lumen. These free-floating cells are defined as digestive cells by Bensoussan et al. (2018) as they have been observed to contain substances of nutritive value such as starch and thylakoid granules (Mothes and Seitz 1981) and degraded plant pigments (Occhipinti and Maffei 2013). Digestive cells increase in

size through several distinct stages of development (**Figure 3**) after budding off the epithelium

and darken from the build-up of waste products.
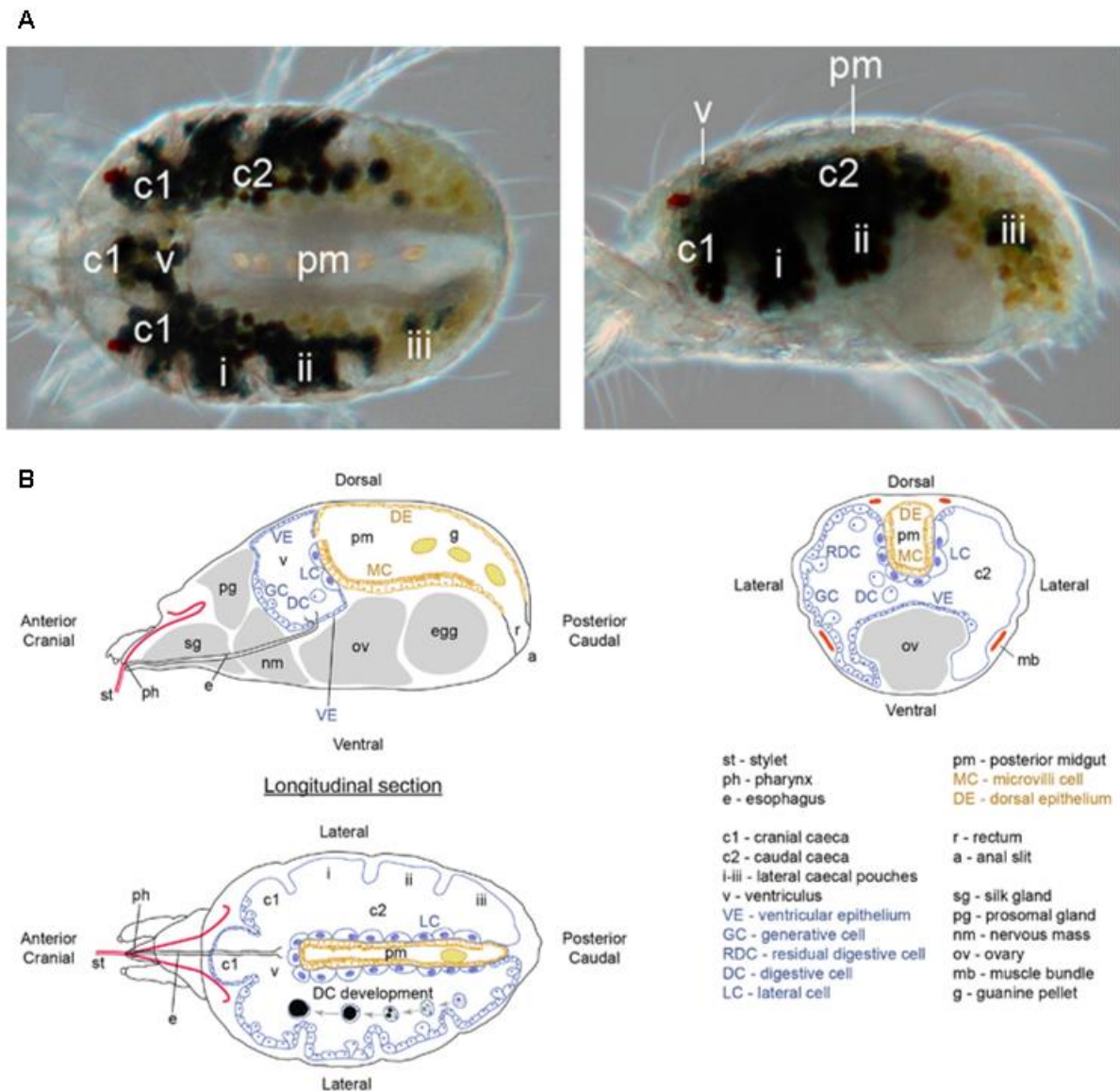


**Figure 2. Anatomical diagram of the digestive tract in *Tetranychus urticae*.**
Digestive anatomy seen from the exterior of a TSSM (A); Diagram of components comprising the digestive tract (coloured) and non-digestive tract organs (grey) (B); Figure modified from Bensoussan et al. (2018).
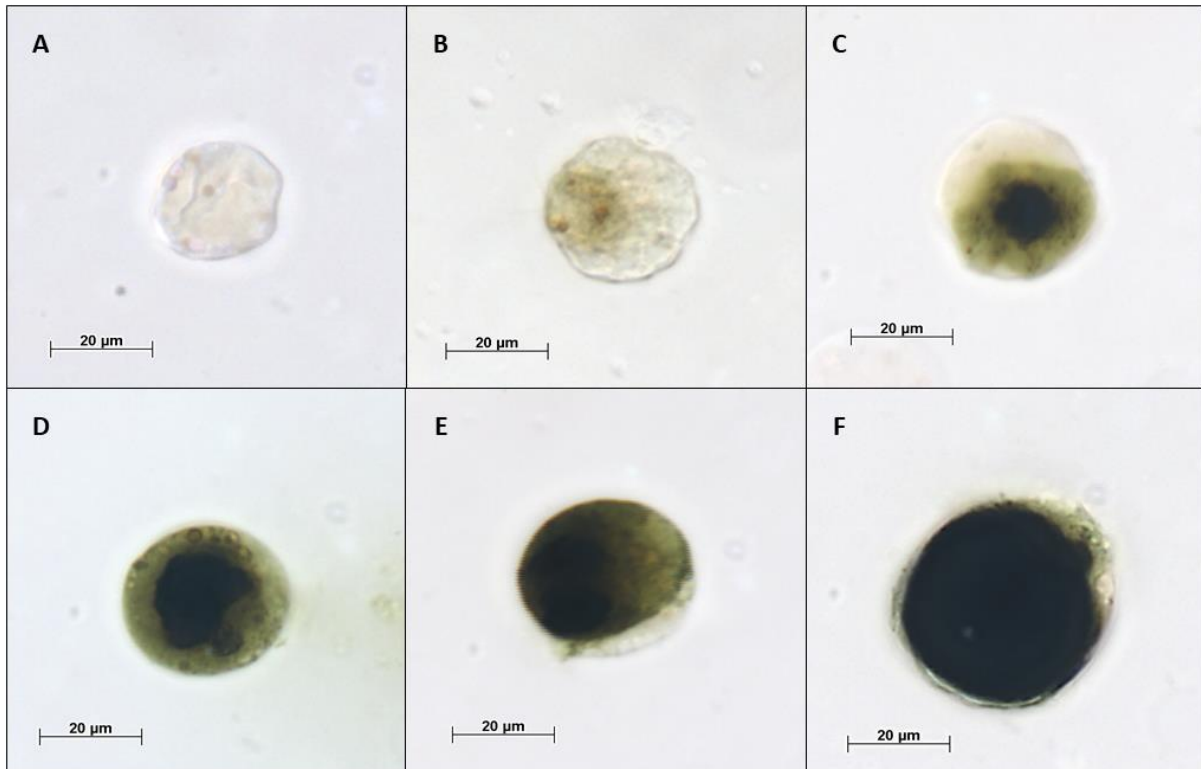
**Figure 3. Stages of development for digestive cells in TSSMs (unstained).**
Cells begin small and clear (A) before absorbing plant cell content from midgut lumen (B). Dark deposits condense in the centre (C) then begin to grow as more plant cell content fills up the rest of the cell (D). The dark deposits occupy most of the cell's volume (E) before maturing (i.e.: terminal stage) where the cell is largest and entirely dark with only a thin layer of cytoplasm and nucleus remaining (F).

Any remaining undigested material and terminal-stage digestive cells enter the posterior midgut and are excreted from the body through the hindgut as faecal pellets, together with other waste products including urine and guanine pellets (Mothes 1985). The TSSM digestive system shares similarities with other Acari, including ticks, which feed slowly on their host and process blood food in acidic, intracellular compartments of gut epithelia (Grandjean and Aeschlimann 1973). The characterization of digestive and/or detoxification processes that occur within digestive cells and gut compartments in *T. urticae* is lacking. The identification of various enzymes in the digestive tract that facilitate the conversion of ingested material into useful nutrients or innocuous substrates can be used as a proxy to understand where these processes may take place. Certain factors that influence the rate of enzymatic

activity, such as pH, may be used to determine where these enzymes are more likely to be localized in the digestive tract.

## 1.4   pH is a key factor that affects enzymatic activity

Digestive system pH of herbivores influences the performance of enzymes during digestive and detoxification processes, as well as the performance of defensive enzymes present in the ingested plant cell content (Harrison 2001; Terra and Ferreira 1994). Felton et al. (1992) examined the fate of chlorogenic acid in the digestive tracts of the Colorado potato beetle *Leptinotarsa decemlineata* and the corn earworm *Helicoverpa zea* when fed with tomatoes. Chlorogenic acid was oxidized by polyphenol oxidase substantially less in the acidic gut of *L. decemlineata* (pH 6.5) than in the alkaline gut of *H. zea* (pH 8.5%). The presence of polyphenol oxidase in ingested plant material, along with phenolic substrates like chlorogenic acid, promote the formation of orthoquinone which reduces the nutritive quality of dietary proteins (Felton et al. 1989). This is why a mildly acidic gut pH benefits *L. decemlineata* as the activity of polyphenol oxidase is higher in alkaline environments, such as in *H. zea*, which feeds on fruiting bodies where there is a lower presence of the enzyme rather than in foliage (Felton et al. 1989). It is thus important to study the digestive tract pH of herbivorous arthropods as it reflects the repertoire of enzymes used to facilitate proper digestion and detoxification.

Previous studies have documented enzymatic activities using extracts from various mite species including *T. urticae*. Sanchez-Monge et al. (1996) observed activity of amalayse in extracts from dust mites (*Dermatophagoides pteronyssinus* and *D. farinae*) and storage mites (*Lepidoglyphus destructor* and *Tyrophagus putrescentiae*), resulting in a collective pH optima of 5.0-6.5. Nisbet and Billingsley (2000) studied how enzymes in extracts from spider

mites (*T. urticae*), flour-feeding mites (*Acarus siro*), bird mites (*Dermanyssus gallinae*) and

sheep mites (*Psoroptes ovis*) hydrolyze haemoglobin and concluded that hydrolysis occurred

optimally at a pH range of 3-5. The enzymes in *T. urticae* hydrolyze dietary proteins from

ingested plant cell contents rather than haemaglobin. Nevertheless, the 3-5 pH range

determined by Nisbet and Billingsley (2000) corresponds with the pH optima of several

enzymes extracted from *T. urticae* examined by Santamaría et al. (2015) and Carrillo et al.

(2011) which include: aspartyl proteases (pH=3.5), legumain (pH=4.5), cathepsin B (pH=5.5)

and cathepsin L (pH=5.5). The pH optima of enzymes from *T. urticae* extracts closely

resemble pH values determined in the digestive tract compartments of non-TSSM species,

suggesting that the digestive tract in *T. urticae* may have a similar range of pH. Gut

compartments with differing pH values described in various mite species (Erban and Hubert

2010) suggest that gradients may also be present within or among the individual

compartments of the TSSM digestive tract. The establishment of pH gradients in the digestive

tract would be actively maintained by proton pumps, such as the membrane-bound vacuolar-

type $H^+$-ATPase (V-ATPase) (D'Silva et al. 2017; Dow 1992; Erban and Hubert 2010;

Overend et al. 2016).

## 1.5  V-ATPase

V-ATPase is a multi-subunit protein complex present in virtually all eukaryotic

organisms (Finbow and Harrison 1997). It is responsible for establishing and maintaining pH

gradients by actively transporting $H^+$ ions across a membrane and into the lumen of organelles

(Beyenbach and Wieczorek 2006; Forgac 2007), which facitlitates enzymatic activity in

endosomes and lysosomes (Scott et al. 2014). V-ATPase is composed of a catalytic and a

membrane-bound domain. The catalytic domain hydrolyzes ATP to fuel the movement of $H^+$

ions facilitated by the membrane-bound domain (Couoh-Cardel et al. 2015; Finbow and

Harrison 1997; Zhang et al. 2008). V-ATPase regulates pH in endocytotic and exocytotic organelles to generate specific pH for enzymatic activity (Beyenbach and Wieczorek 2006). Theoretically, enzymes associated with digestion or detoxification processes in *T. urticae* would not function properly if the mechanism of V-ATPase regulating pH gradients is preturbed.

Suzuki et al. (2017b) reported increased mortality in TSSMs following the silencing of the *tetur09g04140* gene coding for the A subunit in V-ATPase. This was strongly correlated with a completely dark body phenotype (**Figure 4**) not observed in negative control knockdown TSSMs. It is not clear whether these morphological changes in the TSSM digestive tract correspond to changes in digestive tract pH. For my thesis, I predicted that silencing the expression of *tetur09g004140* would perturb the regulation of pH in the TSSM digestive tract, which would subsequently hinder the enzymatic activity necessary for facilitating
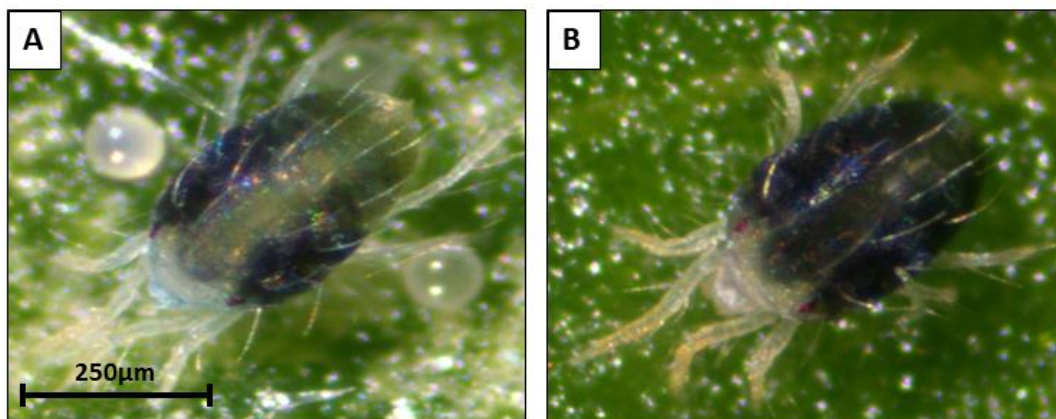


**Figure 4. Whole-body TSSM phenotypes associated with "normal" control/negative control (A) and "dark body" *tetur09g04140*-knockdown TSSMs (B).**
The dark body phenotype is produced by a build-up of degraded plant pigments retained in gut compartments, whereas the wild type body phenotype in untreated mites and negative controls exhibit the signature two spots of the sides of the TSSM's body.

digestion and detoxification processes. The difference in digestive tract pH between *tetur09g04140*-knockdown TSSMs (here referred to as VATP) compared with negative control (here referred to as F3R3) and control TSSMs was measured using pH indicator dyes

## 1.6 Measuring pH in small arthropods

Microscopic electrical probes or "microelectrodes" (with tip diameters ranging from 10 µm to 30 µm) have been used to measure pH in larvae of the freshwater moth *Acentria epemerella* (Gross et al. 2008) and in the digestive tract of the termite *Nasutitermes lujae* (Brune et al. 1995). However, given the small size of *T. urticae* (**Figure 1**), using such microelectrodes would damage digestive tract tissues and cause physiological reactions that could severely compromise the *in vivo* study of internal pH. As a safer alternative, pH indicator dyes can be used by feeding them to small organisms like *T. urticae* and are more affordable than electronic probes. A wide variety of pH indicators are available for research purposes and their chemical properties have been extensively documented (Sabins 2008).

### 1.6.1 How pH indicator dyes work

pH indicator dyes are weak acids or bases that produce a specific colour depending on the pH of a solution or material. When dissolved in a solvent (ex: water, ethanol, benzene, etc.), an indicator dye dissociates into a protonated (acidic) and deprotonated (alkaline) state. The relationship between protonated and deprotonated states of dyes can be summarized by the following formula previously used by Xu et al. (2006):

$$HIn + H_2O \rightleftharpoons H_3O^+ + In^-$$
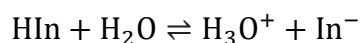
The colours of pH dyes are produced by the weak acid or base (HIn) and its conjugate form (In$^-$) while a freed proton immediately binds with water to form a clear hydronium ion ($H_3O^+$). The overall colour of the solution is determined by the ratio between HIn and In$^-$

concentrations, which is dependent on pH of the solution and dissociation constant (p*Ka*) of the indicator dye (Xu et al. 2006). When observing an indicator dye across an array of pH values, colours remain consistent beyond a narrow set of pH where the dye shows intermediate colours. This narrow region of colour conversion is defined as the transition range. An assortment of indicator dyes with different transition range values can be used to determine the parameters of pH in a solution or specimen (**Figure 5**).
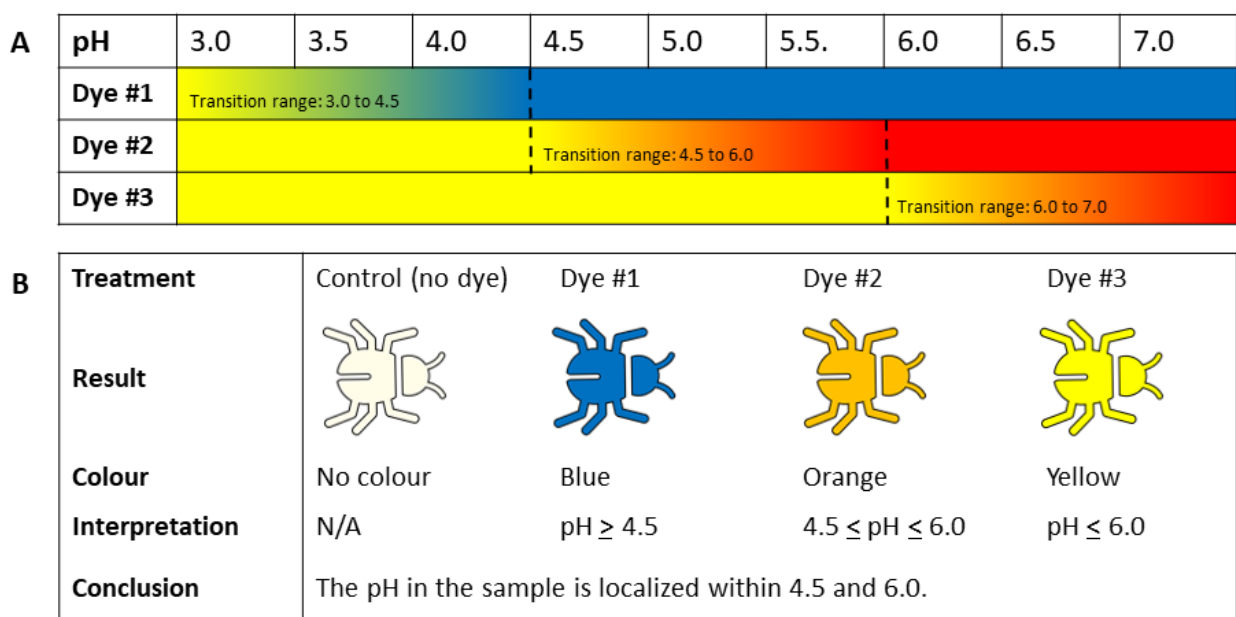


**Figure 5. How indicator dyes with varying transition ranges can be used to determine pH.** Two indicator dyes are used to determine the higher (dye #3) and lower (dye #1) limits of pH while a third dye (dye #2) is used to confirm the pH within the established range (A). In this example, the dyes indicate the pH in the specimen is between 4.5 and 6.0 (B).

### 1.6.2 Previous studies using pH indicator dyes in small arthropods

Digestive tract pH values have been identified in various small arthropods fed with pH indicator dyes. Overend et al. (2016) fed dye-infused media to *Drosophila melanogaster* larvae and found multiple pH gradients throughout the midgut (**Figure 6**), ranging from 2 to 9.5. Corena et al. (2005) fed various indicator dyes to *Aedes aegypti*, *Anopheles gambiae* and *Culex tarsalis* and reported pH ranges of 8.0 to 9.5 in *A. aegypti* and 8.5 to 9.5 in *A. gambiae* and *C.*

*tarsalis*. Indicator dyes have also been used to determine pH in mites. Hughes (1950) fed coarse

meals infused with indicator dyes, such as phenol red and neutral red, to the flour mite

*Tyroglyphus farinae* and determined the midgut pH to be between 5 and 6.
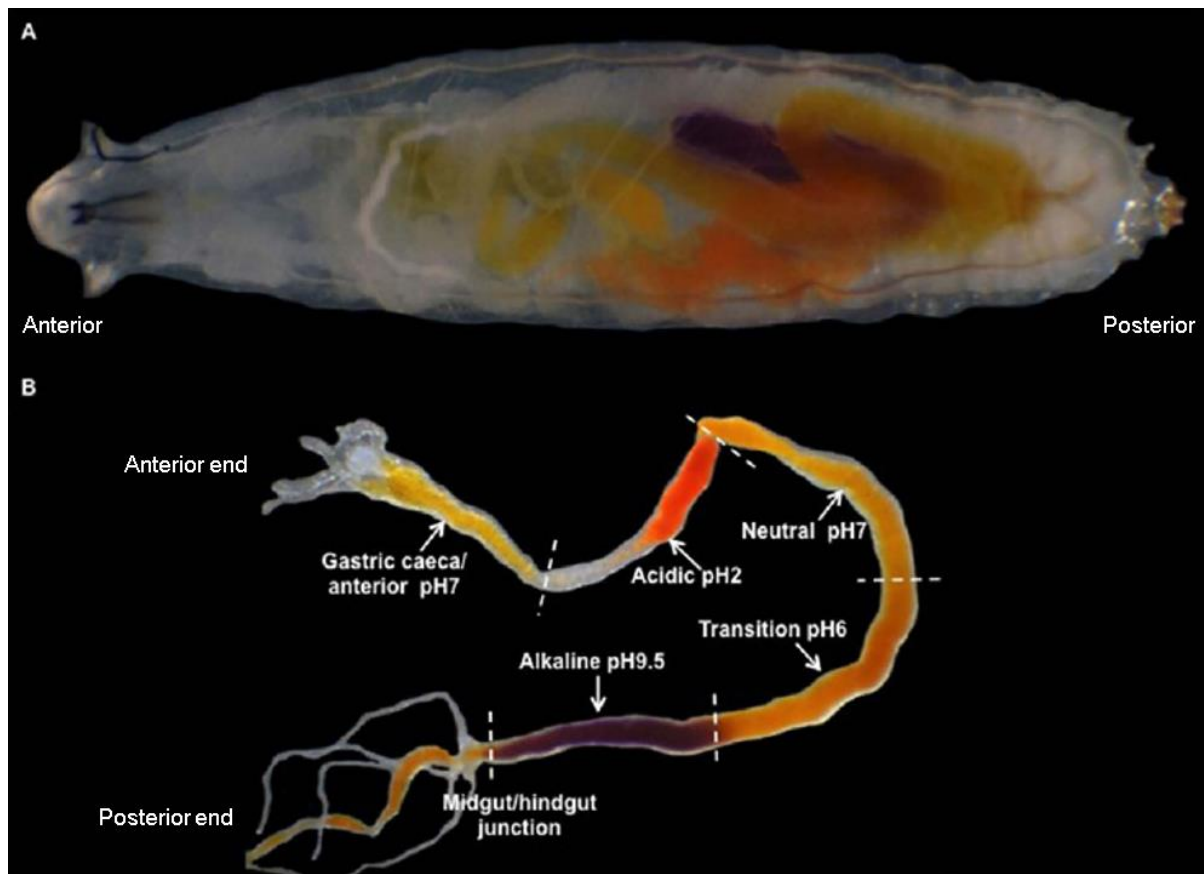


**Figure 6**. **The midgut of *Drosophila melanogaster* (Canton-S strain) stained with *m*-Cresol purple.**
Ingested *m*-Cresol purple produced red (pH < 2.4), yellow (pH = 2.5-8.0) and purple (pH > 8)
colours when staining the midgut, shown here inside (A) and excised out of (B) a larva.
Figure modified from Overend et al. (2016).

Erban and Hubert (2010) fed an assortment of indicator dyes infused in a wheat

powder food product to 12 acaridid dust mite species (Acari: Astigmata) to determine exact

pH and acidic/basic limits (**Figure 7**), which varied between 4-8 depending on species and

gut compartment. This pH range overlaps most pH optima of enzymes identified in *T. urticae*

extracts and provided a reference when selecting indicator dyes for determining pH in the

TSSM digestive tract. The gut compartments of TSSM are too frail to excise as they are composed of a single-layer epithelium (Bensoussan et al. 2018). Nevertheless, coloured solutions are clearly visible inside the gut compartments of TSSMs. In my thesis, imaging stained TSSMs generated both qualitative and quantitative data from visual inspection and digital analyses (respectively) for determining the pH of digestive tract compartments in *T. urticae*.
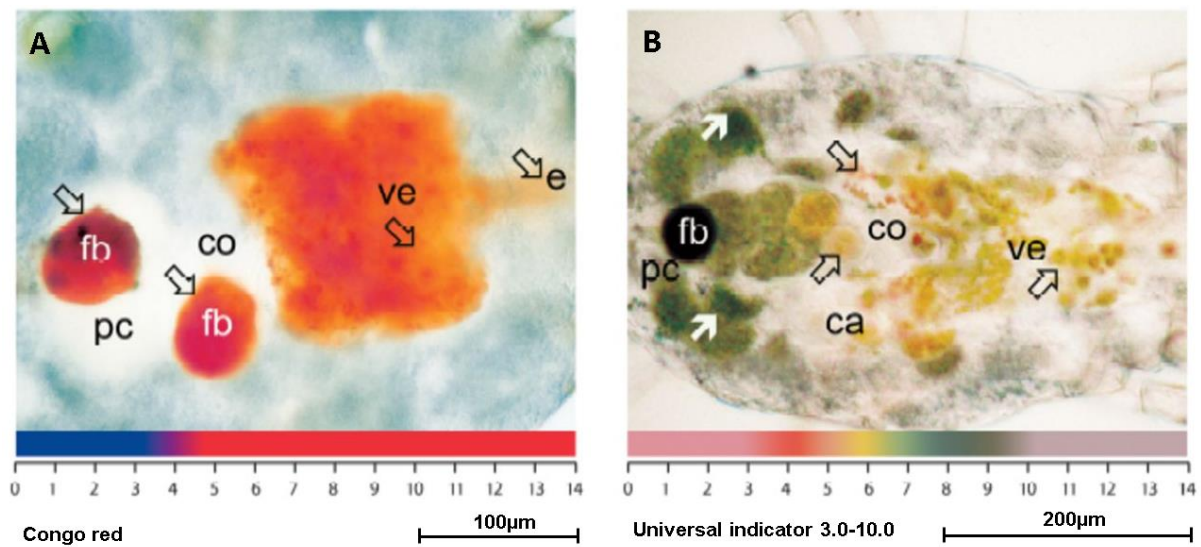


**Figure 7. Digestive tract compartments in *Dermatophagoides farinae* (A) and *Tyrophagus putrescentiae* (B) stained with indicator dyes.**
Congo red (transition range 3-5) produced a red colour throughout the entire digestive tract in *Dermatophagoides farinae* and a universal indicator composed of multiple dyes (total transition range 3-10) showed a variety colours in *Tyrophagus putrescentiae*; Compartments stained were the ventriculus (ve), esophagus (e), colon (co), postcolon (pc) and caeca (ca) when indicator dyes leaked from a food bolus (fb). Figure modified from Erban and Hubert (2010).

# 2 Objectives

## 2.1 Objective 1 – Characterizing pH in the digestive tract of TSSMs

My first objective was to characterize the pH environment within the digestive tract of TSSMs with and without the presence of plant cell contents. These pH values served as a reference to compare and contrast with TSSMs treated with dsRNA.

## 2.2 Objective 2 – Characterizing pH in the digestive tract of *tetur09g04140*-knockdown TSSMs

My second objective was to investigate the role of V-ATPase in regulating pH within the digestive tract of TSSMs. This was accomplished by feeding dsRNA solution to induce an RNAi response and then measuring pH following non-feeding and feeding regimens. Differences in the colours of indicator dyes between control and knockdown TSSMs would illustrate what effect silencing *tetur09g04140* has on pH regulation.

# 3  Methods

## 3.1  Generating TSSM specimens

Protocols described by Suzuki et al. (2017a) were followed when maintaining TSSM stock populations and synchronizing life cycles (**Figure 8**) for experiments. The following terminologies are used in this thesis to describes the various environments where activities and incubation periods of TSSMs were hosted:

**Colony lab**  A lab where the TSSM colony is reared at room temperature and humidity.

**Dark room**  A 20°C room where lights are kept off to reduce the influence of light on specimens and solutions.

**Incubation chamber**  A climate-controlled chamber with a constant temperature of 26°C, 50% relative humidity and a 16:8 h light:dark photoperiod.
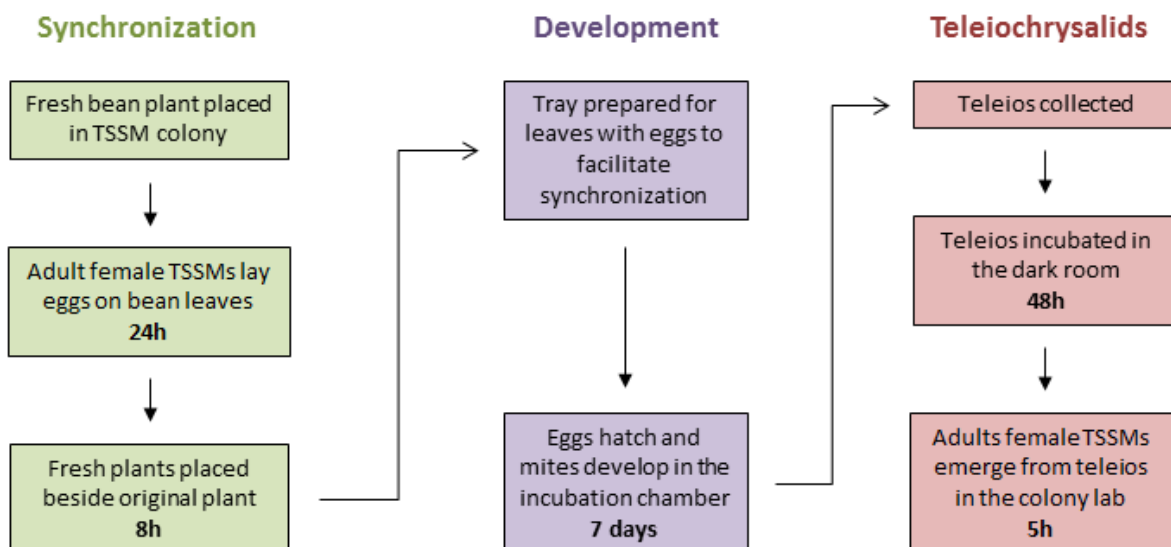


**Figure 8. Overview for synchronizing the life cycles of adult female TSSMs.**
Teleiochrysalids abbreviated to "teleios" for short.

### 3.1.1 Rearing TSSMs on bean plants

*Tetranychus urticae* (London strain, Grbić lab) TSSMs were reared on red kidney beans (*Phaseolus vulgaris* var. California Red Kidney) in the colony lab. Lighting was provided by Philips Fluorescent Plant Light bulbs (Philips, Amsterdam, Netherlands) with a flux density of 150 µmol m$^{-2}$ s$^{-2}$ set to a 16:8 h light:dark photoperiod. Older infested bean plants were discarded and replaced every 6-8 days to maintain TSSM colony size.

### 3.1.2 Synchronizing TSSM development to produce newly moulted adult females

A fresh bean plant was placed in the TSSM colony. Adult female TSSMs were given 24 h to lay eggs on the bean leaves. Fresh bean plants were subsequently placed adjacent to the original plant for 8 h to attract TSSMs from the original plant. Leaves from the original bean plant were cut at the base of the petiole then placed on the paper of a tray with fresh bean leaves (**Figure 9**).



**Figure 9. Tray prepared with TSSMs on bean leaves to ensure host life cycle synchronization.**
The supplement of fresh bean leaves provided TSSMs with a week-long food source as they developed. Leaves were pressed down against the wet paper to prevent TSSMs from climbing underneath.

TSSMs were incubated for 7 days in the incubation chamber, with 2-3 fresh bean leaves placed along the row of older infested leaves on the 6th day. The tray was removed from the incubation chamber and teleiochrysalids were collected using a vacuum air pump (Cazaux et al. 2014), then placed in a small Petri dish lid suspended on a wet cotton pad in a plastic container. The container was sealed with a non-ventilated lid to maintain high air moisture which suppressed TSSMs emerging from their teleiochrysalids (Ikagemi et al. 2000; Suzuki et al. 2017a). It was placed in the dark room for 48 h then moved to the colony lab where it was opened to reduce air moisture content and allow TSSMs to emerge. The newly moulted adult female TSSMs were collected 5 h post-emerging for experiments. TSSMs collected from the same synchronized population constituted an individual trial for a total of 3 trials per experiment.

## 3.2  Generating knockdown TSSMs

### 3.2.1  Synthesis of dsRNA

dsRNA solutions were prepared for an intergenic region (genomic scaffold 12) acting as a negative control (F3R3) and for *tetur09g04140* (VATP) (Suzuki et al. 2017b). Forward and reverse primers for VATP and F3R3 (**Table 1**) were used to synthesize dsRNA following the protocols described by Suzuki et al. (2017b). The final dsRNA solutions (160 ng/µL 0.1% v/v Tween 20[®]) were stored at -20°C in 1.5 mL Eppendorf tubes.

**Table 1. Primers used for the synthesis of dsRNA solutions.**
Each primer is described in 5'-3' direction (Suzuki et al. 2017b).

|  | F3R3 | VATP |
|---|---|---|
| Forward primer | CCGTGATATGGGTTACCATG | GAAGAGGTACGAAATCTGGG |
| Reverse primer | GCCCTCTCCTGGTTGTAAACTT | CGACCCCATCAGGCTATTGA |
| Fragment Size | 382 base pairs | 416 base pairs |

### 3.2.2  Application of dsRNA to facilitate RNAi in TSSMs

A  2.5 mm$^2$ Kimwipe square was placed at the centre of a small Petri dish and soaked with 15 µL of dsRNA solution using a micropipette. A cohort of ~30 newly moulted female TSSMs was collected and placed onto the wet Kimwipe square with the ventral surface of all TSSM bodies facing down (**Figure 10**). The Petri dish was sealed with Parafilm to prevent evaporation and placed in the dark room for 24 h. For experiments, the Kimwipe square was removed from the Petri dish and given 15-20 minutes to dry on a feeding regimen surface, then discarded when TSSMs regained motility to move off the square. Motile TSSMs with legs that were stuck on the dried Kimwipe were gently pushed with an eyelash probe to free them.
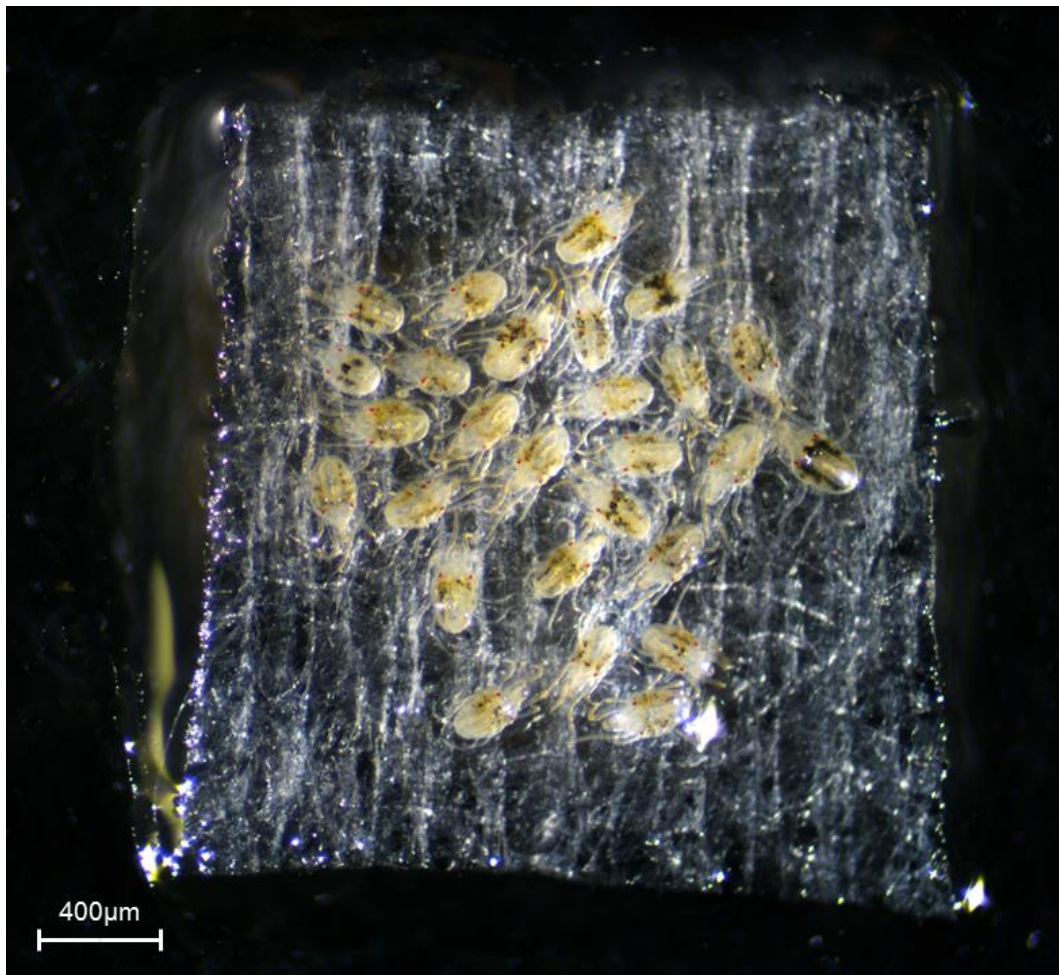


**Figure 10. Newly moulted adult female TSSMs on a 2.5 mm$^2$ Kimwipe paper soaked with dsRNA solution.**

## 3.3 Non-feeding and feeding regimens

TSSMs underwent a non-feeding regimen when given only indicator dye solutions, either orally for 24 h or by immediate microinjection (**Figure 11**), as they did not provide any nutritional value other than water. TSSMs were subject to different feeding regimens to establish digestive tract pH during digestion/detoxification of ingested plant cell content in control and dsRNA-treated TSSMs (here referred to as just RNAi) (**Figure 12**).
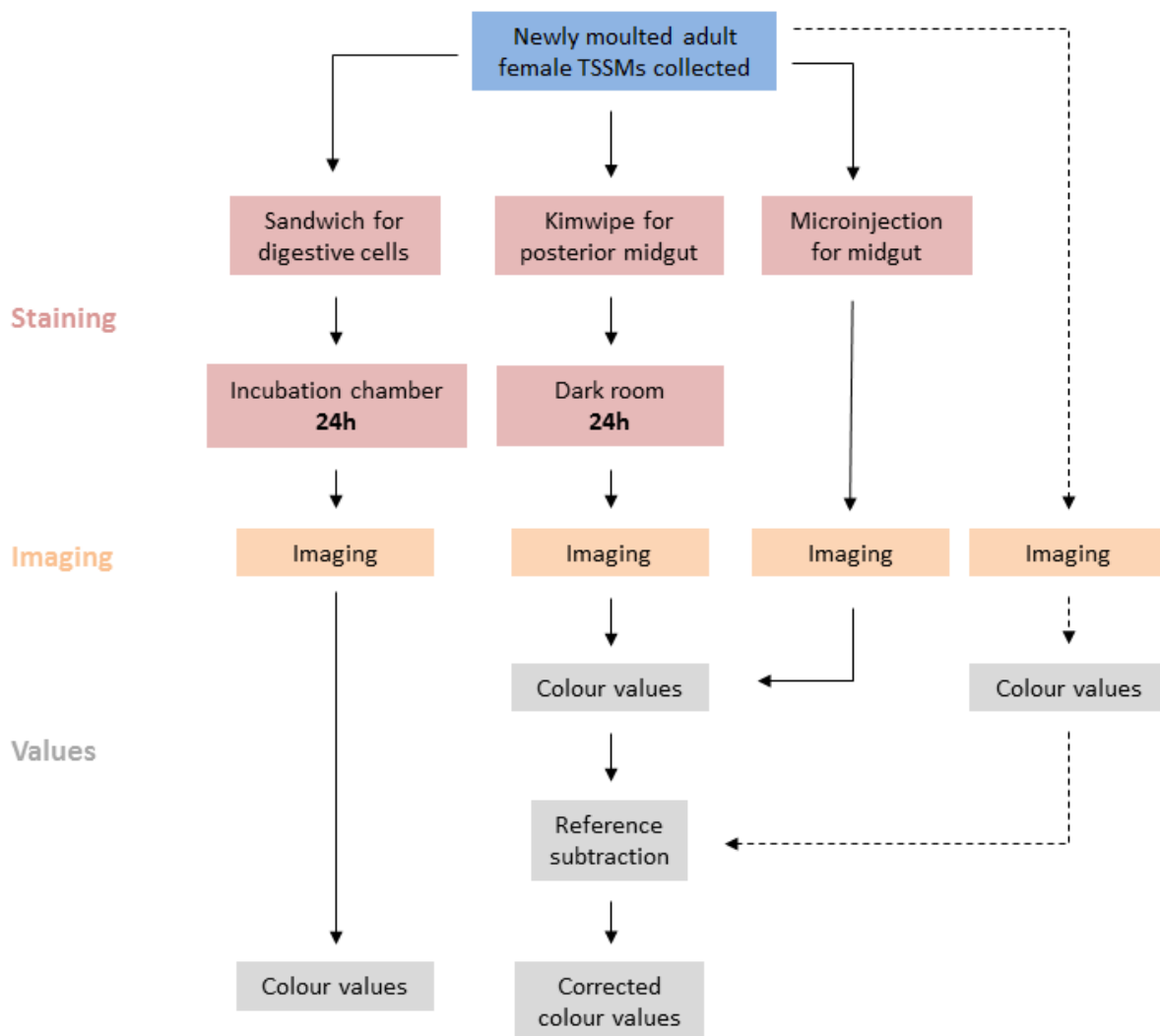


**Figure 11. Overview of experimental protocols used to generate data for determining pH in non-fed TSSMs.**
Dotted lines represent untreated TSSMs used to establish reference values.
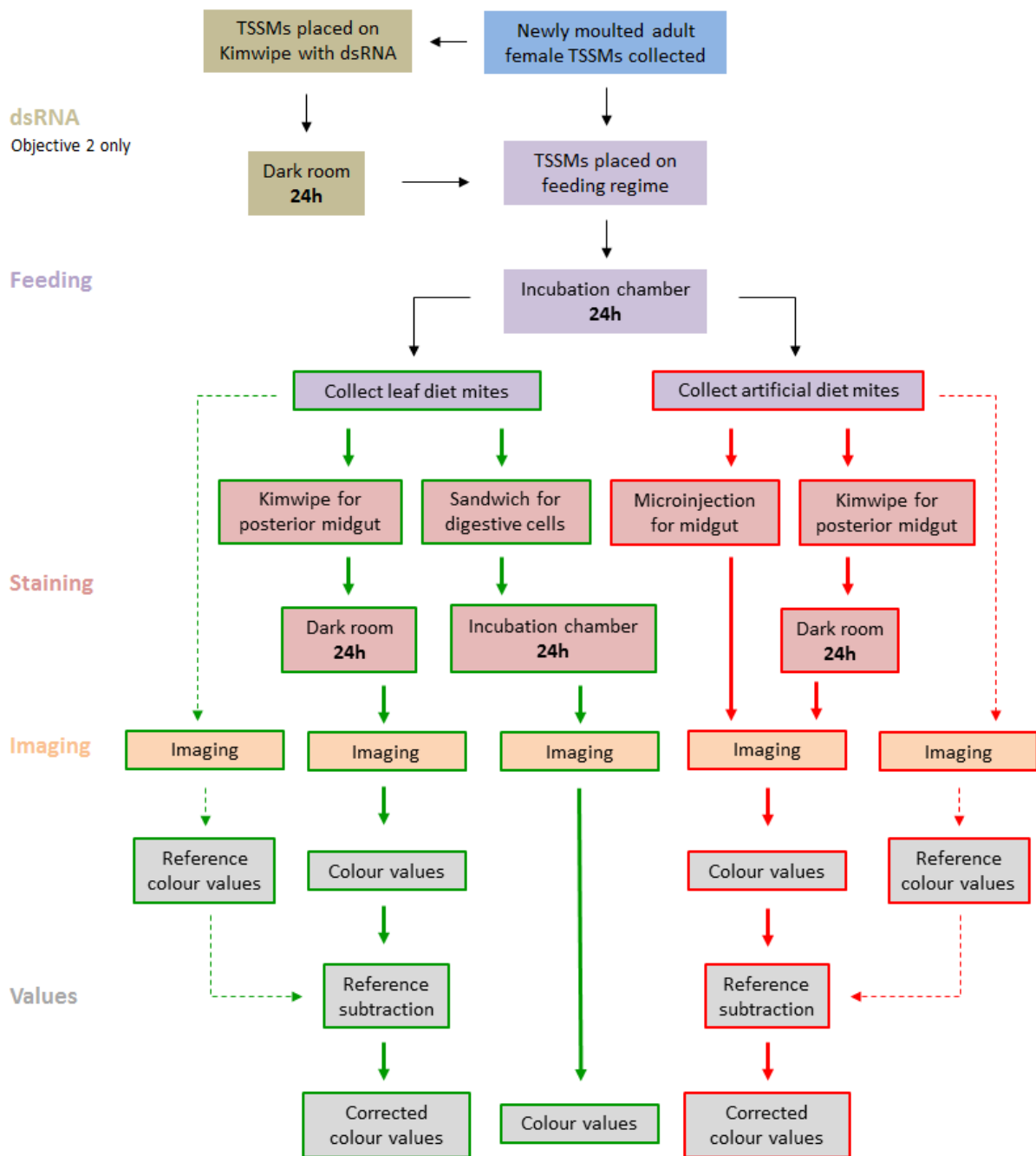
**Figure 12. Overview of experimental protocols used to generate data for determining pH in fed TSSMs.**
Dotted lines represent unstained, fed TSSMs used to establish reference values. Green borders and arrows represent experiments for leaf-fed TSSMs. Red borders and arrows represent experiments for TSSMs fed with artificial diet. TSSMs not treated with dsRNA for Objective 2 experiments were controls.

### 3.3.1  Bean leaf diet

A 2x3 cm square was cut from the base of a bean leaf, with ~2 mm of the petiole kept intact to maintain leaf hydration. The leaf square was placed on a wet cotton pad with the abaxial side facing down and lightly pressed to seal any gaps along the edges. Kimwipe strips overlapped the edges of the leaf square to prevent TSSMs from escaping. TSSMs were placed on the leaf and the cotton pad placed in a plastic container that was sealed with an air-permeable lid then placed in the incubation chamber for 24h. The container was sheltered under an opaque barrier to reduce UV stress from overhead lights in the chamber (Suzuki et al. 2013). The opaque barrier was applied for subsequent feeding experiments in the incubation chamber.

### 3.3.2  Artificial diet

A nutritive artificial solution was used as a substitute for bean leaves to produce a clear midgut lumen without the presence of plant cell content. A variety of *L*-amino acids and nutrients (**Table 2**) described by Febvay et al. (1987) were mixed in 80 mL of distilled water to create a final volume of 100 mL. A serial dilution was conducted by mixing 1 mL of stock solution in 9 mL of distilled water, repeated 2 times, to produce a final 1,000x diluted solution; solutions diluted 10x and 100x were attempted but resulted in TSSM mortality after 24 h feeding whereas TSSMs survived on the 1,000x dilution. A volume of 10 mL of the diluted artificial diet was poured into 15 mL high-capacity polypropylene Cornical™ Falcon tubes and stored at 4°C for no longer than 3 months (Suzuki et al. 2017a). TSSMs were placed on a micromesh "sandwich" (**Figure 13**) infused with artificial diet in a plastic container. The sandwich container was sealed with a breathable lid and placed in the incubation chamber for 24 h.

**Table 2. Ingredients for the aphid diet described by Febvay et al. (1987) and quantities (mg) used to create 100 mL of stock TSSM artificial diet.**

| L-amino acids | Quantity | Vitamins | Quantity | Other Nutrients | Quantity |
|---|---|---|---|---|---|
| Alanine | 178.7 | p-Aminobenzoic acid | 10 | Copper sulfate | 0.47 |
| ß-Alanine | 6.2 | L-Ascorbic acid | 100 | Iron (III) chloride | 4.45 |
| Arginine | 244.9 | Biotin | 1 | Manganese (II) chloride | 0.65 |
| Asparagine | 298.5 | D-Calcium pantothenate | 5 | Sodium chloride | 2.54 |
| Aspartic acid | 88.3 | Choline chloride | 50 | Zinc chloride | 0.83 |
| Cysteine | 29.6 | Folic acid | 1 | Calcium citrate | 10 |
| Glutamic acid | 149.3 | i-Inositol | 42 | Cholesteryl benzoate | 2.5 |
| Glutamine | 445.6 | Nicotinamide | 10 | Magnesium sulfate | 242 |
| Glycine | 166.6 | Pyridoxin HCl | 2.5 | Potassium dihydrogen phosphate | 250 |
| Histidine, HCl, $H_2O$ | 136 | Riboflavin | 0.5 | Sucrose | 28,920 |
| Isoleucine (allofree) | 164.7 | Thiamine di-HCl | 2.5 | | |
| Leucine | 231.5 | | | | |
| Lysine mono HCl | 351 | | | | |
| Methionine | 72.4 | | | | |
| Ornithine mono HCl | 9.4 | | | | |
| Phenylalanine | 169.98 | | | | |
| Proline | 129.3 | | | | |
| Serine | 124.3 | | | | |
| Threonine (allofree) | 127.1 | | | | |
| Tryptophan | 42.7 | | | | |
| Tyrosine | 38.6 | | | | |
| Valine | 190.8 | | | | |
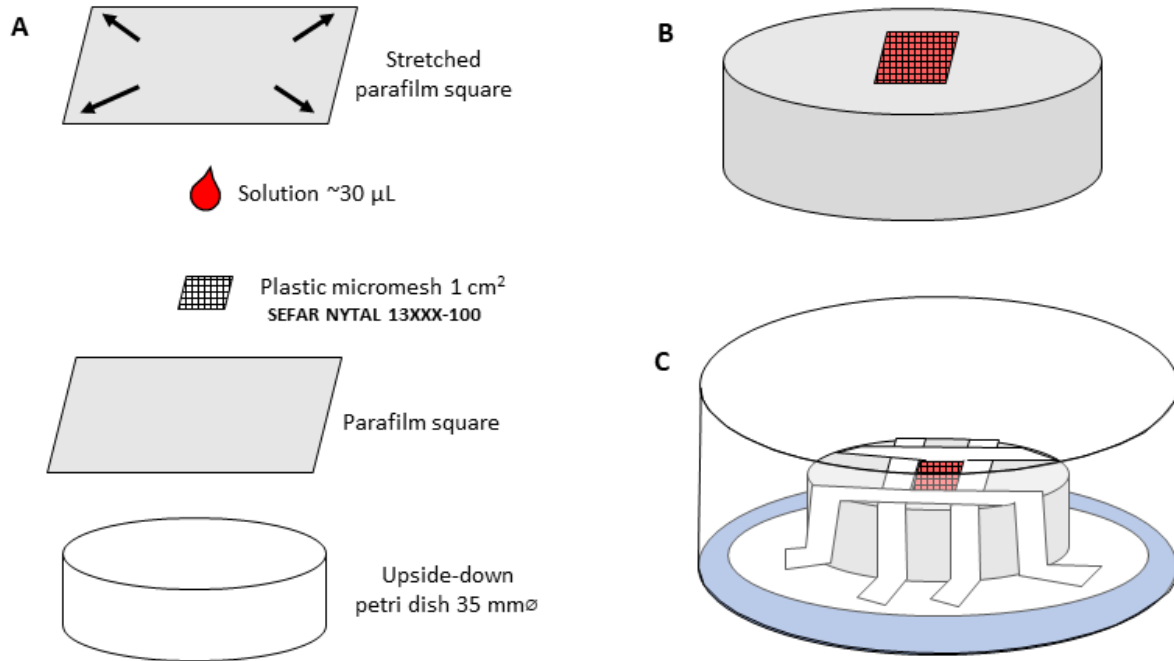
**Figure 13. Micromesh sandwich used to simulate a leaf-like surface for feeding TSSMs.** Components of a plastic micromesh sandwich in top-bottom consecutive order (A); A completed sandwich (B); Micromesh sandwich in a plastic container on a water-soaked cotton pad with Kimwipe strip barriers establishing a feeding area (C).

### 3.3.3  Determining viability of artificial diet as substitute for bean leaves

Control, F3R3 and VATP TSSMs were placed on micromesh sandwiches with artificial diet in plastic containers. Each container constituted an individual trial for a total of 3 replicates per control and knockdown TSSM. Populations began with ~14 TSSMs. The containers were sealed with air-permeable lids and placed in the incubation chamber for 24 h. Population numbers were recorded daily for 7 days.

## 3.4  Preparing indicator dye solutions

Various water-soluble pH indicator dyes were selected for the experiments (**Table 3**). A sufficient quantity of dye powder (~2-4 mg) was added to 10 mL of double distilled water in a 15 mL Falcon tube to produce a fully saturated solution, vortexed for 10 sec, followed by 5 min on a rotary shaker and then vortexed again for 10 sec. Saturation of dye in water was

indicated by the presence of undissolved powder. The dye solution was filtered into a new 15

mL Falcon tube and stored in the dark room.

**Table 3. Stock dye powders and product information.**
Indicator dyes were selected based on transition range pH values within or near the collective
4-8 range of digestive tract pH in mites established by previous research. SS = sodium salt.

| Stock dye | Transition ranges | Manufacturer | CAS number |
| --- | --- | --- | --- |
| Alizarin Red S | 3.4 to 5.5<br>9.4 to 12.0 | Acros Organics | 130-22-3 |
| Bromocresol Green SS | 4.0 to 5.6 | Sigma-Aldrich | 62625-32-5 |
| Bromocresol Purple | 5.2 to 6.8 | Sigma-Aldrich | 62625-32-5 |
| Bromophenol Blue | 3.0 to 4.6 | Sigma Chemical Co. | 115-39-9 |
| Bromophenol Red | 5.2 to 6.8 | Acros Organics | 2800-80-8 |
| Chlorophenol Red | 4.8 to 6.4 | Alfa Aesar | 4430-20-0 |
| Cresol Red | 0.2 to 1.8<br>7.2 to 8.8 | Sigma-Aldrich | 1733-12-6 |
| *m*-Cresol Purple | 1.2 to 2.8<br>7.4 to 9.0 | Sigma-Aldrich | 2303-01-7 |
| Eriochrome Black T | 6.0 to 7.0 | Sigma-Aldrich | 1787-61-7 |
| Neutral Red | 6.8 to 8.0 | Sigma-Aldrich | 553-24-2 |
| Phenol Red SS | 6.8 to 8.4 | Acros Organics | 34487-61-1 |
| Resazurin | 3.8 to 8.4 | Sigma-Aldrich | 62758-13-8 |
| Thymol Blue SS | 1.2 to 2.8<br>8.0 to 9.6 | Sigma-Aldrich | 62625-21-2 |

## 3.5   Delivery of pH indicator dyes to TSSM digestive tract compartments

### 3.5.1   Oral delivery of dyes

A Kimwipe square was placed in a small Petri dishes and soaked with 15 µL of indicator

dye solution and 2 µL of Tween 20 (1%) using a micropipette. TSSMs were placed, ventral

side down, on the Kimwipe square. The Petri dish was sealed with Parafilm and placed in the dark room for 24 h. Micromesh sandwiches were also used for feeding dyes to TSSMs. Micromesh sandwiches were prepared with ~30 µL of indicator dye solution and 5 µL of Tween 20 (1%). TSSMs were placed onto the micromesh feeding area of the sandwich. The micromesh sandwich container was sealed with an air-permeable lid and placed in the incubation chamber for 24 h.

### 3.5.2  Microinjection of dye to midgut caeca and ventriculus

Thin strips of double-sided tape were cut and placed on a glass slide under a dissecting microscope. TSSMs were individually collected from a small Petri dish using an eyelash probe then placed on the tape with the ventral sides of their bodies facing down. Legs were gently pressed down against the tape to restrain them. A volume of dye sufficient for injecting 30 TSSMs (~0.3 µL) was added to a microinjection needle, which was secured onto the microinjection console with the needle tip positioned adjacent to the TSSM tape strip. The needle tip was opened in a droplet of water with constant injection air pressure activated until dye began to spray into the water. The needle tip was then inserted into midgut caeca along the sides of the body. A preset injection air pressure of 150-250 psi or careful application of constant needle-cleaning air pressure was sufficient for effective injection while avoiding tissue damage. Injections resulted in an entirely stained midgut and a slight increase in body size (**Figure 14**). In most cases, the dye solution diffused through the epithelium and stained the rest of the body, though this did not impact the dye colour in the midgut. The tape strip was carefully peeled off and placed onto a new microscope slide. Injected TSSMs were soaked with coverslip mounting medium to reduce adhesion of the tape. Special care was taken when removing TSSMs from the tape with an eyelash probe to avoid rupturing bodies or legs ripping

off, as this could have resulted in leaked dye and possible physiological reactions affecting gut pH.
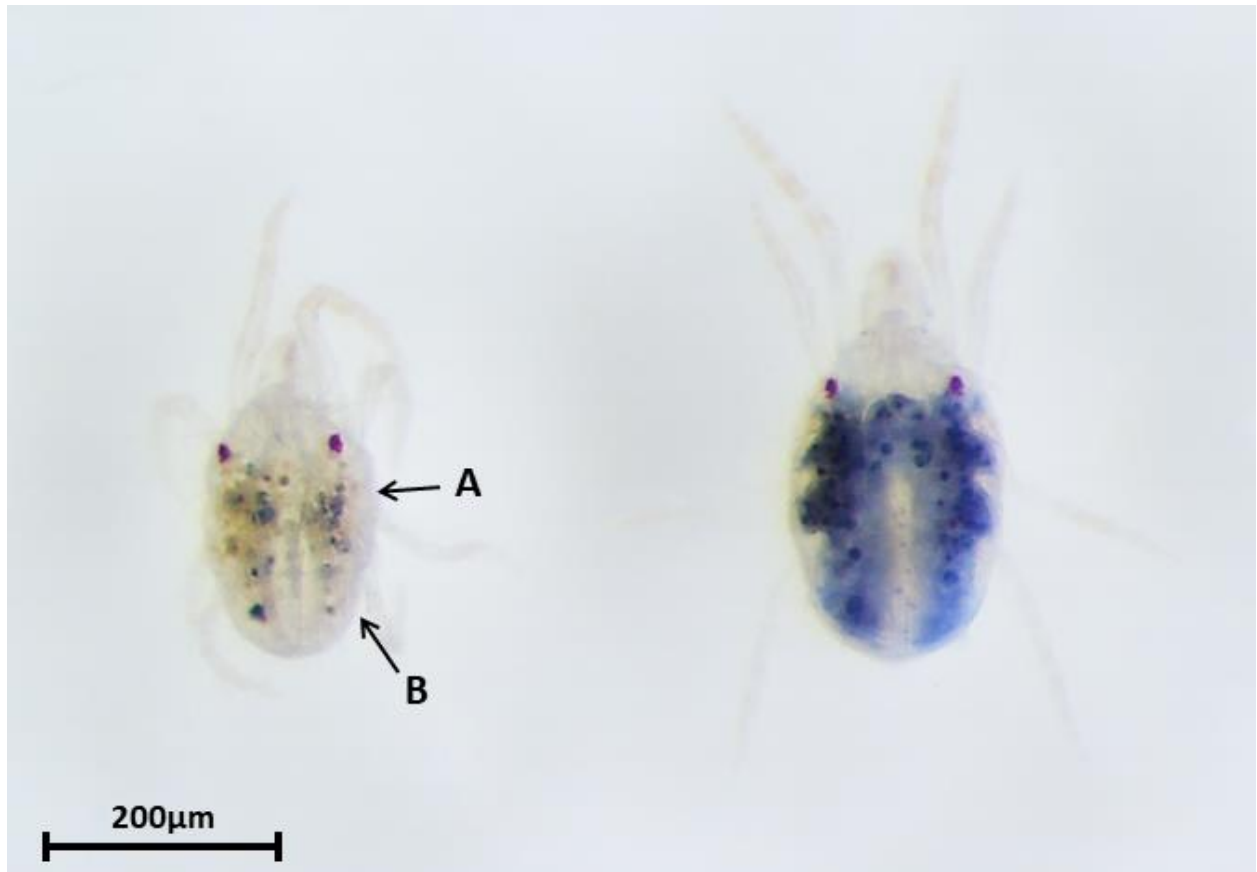


**Figure 14. Newly moulted adult female TSSMs before (left) and after (right) microinjection.**
Dyes were injected either in caeca adjacent to the ventriculus (A) or caudal caeca at the posterior end of the midgut (B).

## 3.6 Creating indicator dye colour standards

### 3.6.1 Preparation of Britton-Robinson buffer solutions

Aqueous universal Britton-Robinson buffer solutions were prepared for pH values from 2 to 12 following protocols described by Joseph et al. (2013). A 100 mL volume of distilled water was poured into a 250 mL glass beaker with a small magnet and placed on a magnetic stirrer. A pH probe set to 0.01 units was turned on and given 30 sec to calibrate in a buffer solution with a pH of 7.0. The pH probe was washed with distilled water and placed in the 250

27

mL beaker. The magnetic stirrer was turned on. Various acids required for the Britton-Robinson buffer (**Table 4**) were mixed into the beaker and given 2 min to dissolve. The buffer was titrated with 0.2 M NaOH, after an initial pH reading of 2.1±0.1 was stable for 30 sec, to a desired pH ±0.02 units. The buffer was poured into a 100 mL glass bottle after the desired pH was stable for 20 sec then sealed with a plastic cap. Buffers of 0.25 increments were prepared for pH values within and near the transition ranges of indicator dyes selected for statistical analysis. The buffer bottles were stored in the dark room.

**Table 4. Components used to create Britton-Robinson buffer for pH indicator dyes.**

| Compound | Stock [ ] | Molar Mass | Quantity | Molarity |
|---|---|---|---|---|
| Acetic acid | 95% | 60.05g/mol | 23 µL | 0.04 Mm |
| Boric acid | 99.7% | 61.83g/mol | 247.56 mg | 0.04 Mm |
| Phosphoric acid | 85% | 97.99g/mol | 270 µL | 0.04 Mm |

### 3.6.2 Preparation of colour standards for indicator dyes

The wells of a 3x4 white ceramic well plate were filled with 300 µL of buffer solution for each pH in the 2-12 or transition range series. The buffer solutions were mixed with 1 µL of dye pipetted to each well (**Figure 15**). A 1:10 dye:buffer dilution was prepared for chlorophenol red and phenol red to reduce saturation of colour. The well plate was placed under a dissecting microscope equipped with a ring light and a Canon EOS Rebel T5i camera. The magnification was increased until the ring light's reflection in the well was completely outside the image frame. A white balance was set using an empty well plate as a reference. Lighting was set to automatic which retained consistency in brightness. Each image constituted an individual colour swatch representing the indicator dye at a specific pH value. A completed series of pH constituted an individual replicate. Imaging was repeated for a total of 3 replicates for each indicator dye.
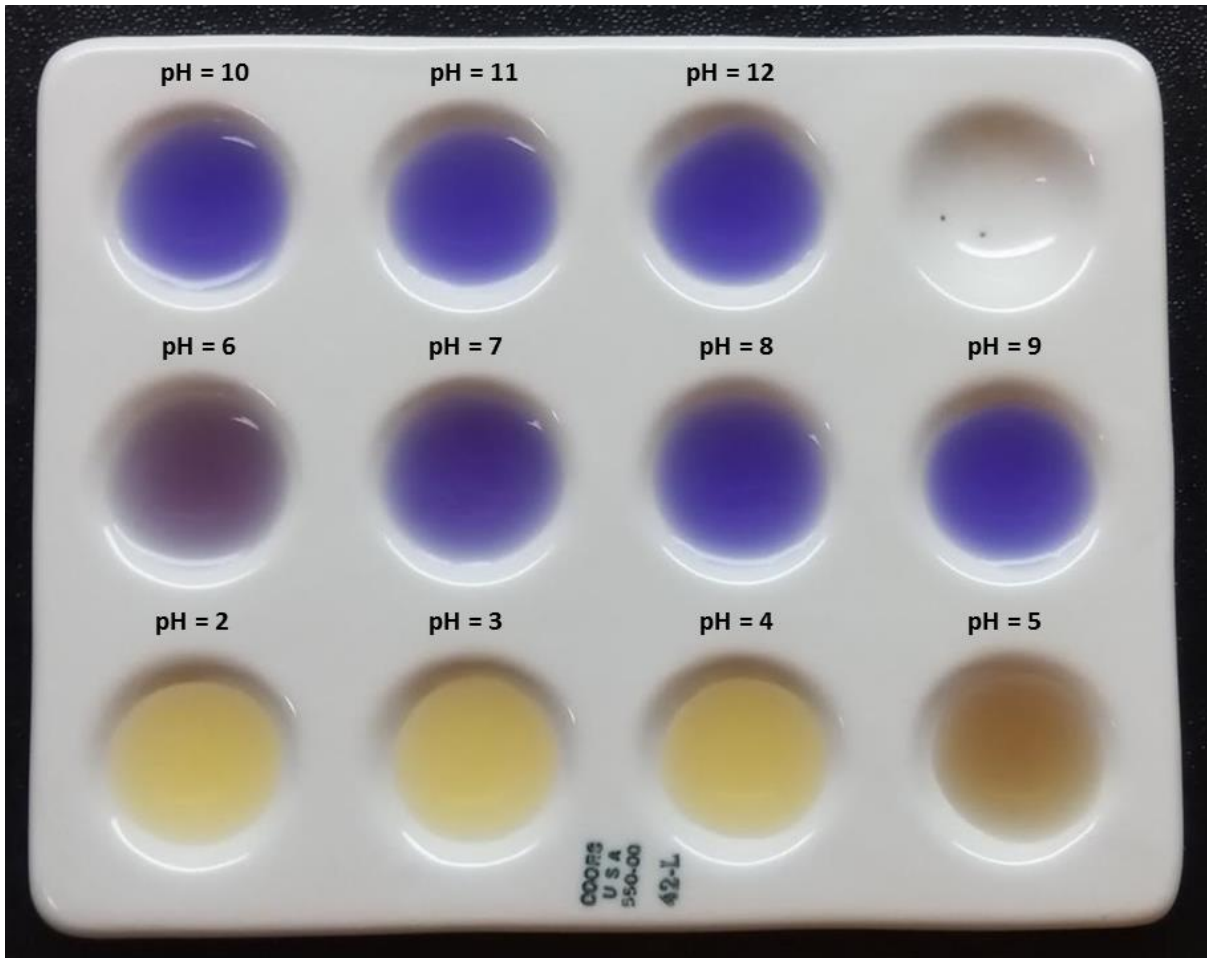
**Figure 15. Well plate with a complete series of pH from 2 to 12 stained with bromocresol purple.**
The transition range of bromocresol purple was 5.2 to 6.8 (Sabins 2008).

## 3.7  Imaging and obtaining colour values from images

### 3.7.1  Mounting TSSMs on microscope slides

A coverslip with plasticine spacers was placed on a glass slide and lightly pressed down. Mounting solution (50% glycerol + 49% PBS + 1% Tween 20 [1% v/v PBS]) was injected under the coverslip using a syringe. TSSMs were transferred to the slide using an eyelash probe and placed on excess mounting medium outside the coverslip. The TSSMs were then pushed underneath the coverslip with the ventral surface of their bodies facing down (**Figure 16**). The coverslip was pressed down until the TSSMs were slightly flattened.
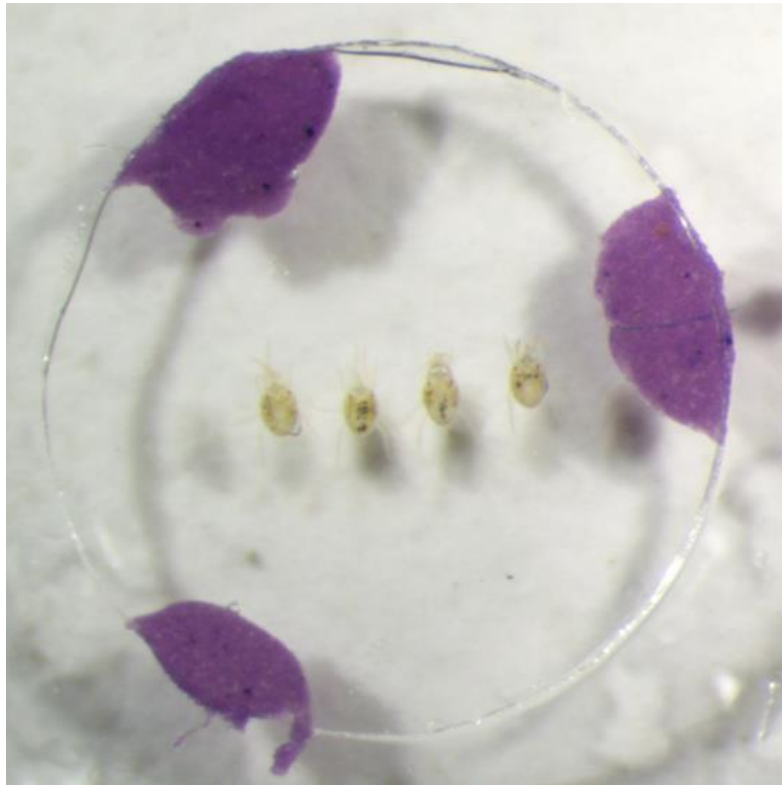
**Figure 16. TSSMs mounted under a 35 mm round coverslip.**
The TSSMs were pushed underneath the coverslip and oriented in a row using an eyelash probe for easier imaging.

### 3.7.2  Mounting digestive cells on microscope slides

A small droplet of mounting solution (50% glycerol + 49% PBS + Tween 20 [1% v/v PBS]) was added to a glass slide with a syringe. TSSMs were placed in the droplet and dissected to release digestive cells. A coverslip with plaster legs was placed on top of the droplet. The coverslip was pressed down to secure it in place and to expand the droplet.

### 3.7.3  Standardizing colours in images using a neutral background

Specimens were imaged using a Zeiss AxioCam Colour HRc CCD 412-312 camera using Zeiss Axioplan II software. A "blank" coverslip with only mounting medium was prepared adjacent to the coverslip with the specimen to generate a neutral background. The neutral background was generated by first establishing black and white references, then

applying a white balance, resulting in a light grey or white background. TSSM bodies were imaged at 100x magnification with lighting set to a pre-set 3200K colour temperature. Digestive cells were imaged at 630x magnification with a water immersion objective lens and lighting set to maximum. Consistency in light exposure settings were maintained in software when imaging regardless of magnification or microscope lighting adjustments.

### 3.7.4  Sampling colour values from images

Images of dye colour standards were opened in Adobe Photoshop CS5[©]. The image colour mode was changed from *RGB* (Red, Green and Blue) to *Lab* (*L* = luminance/brightness, *a* = green-to-red colours, *b* = yellow-to-blue colours). *RGB* values represent colour light generated by digital screens using red, green and blue LCDs. The dependence on a lighting factor in *RGB* would heavily skew pH results as darker materials in TSSMs interfere with the colours produced by indicator dyes. The *a* and *b* colour spaces are independent from *L,* which provides consistent representation of colours regardless of electronic devices (**Figure 17**).



| | R | G | B | L | a | b |
|---|---|---|---|---|---|---|
| | 0 | 42 | 0 | 13 | -30 | 30 |
| | 56 | 106 | 42 | 40 | -30 | 30 |
| | 128 | 179 | 110 | 68 | -30 | 30 |
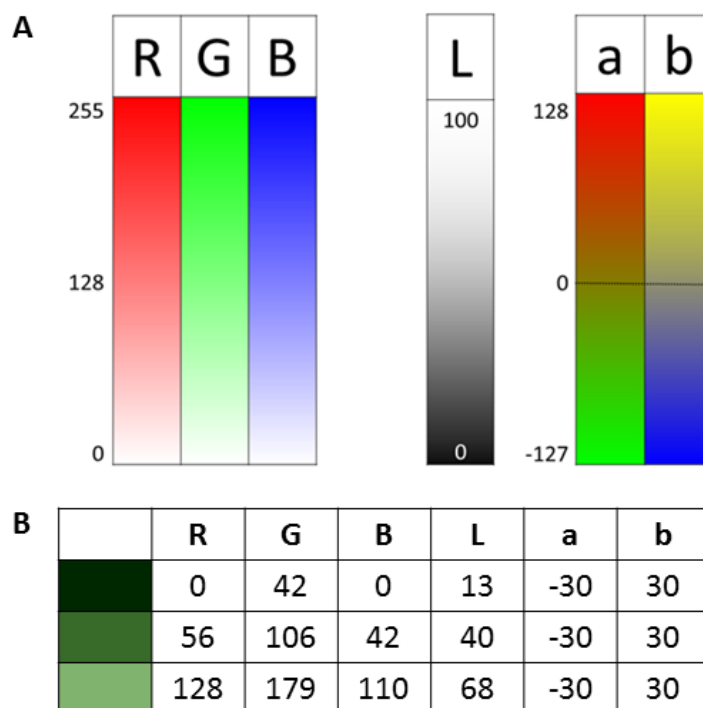
**Figure 17. Numerical scales (A) and an example where only brightness is changed (B) for *RGB* and *Lab* colour space values.**

A Gaussian blur was applied to reduce pixel variation. The *a* and *b* colour values sampled from the centre of indicator dye images were recorded in a spreadsheet. Sampling from 10 images of unstained TSSMs generated mean *a* and *b* values (here referred to as reference values). The reference values would be subtracted from values representing stained gut compartments to reduce the impact of the TSSM's natural body colour on dye colours. No reference values were required for digestive cells.

Images were opened in Adobe Photoshop CS5$^{©}$. Image mode was changed from *RGB* to *Lab*. *a* and *b* values were recorded from pre-selected sampling sites in body images (**Figure 18**) and z-series images of digestive cells with vesicles in proper focus (**Figure 19**). The sampling sites in gut compartments were used to identify pH gradients and to generate a mean value for subsequent analysis. Only digestive cells in the earliest stages of development were imaged as the presence of plant material in later-stage cells (**Figure 3**) would interfere with dye colour. The colour values were taken from the centre of sampling sites and recorded in a spreadsheet file. Caeca and ventriculus colour values were always sampled from the same TSSMs whereas posterior midgut data was taken from separate populations.
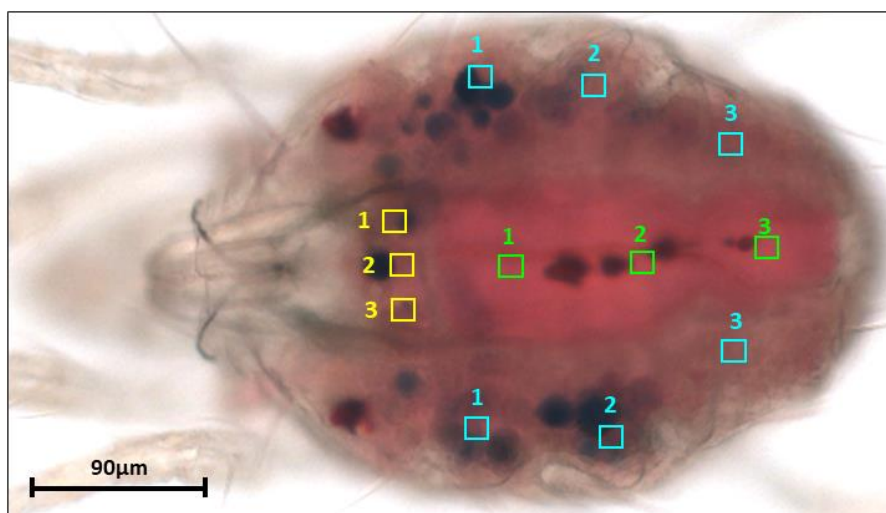


**Figure 18. Sampling sites where colour values were collected from TSSM body images**. Colour values were recorded from the midgut ventriculus (yellow), caeca (blue) and posterior midgut (green). If the dye was obstructed by digestive cells or waste products, the closest unobstructed area near the sampling site would be used instead.
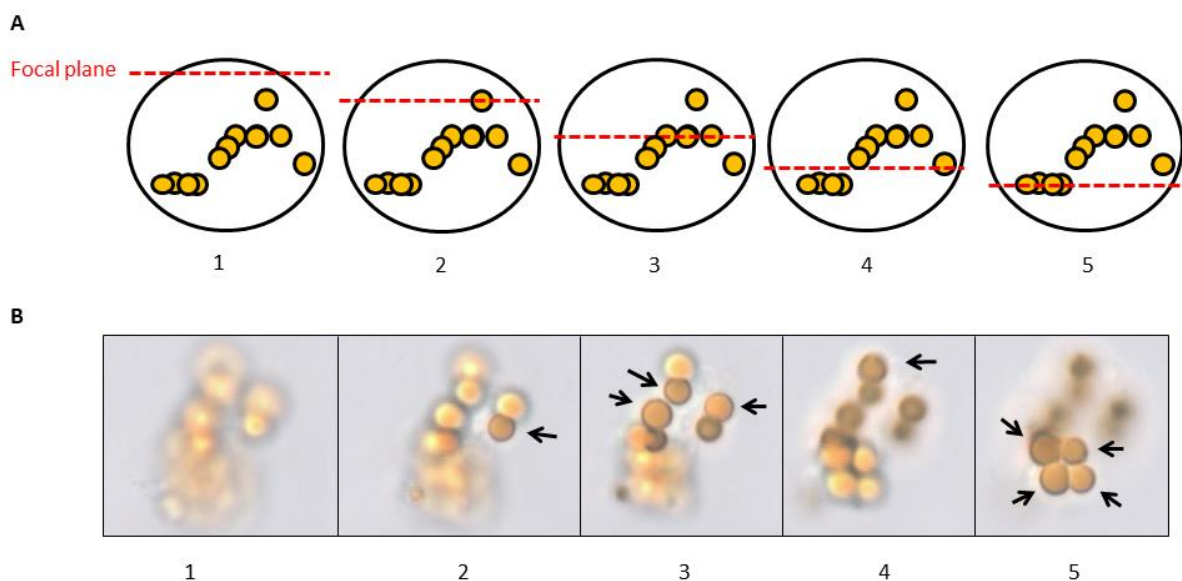
**Figure 19. Digestive cell with stained vesicles imaged in sequential focus.**
Position of the focal plane relative to the dorsal-ventral axis of the digestive cell (A) for each image of the series (B); Arrows point out vesicles in proper focus indicated by sharp vesicle membranes when the focal plane intersects the middle of the vesicles.

## 3.8 Statistical analyses used to determine pH from *a* and *b* colour values

Statistical analyses supplemented the visual determination of pH from indicator dyes when intermediate transition range colours became too ambiguous for the human eye to distinguish. All statistical tests using *a* and *b* colour values were performed with R Studio® (see **Appendix** for program specs and packages).

### 3.8.1 Linear regression models of pH indicator dyes

Linear regression models were used to quantify the changes in colour of dyes reacting to the various pH of Britton-Robinson buffers by predicting the closest match between pH and colour values. All linear models were generated using R Studio®. Linear models were used for indicator dyes that visually established pH parameters and for dyes that produced intermediary transition range colours. The pH values for each indicator dye were estimated using the following formula:

33

$$pH_i = \beta_0 + \beta_1 a_i + \beta_2 b_i$$

where $a$ represents the red-green, and $b$ represents the yellow-blue, colour values of a given sample.

### 3.8.2 Statistical tests for assessing colour data sets

One-way ANOVA and Tukey's HSD tests were performed on image sampling sites, gut compartments, non-feeding/feeding regimens and knockdown TSSMs to determine pH gradients and significant changes in pH. Tukey's HSD test results included 95% family-wise confidence intervals (CI). Individual TSSMs and digestive cell vesicles constituted sample sizes (n) for gut compartments and digestive cell pH results, respectively.

# 4 Results

## 4.1 Characterization of pH indicator dyes

Transition range pH values for indicator dyes were determined according to the manufacturer's suggested range alongside visual inspection of plotted $a$ and $b$ colour values in relation to pH. For prediction of pH values within TSSM gut compartments and digestive cell vesicles, linear regression models encompassing the 2-12 range and transition pH ranges were created for: bromophenol blue (**Figure 20**), chlorophenol red (**Figure 21**), phenol red (**Figure 22**) and thymol blue (**Figure 23**). The combined size of transition ranges from the 4 selected dyes covered a broad pH range of 3.0 to 9.5. The final formulas derived from the analysis of dye calibration data for the dyes within their respective transition ranges (in parentheses) were the following:

Bromophenol Blue (3.0 to 4.5)
$$pH_i = 3.63 + 0.03a_i - 0.05b_i$$
with a residual standard error of 0.19, and adjusted $R^2 = 0.87$.

Chlorophenol Red (4.5 to 6.5)
$$pH_i = 5.05 + 0.07a_i - 0.04b_i$$
with a residual standard error of 0.08, and adjusted $R^2 = 0.99$.

Phenol Red (6.5 to 8.25)
$$pH_i = 7.55 + 0.02 - 0.04b_i$$
with a residual standard error of 0.06, and adjusted $R^2 = 0.99$.

Thymol Blue (8.25 to 9.5)
$$pH_i = 8.35 + 0.01a_i - 0.01b_i$$
with a residual standard error of 0.04, and an adjusted $R^2 = 0.99$.

**A**
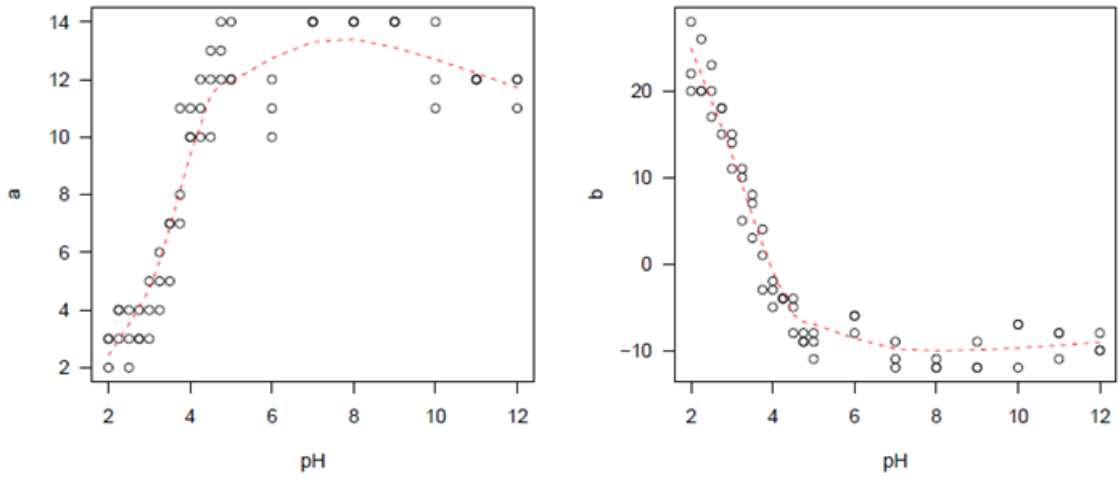


**B**
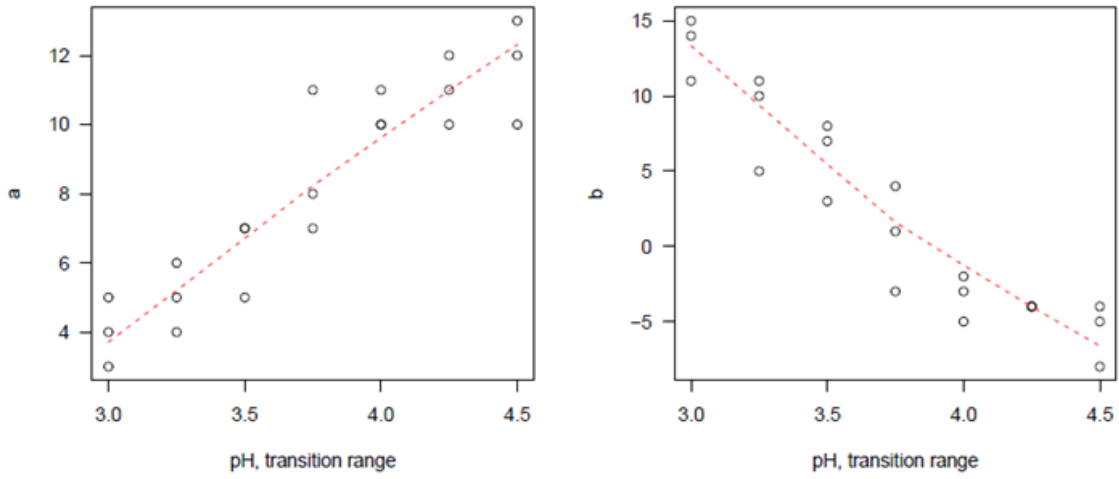


**Figure 20. Bromophenol blue colour value plots encompassing pH values from 2 to 12 (A) and the transition range (B).**
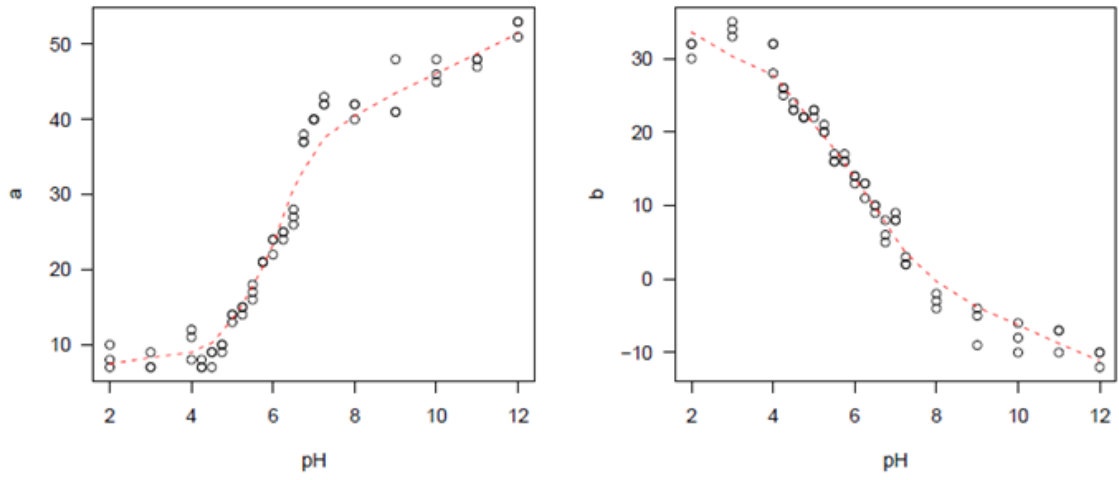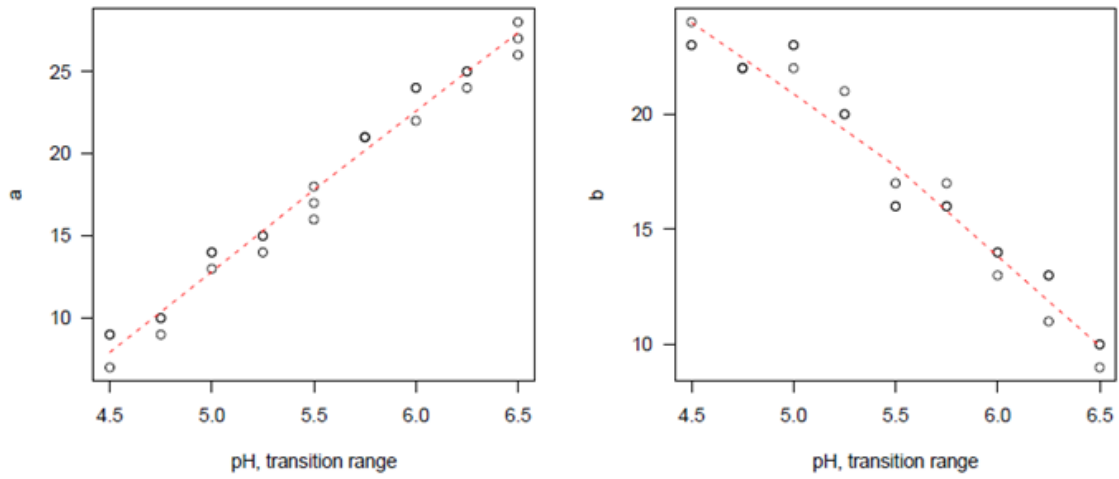
**Figure 21. Chlorophenol red colour value plots encompassing pH values from 2 to 12 (A) and the transition range (B).**
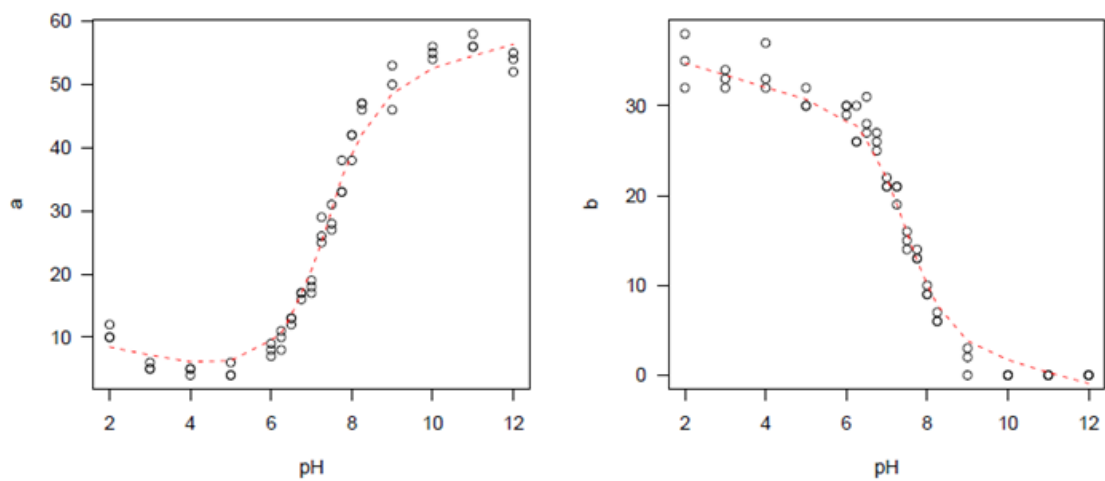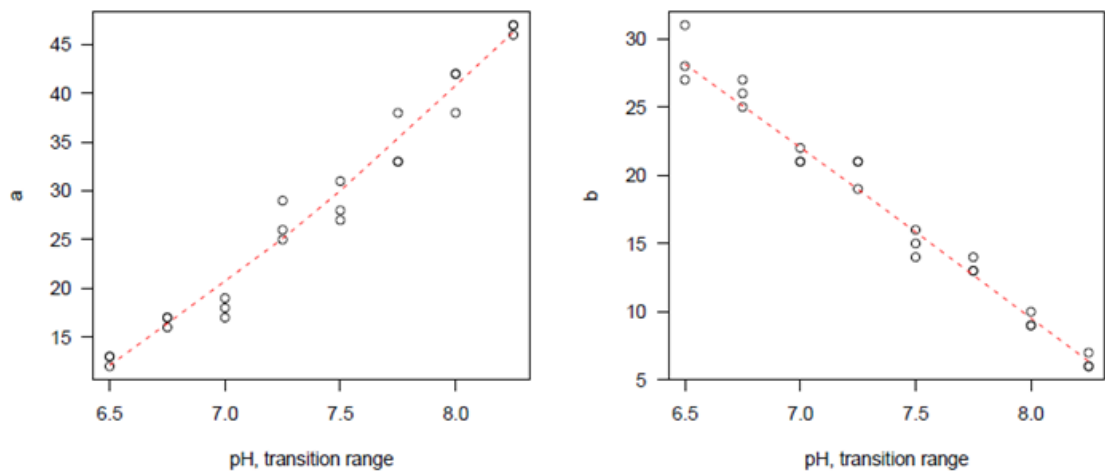
**Figure 22. Phenol red colour value plots encompassing pH values from 2 to 12 (A) and the transition range (B).**
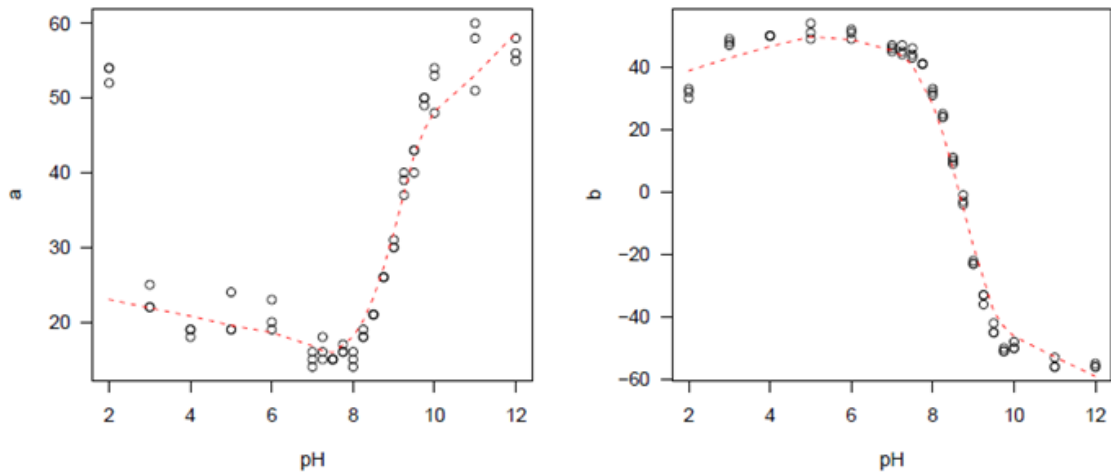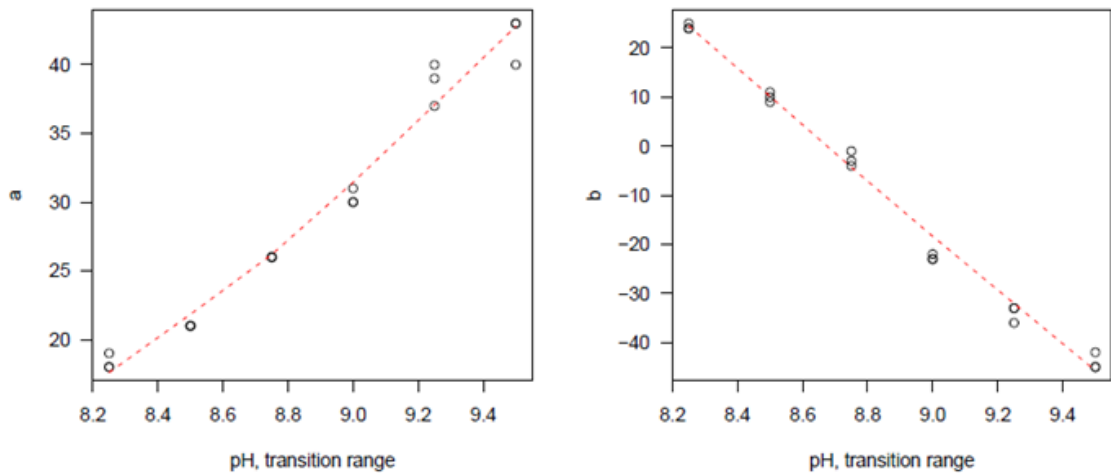
**Figure 23. Thymol blue colour value plots encompassing pH values from 2 to 12 (A) and the transition range (B).**

## 4.2 TSSM survival on artificial diet

Control and F3R3 populations initially began with 15±5 and 15 TSSMs (respectively) then decreased gradually throughout the entire experiment to 10±4 and 10±3 TSSMs (respectively). In contrast, VATP populations began with an initial population of 13±1, sharply declined after day 3 with none surviving on day 7. These trends (**Figure 24**) were consistent

those observed by Suzuki et al. (2017b) when F3R3 and VATP TSSMs were fed on bean leaf discs. Therefore, the artificial diet was proven as a viable alternative to bean leaves.
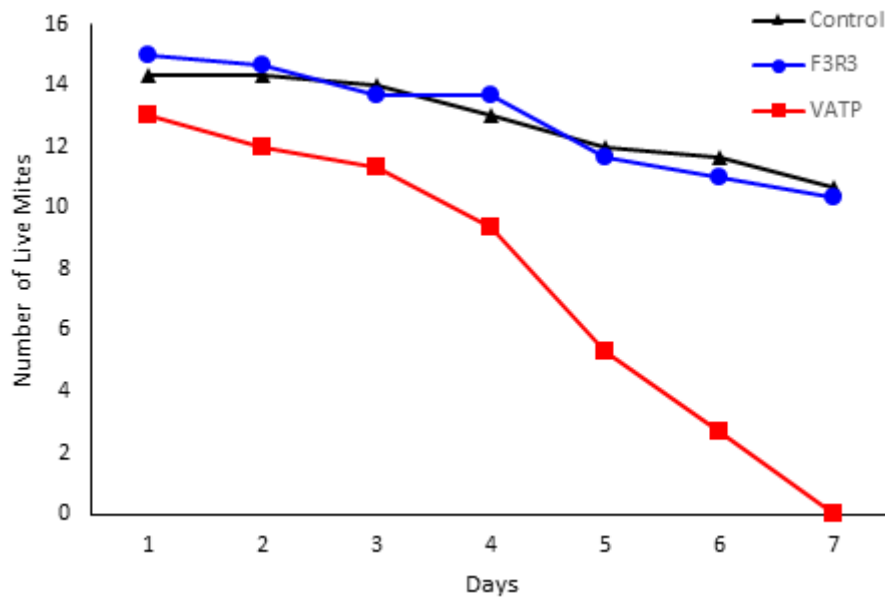


**Figure 24. Survival of control and knockdown TSSM populations on artificial diet micromesh sandwiches.**


## 4.3  Characterization of pH in TSSM digestive tract compartments following non-feeding regimen

### 4.3.1  Gut lumen pH in caeca, ventriculus and posterior midgut

Each indicator dye that stained the posterior midgut (**Figure 25**), caeca and ventriculus (**Figure 26**) produced only a single colour, establishing a lower pH limit of 6.5 using chlorophenol red (**Figure 27**) and an upper limit of 8.25 with thymol blue (**Figure 28**). The values of the midgut ventriculus (7.2), midgut caeca (7.2), and posterior midgut (7.3) were determined within the transition range of phenol red (**Figure 29**), and a one-way ANOVA of the data found no significant differences within or among gut compartments (**Table 5**). Sub-regional data from sampling sites were treated as technical replicates and averaged for subsequent analyses. Midgut caeca, ventriculus and posterior midgut are abbreviated as MC, MV and PM (respectively) for the rest of the thesis.

**Table 5. Results from one-way ANOVA when comparing sub-regional sampling sites within gut compartments of TSSMs.**

| Gut | | df | Sum² | Mean² | F-value | P-value |
|---|---|---|---|---|---|---|
| PM | Sampling sites | 2 | 0.18 | 0.09 | 1.2 | 0.3 |
| | Residuals | 193 | 14.34 | 0.07 | | |
| MC | Sampling sites | 2 | 0.017 | 0.01 | 0.07 | 0.94 |
| | Residuals | 194 | 25.59 | 0.13 | | |
| MV | Sampling sites | 2 | 0.05 | 0.03 | 0.2 | 0.82 |
| | Residuals | 199 | 27.24 | 0.14 | | |
| | | | | | | |
| MV, MC | Compartments | 2 | 0.04 | 0.02 | 0.17 | 0.85 |
| and PM | Residuals | 196 | 21.72 | 0.11 | | |
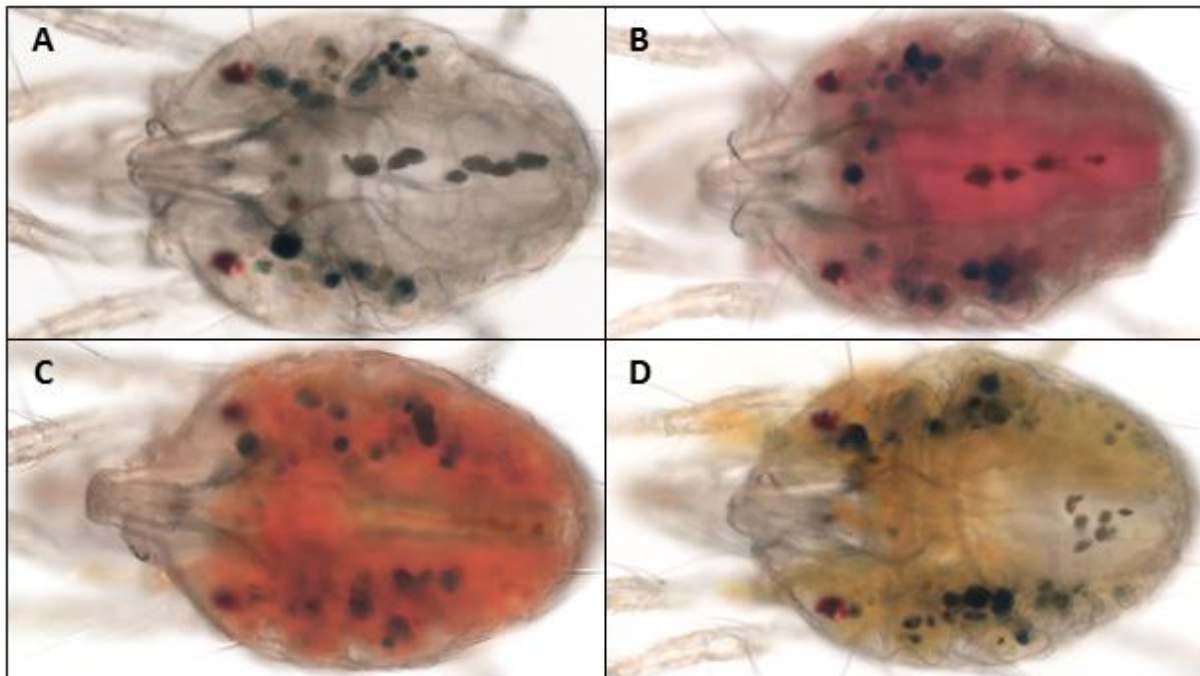


**Figure 25. Caeca and ventriculus in non-fed TSSMs stained with various indicator dyes.**
TSSMs without dye (A), with chlorophenol red (B), phenol red (C) or thymol blue (D).
Phenol red TSSM represents intermediate colour closest to the centre of the transition range.
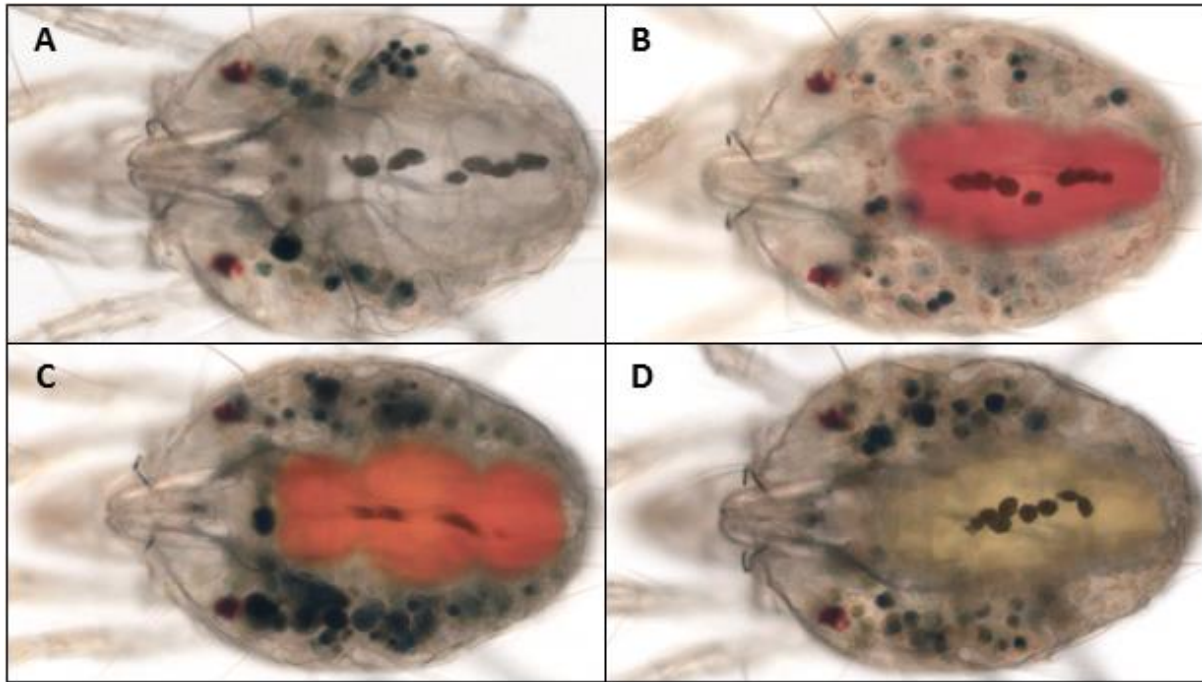
**Figure 26. Posterior midgut in non-fed TSSMs stained with various indicator dyes.**
TSSMs without dye (A), with chlorophenol red (B), phenol red (C) or thymol blue (D).
Phenol red TSSM represents intermediate colour closest to the centre of the transition range.
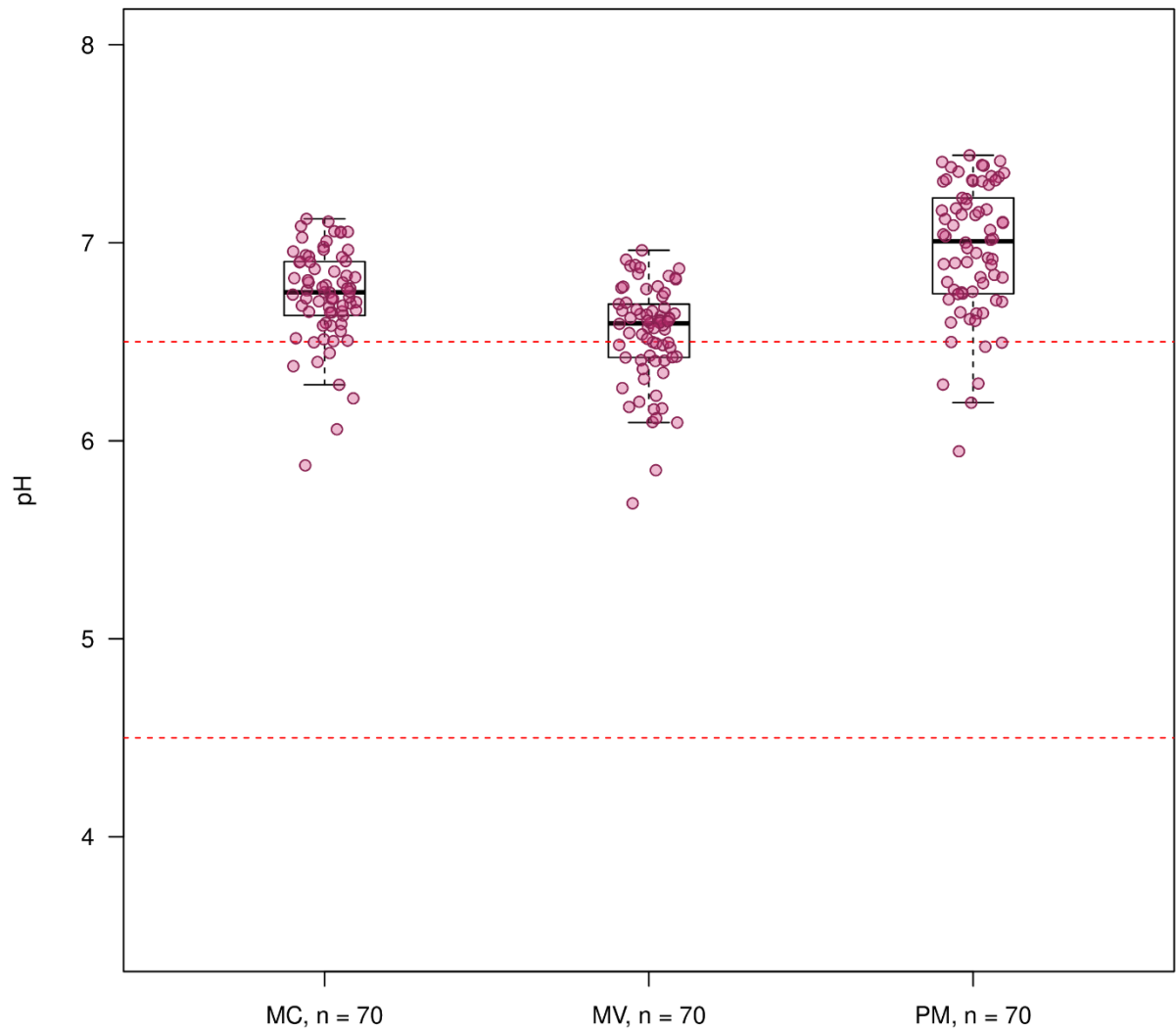
**Figure 27. pH values of lumen in non-fed TSSM gut compartments stained with chlorophenol red.**

Red dotted lines represent predicted transition range pH values of 4.5 and 6.5. Mean values were 6.7 for MC, 6.5 for MV and 7 for PM.
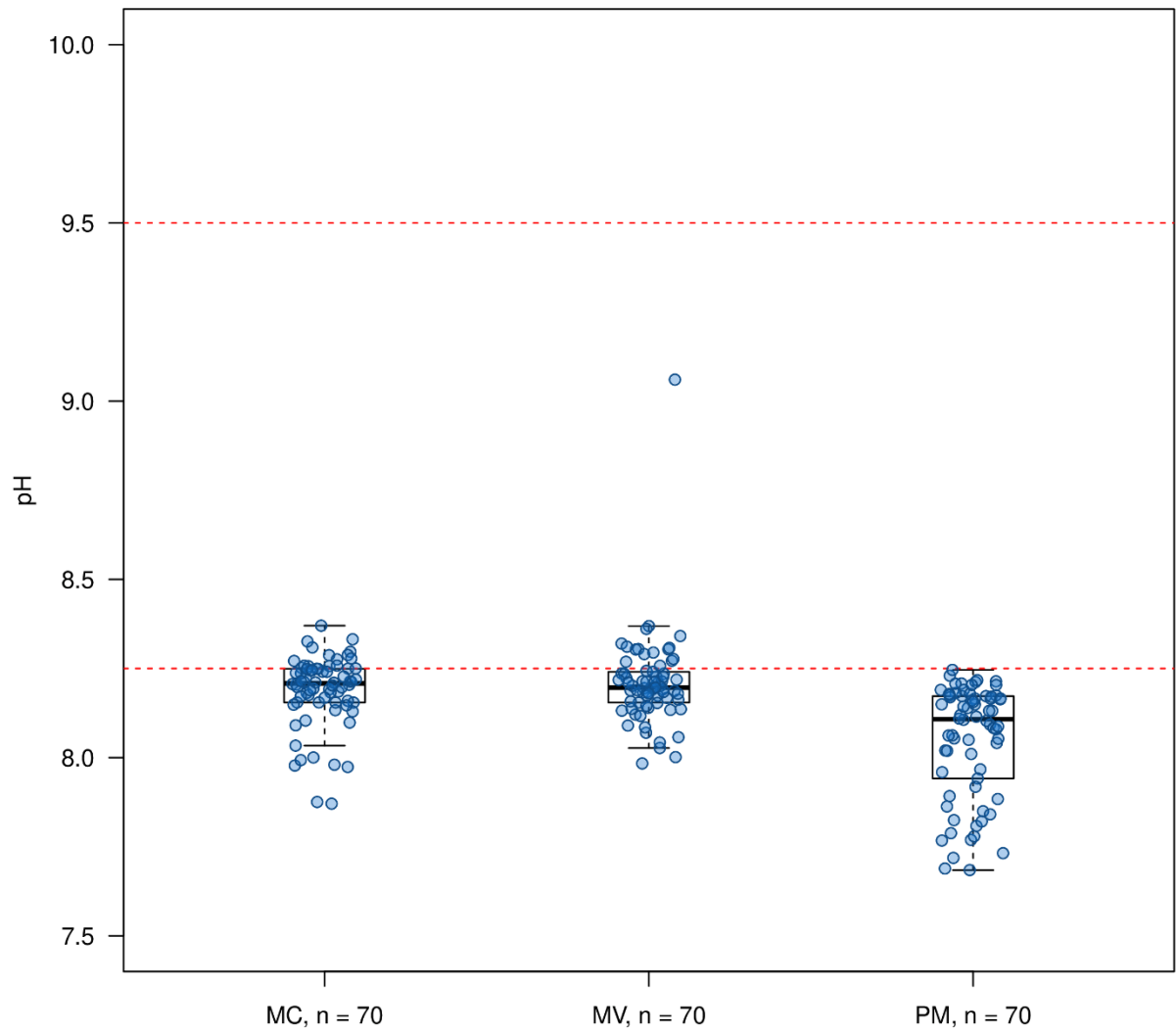
**Figure 28. pH values of lumen in non-fed TSSM gut compartments stained with thymol blue.**
Red dotted lines represent predicted transition range pH values of 8.25 and 9.5. Mean values were 8.2 for MC, 8.2 for MV and 8.1 for posterior midgut PM.
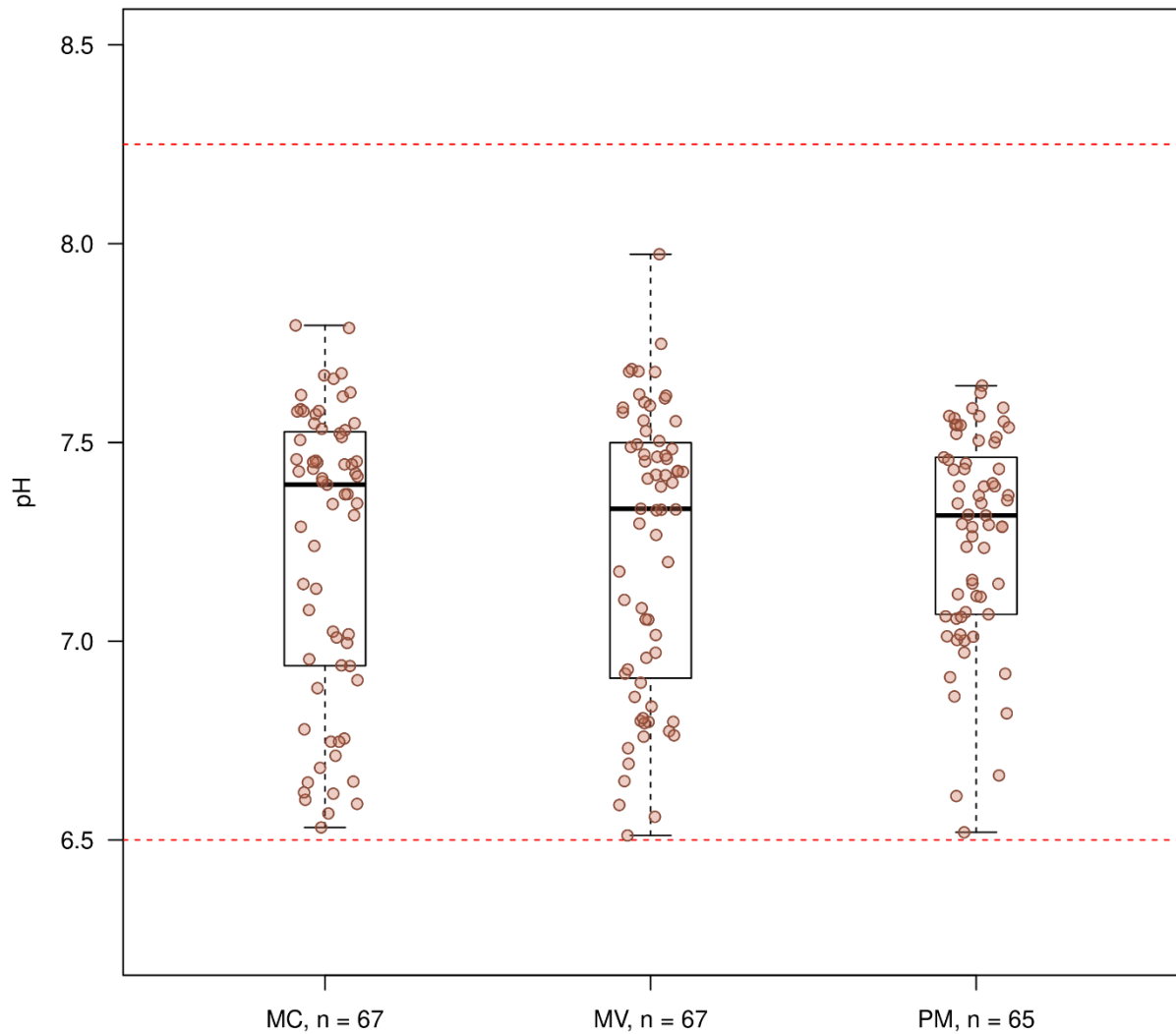
**Figure 29. pH values of lumen in non-fed TSSM gut compartments stained with phenol red.**
Red dotted lines represent predicted transition range pH values 6.25 and 8.25. Mean values were 7.2 for MC, 7.2 for MV and 7.3 for PM

### 4.3.2 Vesicle pH in early-stage digestive cells

Digestive cells at their earliest stage of development with vesicles (**Figure 30**) had a lower pH limit of 4.5 (**Figure 31**) and an upper limit of 6.25 (**Figure 32**), established using bromophenol blue and phenol red, respectively. I then determined vesicle pH within the transition range of chlorophenol red at 5.2 (**Figure 33**).
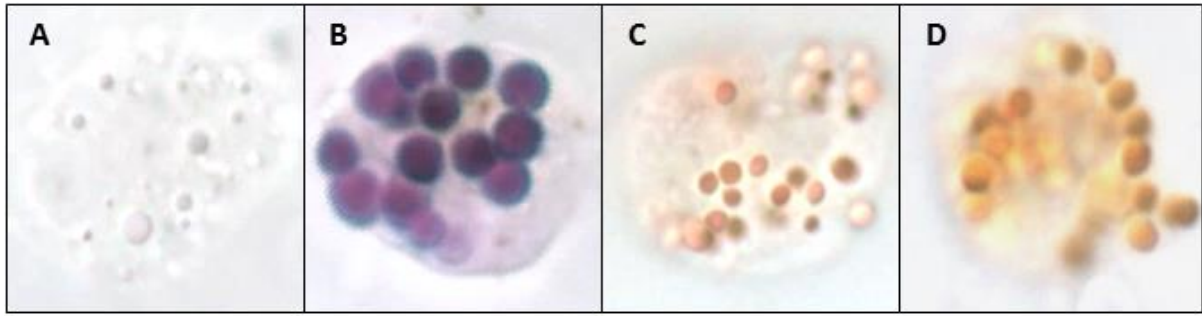
**Figure 30.  Early-stage digestive cells with stained vesicles from non-fed TSSMs.**
Vesicles without dye (A), with bromophenol blue (B), chlorophenol red (C) and phenol red (D). Chlorophenol red digestive cell represents intermediate colour closest to the centre of the transition range.



n = 262
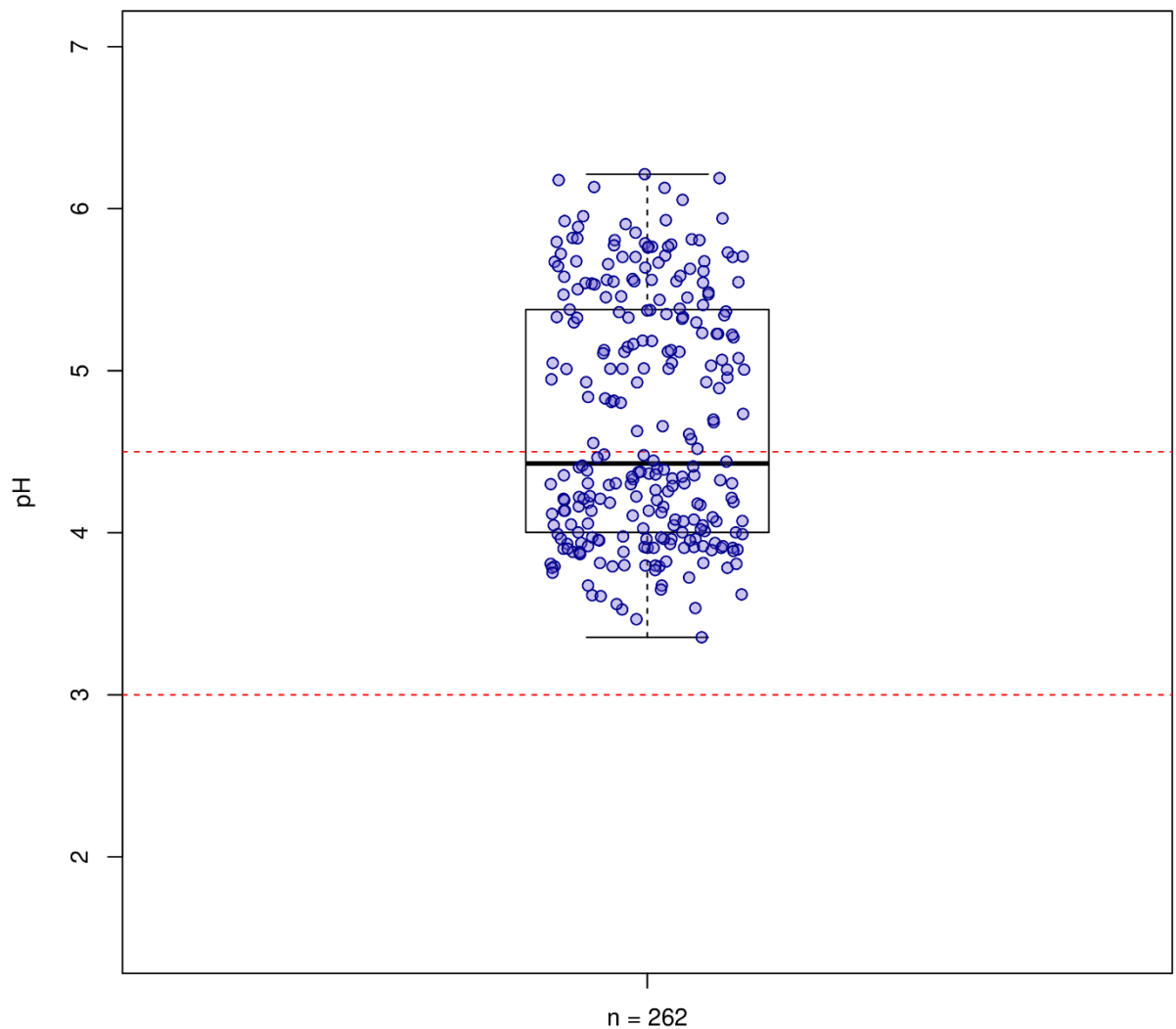
**Figure 31. pH values of lumen in early-stage digestive cell vesicles stained with bromophenol blue from non-fed TSSMs.**
Red dotted lines represent predicted transition range pH values 3.0 and 4.5. Mean value was 4.7.
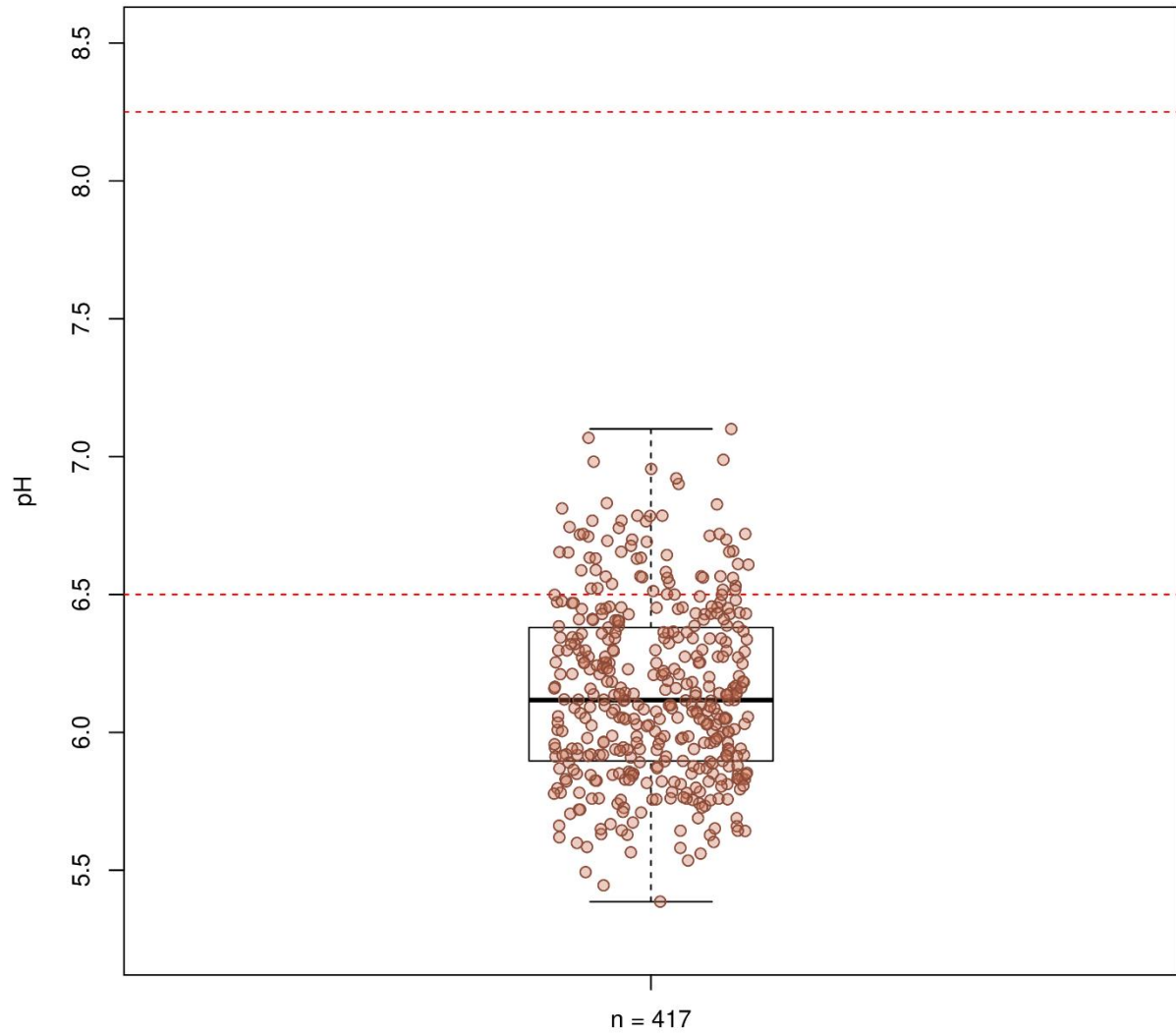
**Figure 32. pH values of lumen in early-stage digestive cell vesicles stained with phenol red from non-fed TSSMs.**
Red dotted lines represent predicted transition range pH values 6.5 and 8.25. Mean value was 6.2.
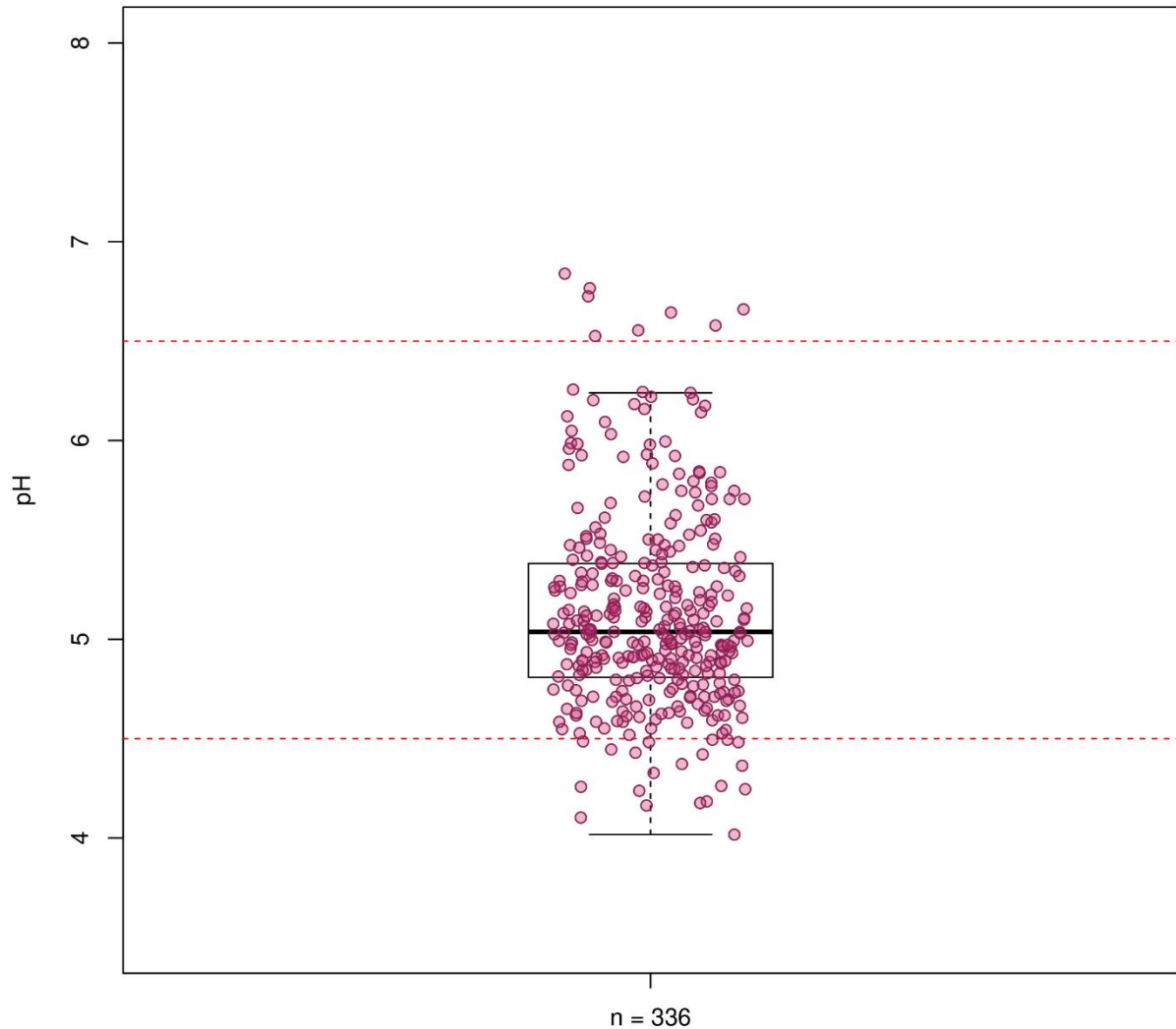
**Figure 33. pH values of lumen in early-stage digestive cell vesicles stained with chlorophenol red from non-fed TSSMs.**
Red dotted lines represent predicted transition range pH values 4.5 and 6.5. Mean value was 5.2.

## 4.4 Characterization of pH in TSSM digestive tract compartments following feeding regimens.

Fed TSSMs, stained with the same indicator dyes as non-fed individuals (**Figure 34**), had a lower pH limit of 6.5 (**Figure 35**) and an upper limit of 8.25 (**Figure 36**) using chlorophenol red and with thymol blue, respectively. The pH within the transition range of phenol red was MV (7.5), MC (7.5), PM (7.3) for those fed artificial diet and PM in those fed leaves (7.4) (**Figure 37**). Several one-way ANOVA tests were conducted and revealed significant differences when comparing artificial diet gut compartments (**Table 6**) and when

48

comparing diet and gut compartments (**Table 7**). However, there were no significant differences among gut compartment sampling sites regardless of diet (**Table 8**). Tukey's HSD tests yielded significant results when comparing non-feeding regimen data with the diets but not when comparing leaf and artificial diet (**Table 9**Error! Reference source not found.). There were also significant differences between MC/MV and PM, but not between MC and MV (**Table 10**)

**Table 6. Results from one-way ANOVA for gut compartments in TSSMs fed with artificial diet.**

|  | df | Sum$^2$ | Mean$^2$ | F-value | P-value |
|---|---|---|---|---|---|
| Region | 2 | 1.26 | 0.63 | 12.27 | 8.34e-6 |
| Residuals | 247 | 12.69 | 0.05 |  |  |

**Table 7. Results from one-way ANOVA for diet and post-feeding TSSM gut compartments.**
P-value significance thresholds: ** = 0.01, *** = 0.001.

|  | df | Sum$^2$ | Mean$^2$ | F-value | P-value |
|---|---|---|---|---|---|
| Diet | 2 | 3.74 | 1.87 | 24.62 | 6.07e-11 *** |
| Compartment | 2 | 0.52 | 0.26 | 3.41 | 0.03 ** |
| Diet-Compartment | 2 | 0.78 | 3.9 | 5.14 | 0.01 ** |
| Residuals | 523 | 39.69 | 0.08 |  |  |

**Table 8. Results from one-way ANOVA for post-feeding TSSM gut compartment sampling sites (Subregions).**

| Diet | Gut |  | df | Sum$^2$ | Mean$^2$ | F-value | P-value |
|---|---|---|---|---|---|---|---|
| Leaf diet | PM | Subregions | 2 | 0.44 | 0.22 | 3.02 | 0.05 |
|  |  | Residuals | 240 |  |  |  |  |
| Artificial diet | PM | Subregions | 2 | 0.03 | 0.02 | 0.18 | 0.84 |
|  |  | Residuals | 267 | 22.89 | 0.09 |  |  |
| Artificial diet | MC | Subregions | 2 | 0.03 | 0.01 | 0.32 | 0.72 |
|  |  | Residuals | 236 | 10.83 | 0.05 |  |  |
| Artificial diet | MV | Subregions | 2 | 0.11 | 0.06 | 1.32 | 0.27 |
|  |  | Residuals | 237 | 10.02 | 0.04 |  |  |

**Table 9. Results from Tukey's HSD test for comparing starvation and feeding regimens (A) as well as comparing post-feeding TSSM gut compartments (B).**
P-value significance thresholds: ** = 0.01, *** = 0.001.

|   | Comparison | Difference | Lower CI | Upper CI | P-value |
|---|---|---|---|---|---|
| **A** | None-Leaf | -0.11 | -0.19 | 0.004 | 0.01 ** |
|   | None-Artificial | -0.18 | -0.25 | -0.12 | 0.00 *** |
|   | Leaf-Artificial | -0.08 | -0.16 | -0.01 | 0.07 |
|   |   |   |   |   |   |
| **B** | MV-MC | -0.02 | -0.09 | 0.06 | 0.85 |
|   | MV-PM | -0.05 | -0.11 | 0.02 | 0.26 |
|   | MC-PM | -0.06 | -0.13 | 0.01 | 0.08 |

**Table 10. Results from Tukey's HSD test for comparing gut compartments in TSSMs fed with artificial diet.**

| Comparison | Difference | Lower CI | Upper CI | P-value |
|---|---|---|---|---|
| MC-MV | -0.03 | -0.12 | 0.05 | 0.61 |
| MC-PM | -0.16 | -0.24 | -0.08 | 1.55E-05 |
| MV-PM | -0.13 | -0.24 | -0.05 | 8.46E-04 |

There was a significant difference in the pH of non-fed and fed mites, indicating acidic conditions in the PM of post-fed TSSMs (**Table 9**), but not between those fed with leaf or artificial diets. Sampling sites within a given compartment did not differ significantly in any of the treatments (

**Table** 11), indicating pH was always uniform within compartments, thus they were treated as technical replicates and averaged for subsequent analyses. Stained gut compartments from non-feeding regimen, leaf diet and artificial diet were all compared using Tukey's HSD test (

**Table 11. Results from Tukey's HSD test for comparing sampling sites (Subregions) in post-feeding TSSMs.**

| Diet | Gut | Comparison | Difference | Lower CI | Upper CI | P-value |
|---|---|---|---|---|---|---|
| Leaf diet | PM | Site 1 – Site 2 | 0.09 | -0.01 | 0.19 | 0.1 |
| | | Site 1 – Site 3 | 0.09 | -0.01 | 0.19 | 0.07 |
| | | Site 2 – Site 3 | 0.01 | -0.09 | 0.1 | 0.99 |
| | | | | | | |
| Artificial diet | PM | Site 1 – Site 2 | -0.01 | -0.11 | 0.1 | 0.99 |
| | | Site 1 – Site 3 | 0.02 | -0.08 | 0.12 | 0.9 |
| | | Site 2 – Site 3 | 0.02 | -0.08 | 0.13 | 0.84 |
| | | | | | | |
| Artificial diet | MC | Site 1 – Site 2 | 0.02 | -0.06 | 0.1 | 0.8 |
| | | Site 1 – Site 3 | -3.81e-03 | -0.08 | 0.08 | 0.99 |
| | | Site 2 – Site 3 | -0.03 | -0.11 | 0.05 | 0.73 |
| | | | | | | |
| Artificial diet | MV | Site 1 – Site 2 | -0.05 | -0.13 | 0.03 | 0.26 |
| | | Site 1 – Site 3 | -0.01 | -0.09 | 0.06 | 0.91 |
| | | Site 2 – Site 3 | 0.04 | -0.04 | 0.11 | 0.48 |

**Table 12**). Every comparison between non-feeding TSSM gut compartments and MC/V in TSSMs fed with artificial diet yielded significant differences. MC with artificial diet was significantly different from both leaf and artificial diet PM. Stained digestive cell vesicles were not observed from either feeding regimen regardless of indicator dye used.

**Table 11. Results from Tukey's HSD test for comparing sampling sites (Subregions) in post-feeding TSSMs.**

| Diet | Gut | Comparison | Difference | Lower CI | Upper CI | P-value |
|---|---|---|---|---|---|---|
| Leaf diet | PM | Site 1 – Site 2 | 0.09 | -0.01 | 0.19 | 0.1 |
| | | Site 1 – Site 3 | 0.09 | -0.01 | 0.19 | 0.07 |
| | | Site 2 – Site 3 | 0.01 | -0.09 | 0.1 | 0.99 |
| | | | | | | |
| Artificial diet | PM | Site 1 – Site 2 | -0.01 | -0.11 | 0.1 | 0.99 |
| | | Site 1 – Site 3 | 0.02 | -0.08 | 0.12 | 0.9 |
| | | Site 2 – Site 3 | 0.02 | -0.08 | 0.13 | 0.84 |
| | | | | | | |
| Artificial diet | MC | Site 1 – Site 2 | 0.02 | -0.06 | 0.1 | 0.8 |
| | | Site 1 – Site 3 | -3.81e-03 | -0.08 | 0.08 | 0.99 |
| | | Site 2 – Site 3 | -0.03 | -0.11 | 0.05 | 0.73 |
| | | | | | | |
| Artificial diet | MV | Site 1 – Site 2 | -0.05 | -0.13 | 0.03 | 0.26 |
| | | Site 1 – Site 3 | -0.01 | -0.09 | 0.06 | 0.91 |
| | | Site 2 – Site 3 | 0.04 | -0.04 | 0.11 | 0.48 |

**Table 12. Results from Tukey's HSD test for comparisons between gut compartments in TSSMs, from non-feeding and feeding regimens, stained with phenol red.**

Feeding regimens: N = none (non-feeding), L = leaf diet, A = artificial diet.
Gut compartments: MC = caeca, MV = ventriculus, PM = posterior midgut
P-value significance thresholds: * = 0.05, ** = 0.01, *** = 0.001.

| Comparison | Difference | Lower CI | Upper CI | P-value |
|---|---|---|---|---|
| AMC-AMV | -0.03 | -0.17 | 0.1 | 1.00 |
| AMC-APM | -0.16 | -0.29 | -0.03 | 0.004 ** |
| AMV-APM | -0.13 | -0.26 | 3.83E-03 | 0.06 |
| LPM-AMC | 0.14 | -0.28 | -0.01 | 0.02 * |
| LPM-AMV | -0.11 | -0.25 | 0.02 | 0.18 |
| LPM-APM | -0.01 | 0.12 | 0.15 | 1.00 |
| NMC-AMC | -0.26 | -0.41 | -0.12 | 4.00e-07 *** |
| NMC-AMV | 0.23 | 0.09 | 0.37 | 2.28e-05 *** |
| NMC-APM | 0.1 | 0.04 | 0.24 | 0.35 |
| NMC-LPM | 0.12 | 0.03 | 0.26 | 0.21 |
| NMV-AMC | -0.26 | -0.4 | -0.12 | 6.00e-07 *** |
| NMV-AMV | -0.23 | -0.37 | -0.08 | 3.22e-05 *** |
| NMV-APM | 0.1 | 0.04 | 0.24 | 0.39 |
| NMV-LPM | 0.11 | 0.03 | 0.25 | 0.24 |
| NMV-NMC | 0.003 | 0.15 | 0.15 | 1.00 |
| NPM-AMC | -0.23 | -0.38 | -0.09 | 1.91e-05 *** |
| NPM-AMV | -0.2 | -0.34 | -0.06 | 6.01e-04 *** |
| NPM-APM | -0.07 | -0.21 | 0.07 | 0.81 |
| NPM-LPM | 0.09 | -0.23 | 0.06 | 0.64 |
| NPM-NMC | 0.03 | 0.12 | 0.18 | 1.00 |
| NPM-NMV | 0.03 | 0.12 | 0.18 | 1.00 |
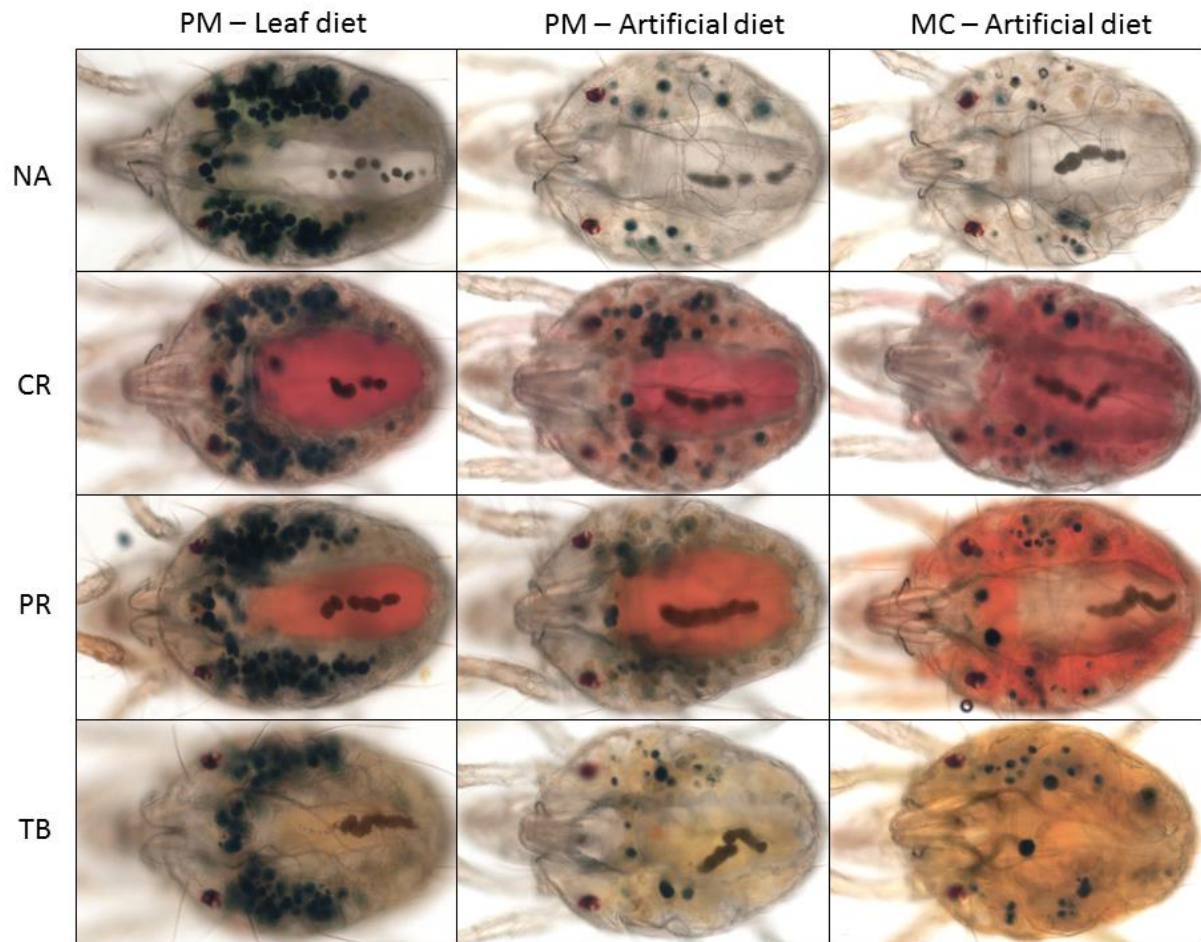
**Figure 34. Gut compartments in fed TSSMs stained with various dyes.**
PM = posterior midgut; MC = midguc caeca; NA = no dye; CR = chlorophenol red; PR = phenol red; TB = thymol blue; Phenol red TSSMs represent intermediate colour closest to centre of the transition range.
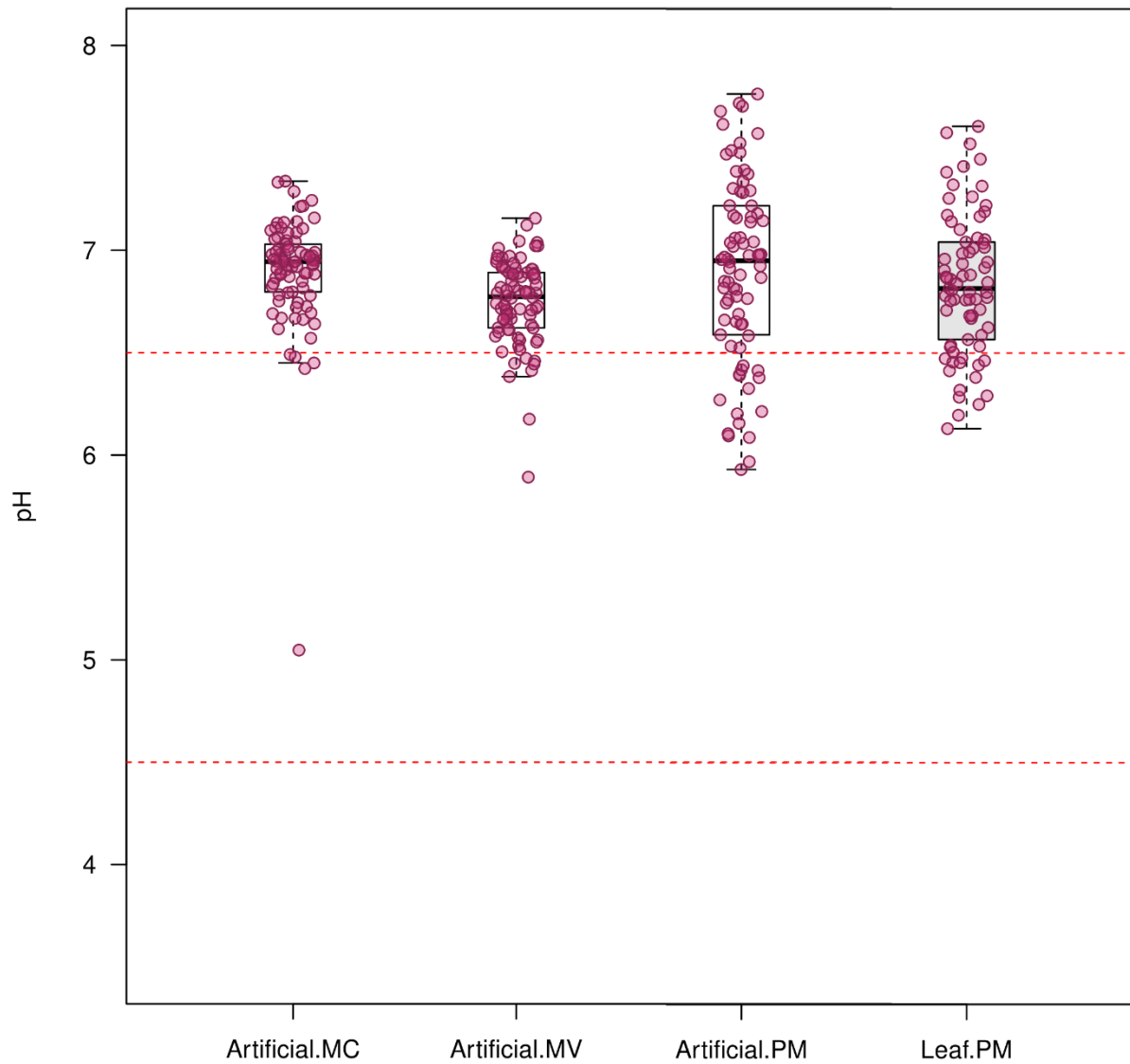
**Figure 35. pH values of lumen in post-feeding TSSM gut compartments stained with chlorophenol red.**

Red dotted lines represent predicted transition range pH values 4.5 and 6.5. Mean values for artificial diet gut compartments were 6.9 for caeca (MC), 6.8 for ventriculus (MV) and 6.9 for posterior midgut (PM). Leaf diet PM mean value was and 6.8.
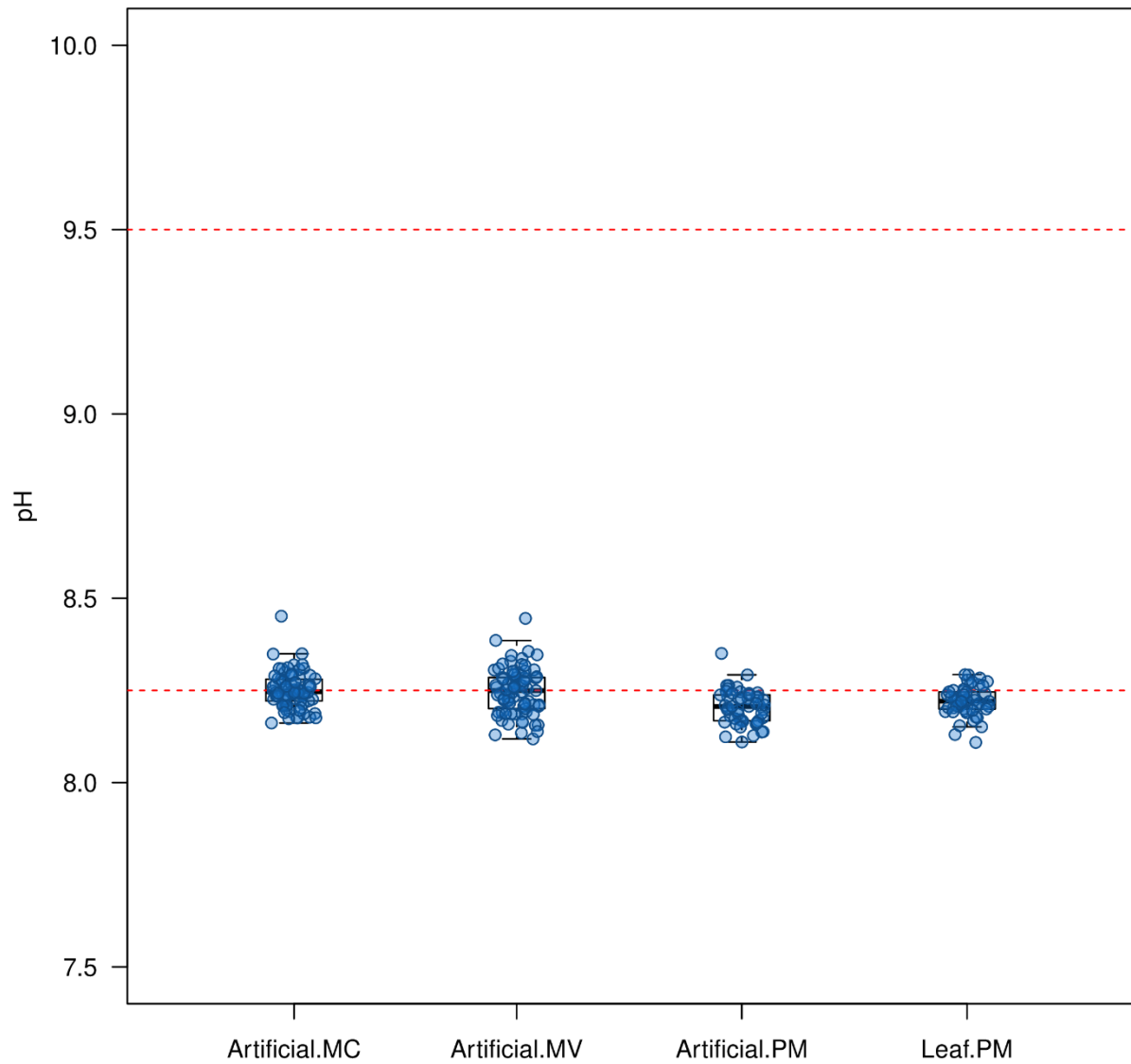
**Figure 36. pH values of lumen in post-feeding TSSM gut compartments stained with thymol blue.**
Red dotted lines represent predicted transition range pH values 8.25 and 9.5. Mean values for artificial diet gut compartments were 8.2 for caeca (MC), 8.3 for ventriculus (MV) and 8.2 for PM. Leaf diet posterior midgut (PM) mean value was 8.2.
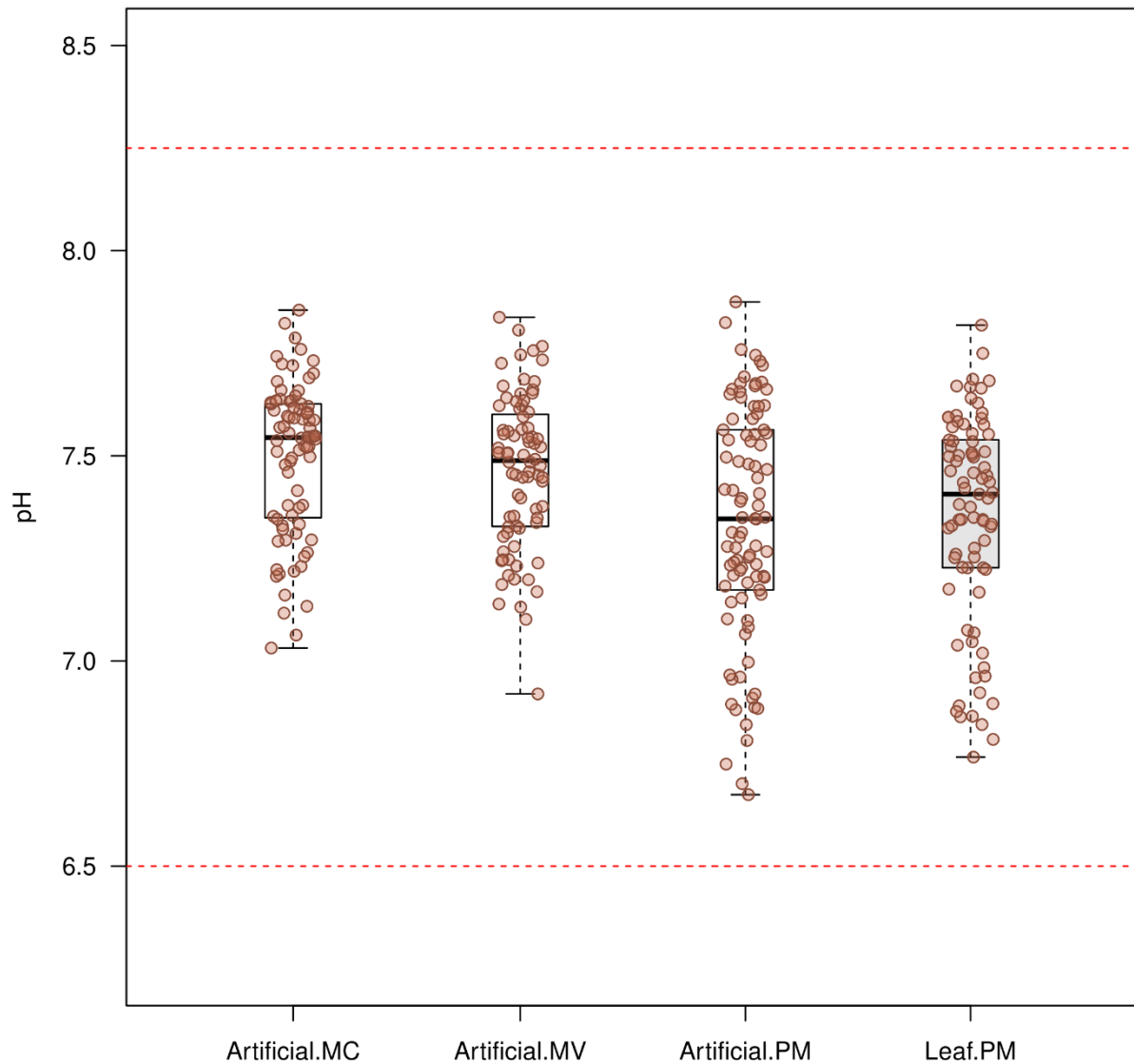
**Figure 37. pH values of lumen in post-feeding TSSM gut compartments stained with phenol red.**
Red dotted lines represent predicted transition range pH values 6.5 and 8.25. Mean values for artificial diet gut compartments were 7.5 for caeca (MC), 7.5 for ventriculus (MV) and 7.3 for posterior midgut (PM). Leaf diet PM mean value was 7.4.

## 4.5   Characterization of pH in control and knockdown TSSMs

### 4.5.1   pH in gut compartments after RNAi and feeding regimens

The MC was selected to represent pH for both caeca and ventriculus as there were no significant differences observed when comparing MC with MV; MC also comprises much of the overall midgut volume. I only used phenol red to determine mean pH in PM (**Figure 38**

and **Figure 39**) and MC (**Figure 40**) for post-feeding control and knockdown TSSMs. Tukey's

HSD test (

**Table 13**) and one-way ANOVA (

**Table 14**) indicated significant results for all comparisons except when comparing PM in leaf-fed control and VATP TSSMs. There were also significant differences identified for sampling sites in PM. Sampling site 1 (anterior end of PM) was significantly different from site 2 (centre of PM) and 3 (posterior end of PM) for leaf-fed TSSMs whereas site 3 was significantly different from sites 1 and 2 in TSSMs fed with artificial diet.

**Table 13. Results from Tukey's HSD test comparing MC and PM in TSSMs following RNAi and feeding regimen.**
n = 10 for each mite. CI = confidence intervals.
P-value significance thresholds: * = 0.05, ** = 0.01, *** = 0.001.

| Diet & gut | Comparison | Difference | Lower CI | Upper CI | P-value |
|---|---|---|---|---|---|
| Leaf diet | CONT-F3R3 | -0.18 | -0.32 | -0.05 | 0.01 * |
| PM | CONT-VATP | 0.08 | -0.06 | 0.21 | 0.36 |
| | F3R3-VATP | 0.26 | 0.13 | 0.39 | 1.73e-05 *** |
| Artificial diet | CONT-F3R3 | -0.16 | -0.28 | -0.04 | 0.005 ** |
| PM | CONT-VATP | 0.23 | 0.11 | 0.35 | 3.70e-05 *** |
| | F3R3-VATP | 0.39 | 0.27 | 0.51 | 0.00 *** |
| Artificial diet | CONT-F3R3 | 0.09 | 0.03 | 0.15 | 0.03 * |
| MC | CONT-VATP | 0.35 | 0.29 | 0.41 | 0.00 *** |
| | F3R3-VATP | 0.26 | 0.2 | 0.32 | 0.00 *** |
| Leaf diet | Site 1 – Site 2 | 0.39 | 0.23 | 0.54 | 1.00e-07 *** |
| PM | Site 1 – Site 3 | 0.4 | 0.25 | 0.54 | 0.00 *** |
| | Site 2 – Site 3 | 0.01 | -0.11 | 0.14 | 0.98 |
| Artificial diet | Site 1 – Site 2 | -0.08 | -0.21 | 0.06 | 0.36 |
| PM | Site 1 – Site 3 | 0.25 | 0.14 | 0.36 | 1.70e-06 *** |
| | Site 2 – Site 3 | 0.33 | 0.2 | 0.45 | 0.00 *** |
| Artificial diet | Site 1 – Site 2 | -0.02 | -0.1 | 0.05 | 0.73 |
| MC | Site 1 – Site 3 | -0.02 | -0.08 | 0.05 | 0.86 |
| | Site 2 – Site 3 | 0.01 | -0.05 | 0.07 | 0.94 |

**Table 14. Results from one-way ANOVA for MC and PM in TSSMs following RNAi and feeding regimen.**

| Diet & gut | | Df | Sum² | Mean² | F-value | P-value |
|---|---|---|---|---|---|---|
| Leaf diet | RNAi | 2 | 1.77 | 9,88 | 11.5 | 2.31e-05 |
| PM | Batch | 2 | 3.7 | 1.85 | 24.08 | 9.36e-10 |
| | Residuals | 145 | 0.08 | | | |
| | | | | | | |
| Artificial diet | RNAi | 2 | 4.66 | 2.33 | 28.71 | 1.36e-11 |
| PM | Batch | 2 | 3.99 | 1.99 | 24.54 | 3.47e-10 |
| | Residuals | 186 | 15.1 | 0.08 | | |
| | | | | | | |
| Artificial diet | RNAi | 2 | 3.7 | 1.85 | 95.46 | 2e-16 |
| MC | Batch | 2 | 0.01 | 0.01 | 0.29 | 0.75 |
| | Residuals | 158 | 3.06 | 0.02 | | |
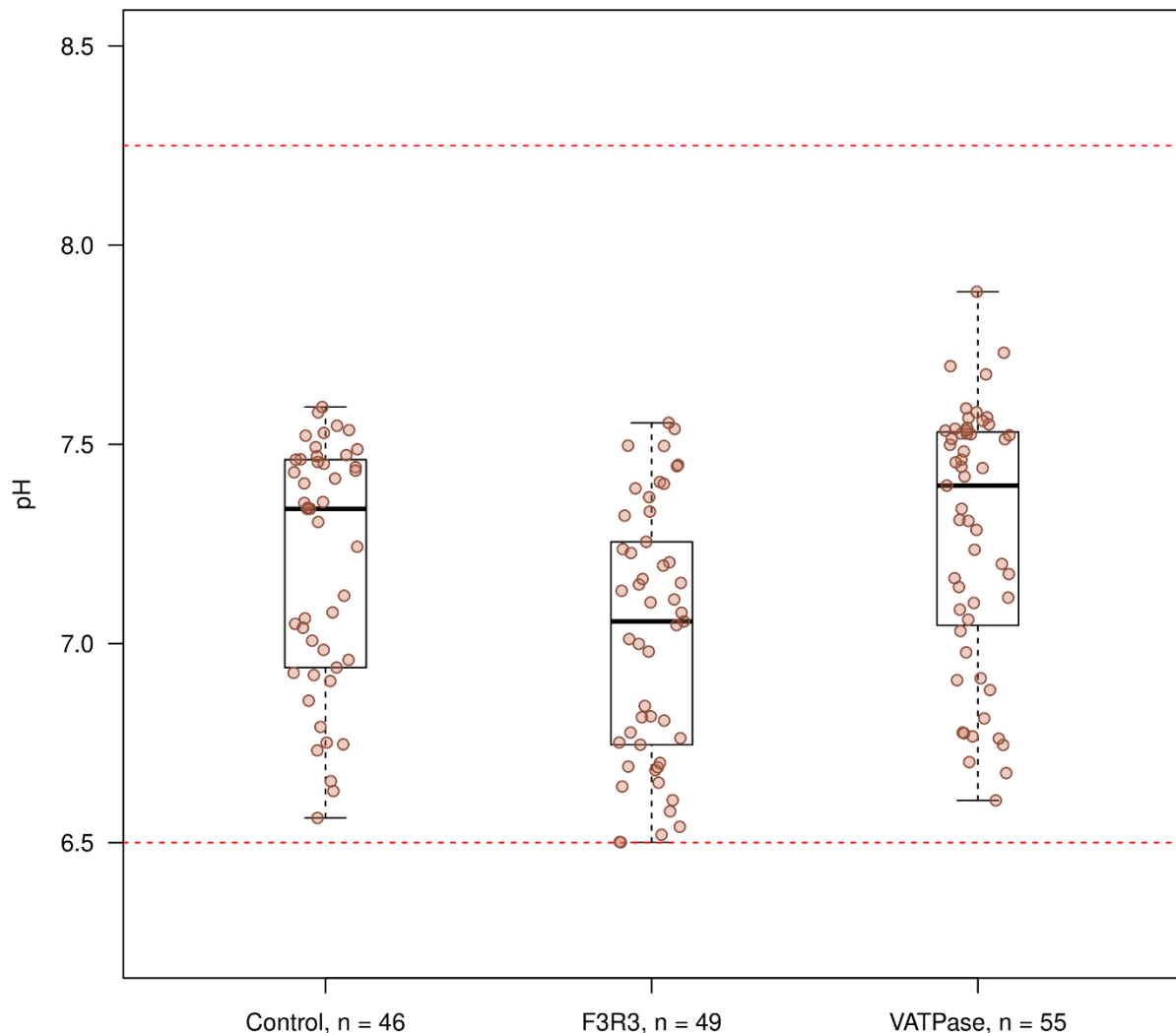


**Figure 38. pH values of the posterior midgut in RNAi TSSMs fed with artificial diet and stained with phenol red.**
Red dotted lines represent predicted transition range pH values 6.5 and 8.25. Mean values were 7.3 for Control, 7.1 for F3R3 and 7.4 for VATPase.
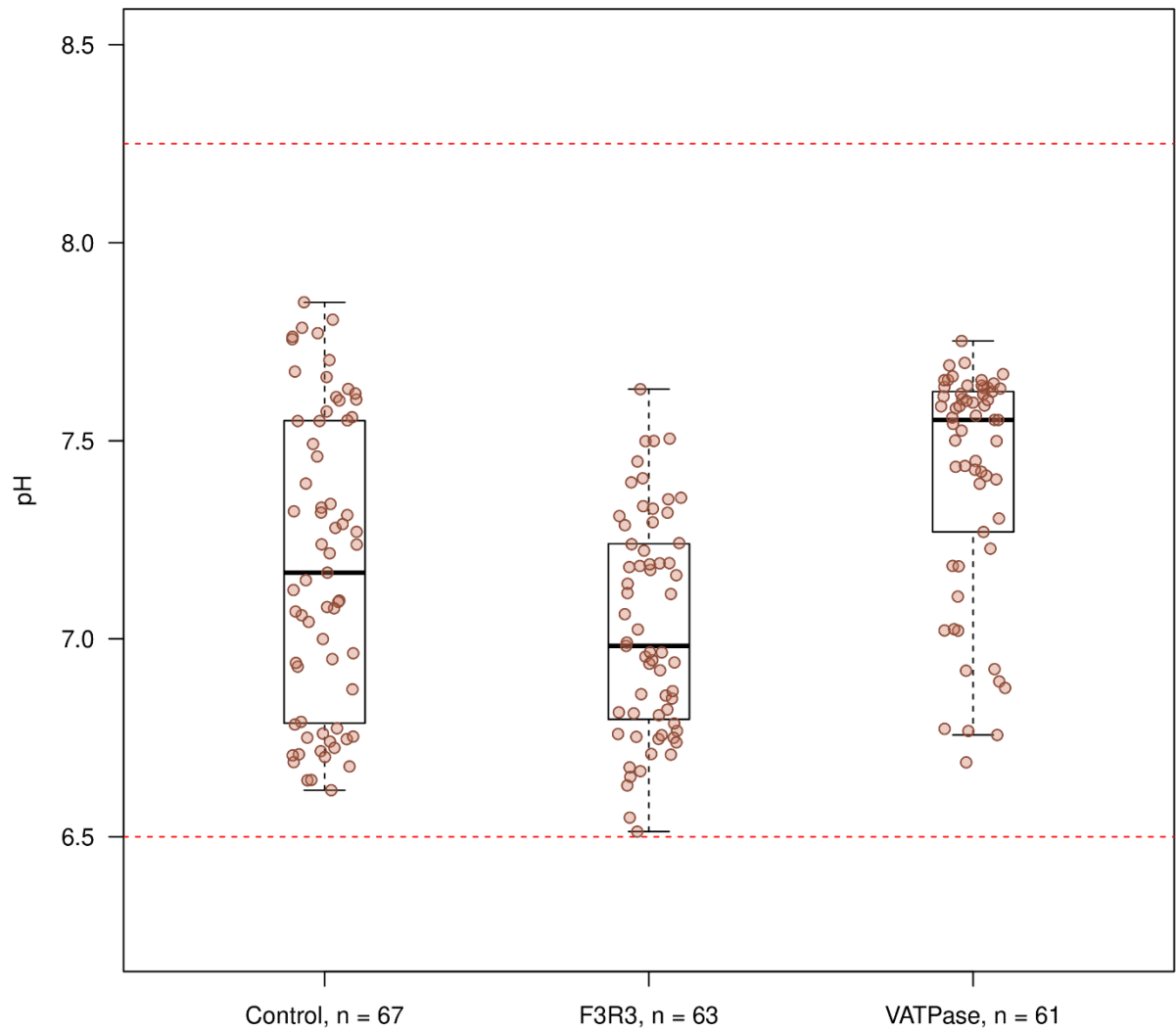
**Figure 39. pH values of the posterior midgut in RNAi TSSMs fed with leaf diet and stained with phenol red.**
Red dotted lines represent predicted transition range pH values 6.25 and 8.25. Mean values were 7.2 for Control, 7.0 for F3R3 and 7.4 for VATPase.
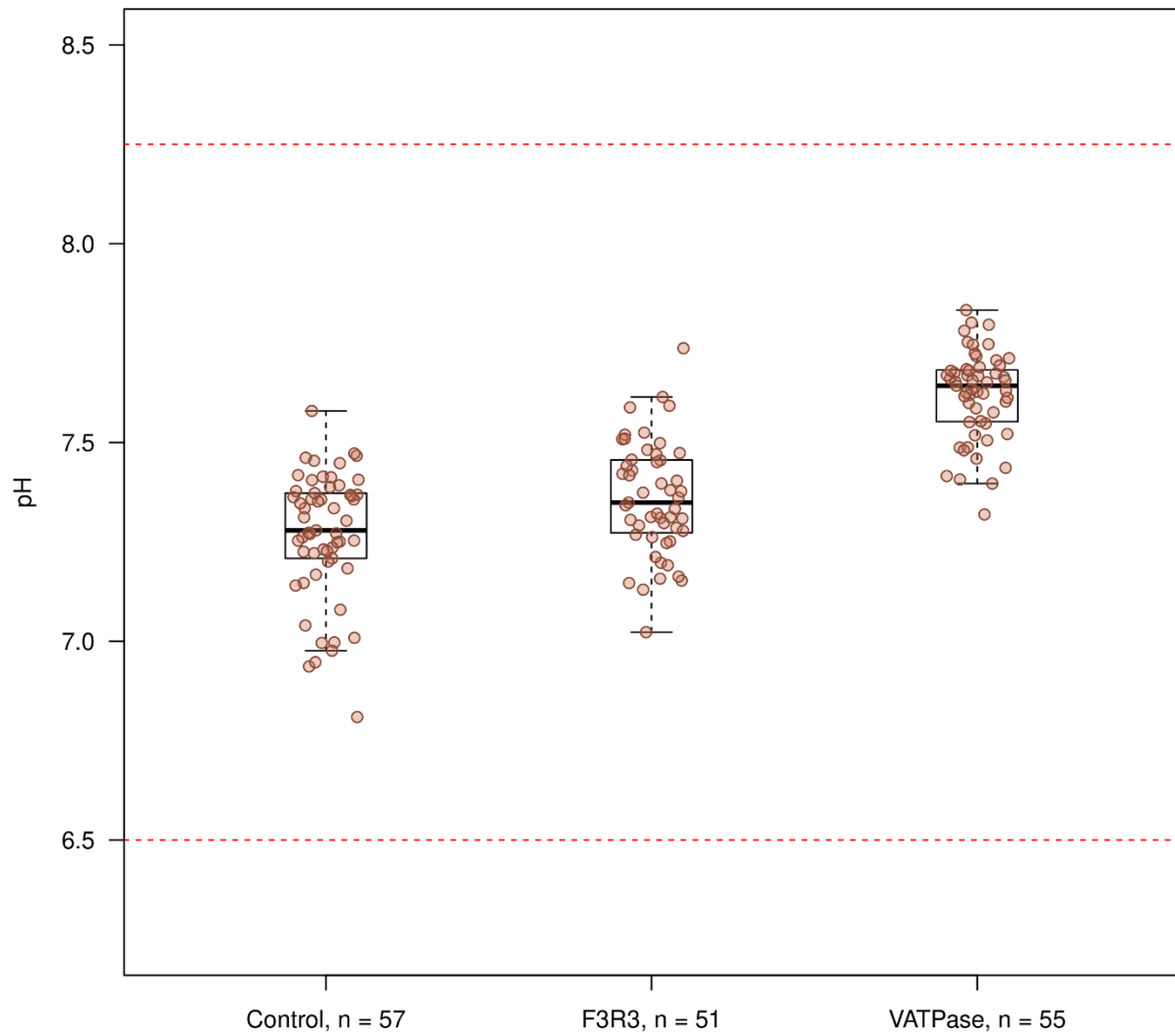
**Figure 40. pH values of the midgut caeca in RNAi TSSMs fed with artificial diet and stained with phenol red.**
Red dotted lines represent predicted transition range pH values 6.25 and 8.25. Mean values were 7.3 for Control, 7.4 for F3R3 and 7.6 for VATPase.

### 4.5.2 pH in early-stage digestive cell vesicles after RNAi and feeding regimen

Stained vesicles were rarely observed in early-stage digestive cells from control and knockdown TSSMs. Several digestive cells with stained vesicles were obtained from 1 trial of leaf-fed TSSMs (**Figure 41**). Vesicle pH was not expected to exceed the upper and lower pH limits previously established with bromophenol blue and phenol red (respectively) in digestive cell vesicles from non-fed TSSMs. I used chlorophenol red to determine the pH of vesicles from control and knockdown TSSM digestive cells (**Figure 42**). Vesicles from control TSSMs were found to be significantly different compared to vesicles from knockdown TSSMs. However, no significant difference was found between F3R3 and VATP vesicles (**Table 15**).

**Table 15. Results from Tukey's HSD test for comparison early-stage digestive cells from control and knockdown TSSMs stained with chlorophenol red.**

| Comp | Difference | Lower CI | Upper CI | P-value |
|------|-----------|----------|----------|---------|
| CONT-F3R3 | -0.26 | -0.35 | -0.17 | 0.00 |
| CONT-VATP | -0.19 | -0.28 | -0.09 | 1.31E-5 |
| F3R3-VATP | 0.07 | -0.02 | 0.17 | 0.16 |
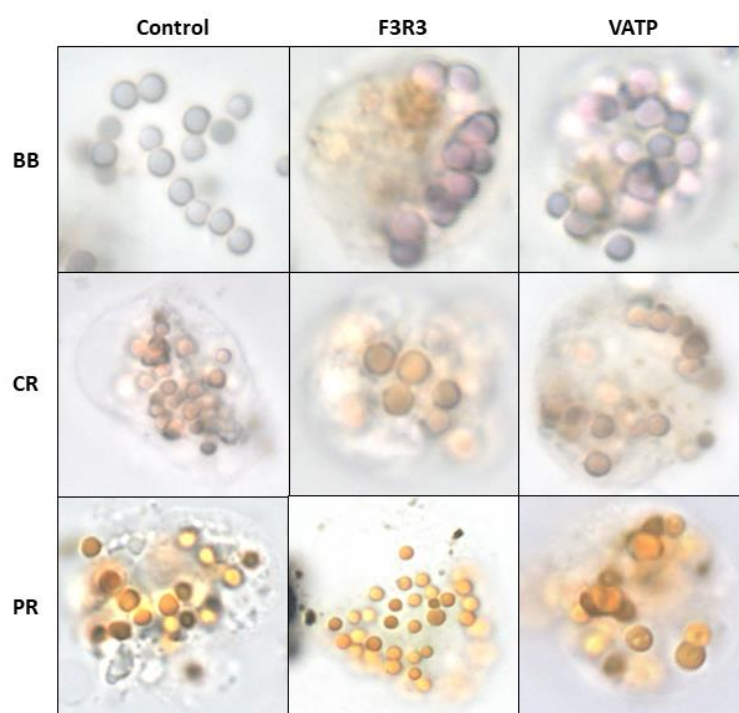


**Figure 41. Stained vesicles in early-stage digestive cells from leaf-fed RNAi TSSMs.**
Vesicles were stained with bromophenol blue (BB), chlorophenol red (CR) and phenol red (PR). Chlorophenol red cells represent intermediate colour closest to centre of the transition range.
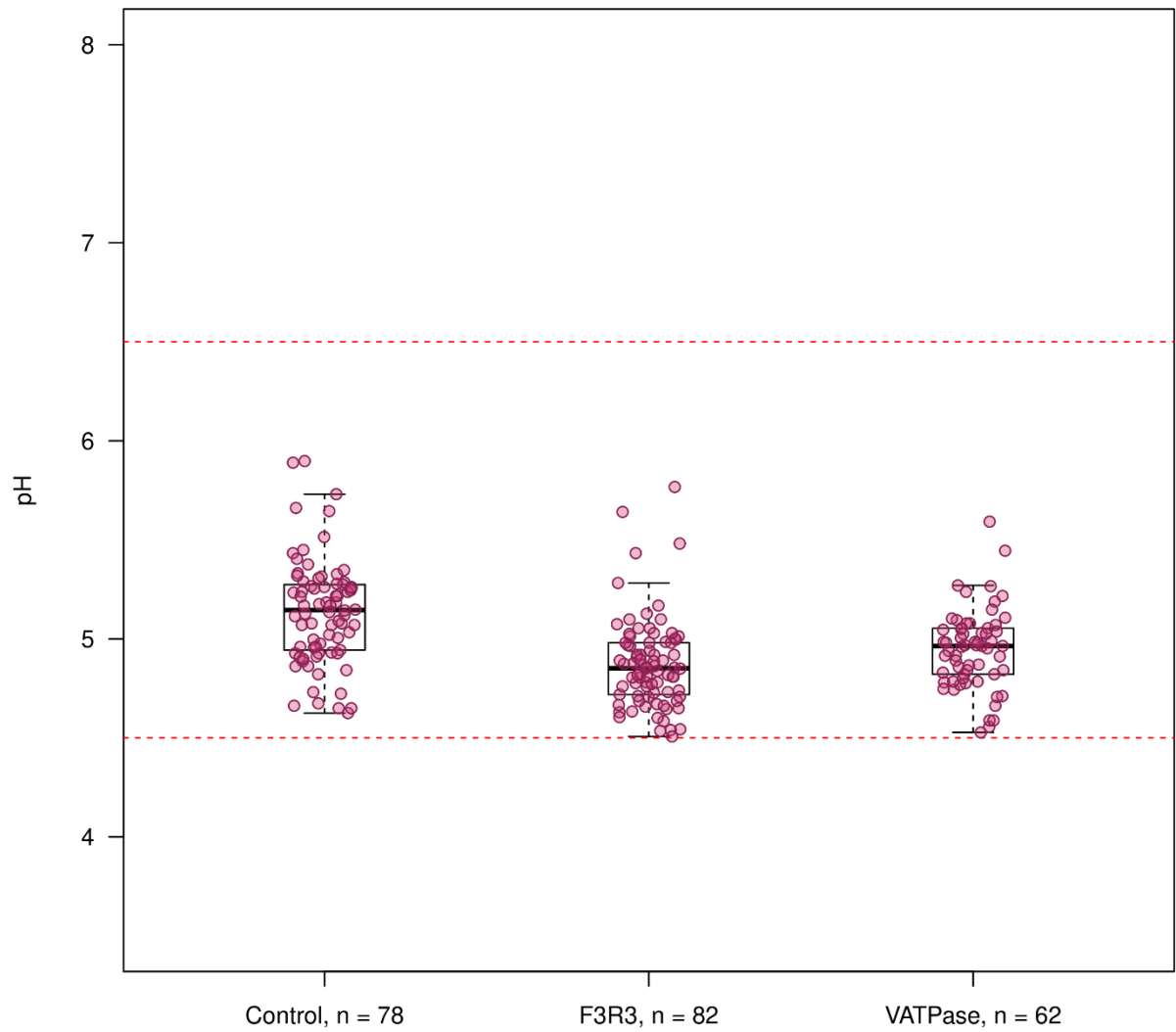
**Figure 42. pH values of lumen in early-stage digestive cell vesicles stained with chlorophenol red from leaf-fed RNAi TSSMs.**
Red dotted lines represent predicted transition range pH values 4.5 and 6.5. Mean values were 5.1 for control, 4.9 for F3R3 and 4.9 for VATP.

# 5 Discussion

## 5.1 pH gradients in the TSSM digestive tract

There were no pH gradients observed within or among TSSM gut compartments from non-feeding or feeding experiments. There were, however, significant differences in sampling sites following RNAi, specifically in leaf-fed TSSMs between sampling sites 1 and 2 compared with site 3 in the PM. These significant differences may have resulted from irregular staining in TSSMs. The colours in the gut may have been too faint in some areas or there may have been too many terminal-stage digestive cells masking the surrounding dye. The colour of the dyes appeared stable regardless of saturation or interference by non-dye objects. Acaridid dust mites, by contrast, produced a variety of colours in different gut compartments when stained with indicator dyes. The universal indicator dye ingested by *Tyrophagus putrescentiae* (**Figure 6B**) produced colours that revealed pH gradients among the digestive tract compartments (Erban and Hubert 2010).

The TSSM gut differs from dust mites as TSSMs are adapted to feed on a large amount of liquified plant cell contents to fuel the rapid production of silk and ovaries/eggs (Bensoussan et al. 2018). Other obligately phytophagous Actinedida mites, including Tetranychoidea and Eriophyoidea superfamilies, share similar physiologies adapted to consuming large amounts of liquids (Krantz and Lindquest 1979). Dust mites chew and ingest individual food boli that do not inflate the gut to the degree of inflation experienced by TSSMs, as TSSM gut compartments occupy nearly half of the body's internal volume upon feeding. $H^+$ ions can easily diffuse freely throughout the liquid lumen in a large, globular gut compartment without physical barriers. Peristalsis occurs in these gut compartments as a result of the activity of dorsal muscle bundles (Bensoussan et al. 2018), creating an active

environment that further mixes gut contents and homogenizes pH. Finer pH gradients may exist in microcrevices (ex: between budding digestive cells and posterior midgut epithelial microvilli) where the movement of lumen is more restricted, though discerning such gradients was beyond the capability of the techniques used for my thesis.

A large, unstable volume would explain why there was only ever a single colour when the indicator dyes stained the lumen of the gut compartments. Corena et al. (2005) observed a similar pattern of uniform colouring indicating a pH of 8.0-9.5 in the midgut of female mosquitoes, which inflate substantially when feeding (Klowden 1995).  A longer, narrower gut would be better equipped for regional-specific pH gradients as intraluminal mixing could be much more restricted. A variety of pH environments could represent different digestion and/or detoxification processes within the gut. Intraluminal pH gradients were characterized in insects including fruit flies (Overend et al. 2016; Shanbhag and Tripathi 2009), aphids (Cristofoletti et al. 2003), mosquitoes (Boudko et al. 2001; Linser et al. 2009) and caterpillars (Dow 1992; Skibbe et al. 1996).  Previous studies have demonstrated that pH gradients may also favour beneficial symbionts and provide protection against ingested pathogens.

Bacterial symbionts such as *Flavobacterium* and *Wolbachia* are universal in TSSMs, though the composition of microbiota may depend on the host plant species (Zhu et al. 2020). The elimination of these bacterial symbionts with antibiotics in *Tetranychus truncatus* compromised bacterial diversity regardless of host plant specialization and severely reduced daily fecundity (Zhu et al. 2020). The pH environment in the gut compartments of *T. urticae* favours the presence of symbionts thriving in neutral to near-neutral alkaline lumen. This also equally disfavours microbes that prefer more extreme pH conditions. However, *T. urticae* lacks pH gradients with strongly acidic (Harrison 2001; Giannella et al. 1973; Overend et al.

2016) or alkaline  (Berebaum 1980; Dow 1992) regions that could offer protection against potential infections by pathogens that thrive in neutral and near-neutral conditions.

Overend et al. (2016) observed an increase in pH of acidic midgut lumen in *Drosophila* larvae following RNAi of V-ATPase gene expression, which resulted in disrupted beneficial gut microbiota and an increase in lethal *Pseudomonas* infections. Gut symbionts alongside pH gradients appear to act as safeguards against the successful establishment of infections in the digestive tract. TSSMs have a relatively impoverished gut microbiota possibly reflecting the aseptic nature of the ingested plant cell contents (Matos et al. 2017) and the lack of a selective advantage for pH gradients. Plant host species may also influence the gut pH (Appel and Maines 1995) which in turn can determine the composition of the TSSM's microbiota (Priya 2012; Zhu et al. 2018, 2020), susceptibility to pathogens and efficacy of digestive or detoxification enzymes. The lack of chemical and biological safeguards would allow pathogens to proliferate and overwhelm the TSSM, which was previously demonstrated with injections of *Escherichia coli* and *Bacillus megaterium* in healthy TSSMs (Matos et al. 2017).

The numerous digestive cells populating the gut compartments may also counter pathogenic agents as the vesicle pH is more acidic (~5.1) than the lumen (~7.3). However, it is unlikely digestive cells participate in containing pathogens as Matos et al. (2017) introduced several strains of bacteria into the TSSM gut, which severely impacted their survival. The activity of enzymes hydrolysing bacteria in the gut lumen of other mites was also previously examined (Erban and Hubert 2008) but not in TSSMs. The pH gradient between gut compartments and digestive cell vesicles may be more effective against defensive compounds, rather than potential pathogens, ingested alongside plant cell contents.

The characterization of pH in my study offers a starting point to determine where such detoxification of harmful compounds would occur in the TSSM digestive tract.

## 5.2 Influence of pH on enzymes associated with digestion and detoxification processes in TSSMs

The pH optima of digestive proteases derived from *T. urticae* bodily extracts and faeces provided a rough estimation for pH environments that may exist in the TSSM digestive tract (Carrillo et al. 2011; Nisbet and Billingsley 2000; Santamaría et al. 2015). The indicator dyes in my thesis revealed a pH range of 7.3-7.5 in fed TSSM gut compartments, which better accommodates the activity of near-neutral alkaline digestive proteases. Enzymes like leucine aminopeptidase with an optimal pH of 7.5 (Carrillo et al. 2011) would thus show higher activity in gut lumen. The acidic lumen of early-stage digestive cell vesicles (pH=5.2) would support the activity of digestive proteases such as legumain and cathepsin L with pH optima of 4.5 and 5.5, respectively (Carrillo et al. 2011; Santamaría et al. 2015). The digestion of haemoglobin in ticks was previously observed to be carried out by cysteine proteases in the vesicles of midgut epithelial cells (Grandjean and Aeschlimann 1973; Lara et al. 2005; Sojka et al. 2013). Possible intracellular digestion of plant cell contents may be carried out in a similar manner carried out by free-floating digestive cells. The data from my thesis support the presence of digestive proteases with acidic pH optima in digestive cell vesicles rather than in the more near-neutral alkaline lumen of gut compartments. The presence of nutritive substances and waste products in later-stage cells (Bensoussan et al. 2018; Mothes and Seitz 1981), as well as the higher activity of aspartyl- and cathepsin L-like proteases previously observed in faeces composed of mostly terminal stage digestive cells (Santamaría et al. 2015), also suggest digestive proteases are more likely to be active in digestive cells.

Enzymes that detoxify harmful substances also require a specific pH environment in the digestive tract to perform at their optimum. Memarizadeh et al. (2010) found that optimal activity of detoxifying esterases was 6.5 in TSSMs resistant and susceptible to abamectin suggesting the enzyme would show greater activity in gut compartments than in digestive cells. In a similar study, van Leeuwen and Tirry (2007) determined a pH optimum of 7.5 for general esterases hydrolyzing *p*-nitrophenyl acetate in bifenthrin-susceptible and resistant *T. urticae* populations. It is unlikely that pH alone is sufficient in countering the effects of acaricides, plant defensive compounds or other xenobiotic substances. Digestive tract pH works in tandem with transcriptional reprogramming to facilitate the activity of detoxification processes against unfamiliar and harmful compounds. The upregulation of gene expression for detoxifying enzymes occurs when TSSM populations encounter pesticides or adapt to new plant hosts (Dermauw et al. 2018; Grbić et al. 2011).

This transcriptional plasticity is critical for TSSMs developing quick resistance to novel xenobiotic compounds such as indole glucosinolates (IGs) synthesized and deployed by Brassicaceae plants, such as Arabidopsis, in response to herbivory. When bean-reared TSSMs were initially fed Arabidopsis plants, mortality was observed to increase (Zhurov et al. 2014). In similar studies, after several generations of TSSM populations being transferred between bean and Arabidopsis hosts, mortality levels were observed to decrease (Ratlamwala 2014; Salehipourshirazi 2018). Arabidopsis-adapted TSSMs upregulated the expression of genes associated with enzymes involved in the detoxification of IGS, including cytochrome P450 monooxygenases, carboxylesterases and glutathione-S-transferases (Salehipourshirazi 2018). The pH in the TSSM digestive tract would allow for the activity of such enzymes to counter IGs. Understanding digestive tract pH environments in TSSM populations when encountered with novel, harmful substances can contribute to understanding modifications in digestive

and/or detoxification processes that allow for their successful adaptation. Whether or not digestive tract pH in bean-adapted TSSMs differs from TSSMs adapted to other host plant species remains unknown.

## 5.3   Influence of diet on TSSM gut pH

Fed adult female TSSMs had a gut pH range of 7.3-7.5 whereas their non-fed counterparts had a range of 7.2-7.3. This suggests that gut pH becomes slightly alkaline when plant cell contents are ingested, which was also supported by significant differences observed when comparing data from the non-feeding regimen with both diets (**Table 14**). When comparing pH in gut compartments from the non-feeding and feeding regimens, significant differences were observed between MC with artificial diet and PM in TSSMs from either diet (**Table 14**). This may be because phenol red injected in MC showed more consistent colours rather than in PM when TSSMs fed on the dye for 24 h. However, there was no difference in pH (p=1.00) when comparing PM in leaf-fed TSSMs with PM in TSSMs fed with artificial diet. This strong similarity suggests that the artificial diet originally created for phloem-feeding aphids (Febvay et al. 1987) diluted 1,000x emulated the pH of ingested plant cell contents. It is unclear whether gut pH is affected by the pH of plant cells or if TSSMs modify the pH when they initially penetrate mesophyll cells with their stylet (Bensoussan et al. 2016) and inject an assortment of hydrolyzing enzymes (Jonckheer et al. 2016). The 0.75µm particle size limit of the stylet suggests plant cell contents are liquefied and pre-digested (Bensoussan et al. 2018) as larger contents like chloroplasts are much too big to enter (Barton 1966). Whether or not the pH in pre-digested plant cell contents has any impact on the gut pH in TSSMs, despite prior liquefication/digestion, has yet to be determined.

The extent of gut pH responses to plant hosts have been previously studied in phytophagous insects. Schultz and Lechowicz (1986) found differences in the gut pH of gypsy moth larvae at various instar stages (*Lymantria dispar*) reared on different hosts plants. A later study on the same species found no effects from host plants when examining post-feeding times in later-stage instars (Appel and Maines 1995), suggesting that younger instars are not as resistant to the influence of ingested plant material pH. The action of powerful cation pumps in the midgut epithelium allows Lepidopteran caterpillars to increase the alkalinity of the midgut to compensate for the presence of relatively acidic ingested plant material including their defensive compounds with lower optimal pH (i.e.: tannins) (Dow 1984). However, establishing and maintaining pH gradients is energy-intensive in Lepidopterans, as 10% of ATP was reported to be used for fuelling $K^+$ ion pumps in *Manduca sexta* (Dow and Peacock 1989). Whether or not the ingestion of liquified plant cell contents elicits a similar response in TSSMs by increasing ATP consumption by V-ATPase has yet to be determined.

The potential effects of plant materials on pH in the digestive tract would be better observed in TSSMs adapting to a novel host as resistance to plant defenses is initially poor but improves over time (Rioja et al. 2017). TSSMs adapted to specific plant hosts would have a narrower tolerance that one might expect given that *T. urticae* has been recorded to exploit over 1,100 host plant species. Gene expansions and transcriptional reprogramming have been proposed as the source for rapid TSSM adaptations to new plant hosts, specifically against defensive compounds (Grbić et al. 2011; Wybouw et al. 2015). The impact of novel xenobiotic compounds on non-resistant TSSMs adapting to a new plant host species has been extensively studied (Agrawal et al. 2002; Fry 1989; Rioja et al. 2017; Wybouw et al. 2015).

However, the impact of unfamiliar plant cell contents on digestive tract pH and how it might affect the overall survival of non-resistant TSSMs is not yet understood.

## 5.4   Stained vesicles in early-stage digestive cells

Vesicles in later-stage digestive cells were regularly stained with the same colours observed in early-stage cells suggesting the pH is consistent throughout the cell's development. Early-stage digestive cell vesicles in non-fed TSSMs were frequently stained while those from fed individuals were not, even when dyes were visible in the midgut. This suggests dyes that enter the vesicles may have been masked by the presence of additional absorbed substances or that digestive cells discriminated between plant cell content and indicator dyes. Either way, the role of digestive cell vesicles in absorbing and processing plant cell contents remains unclear. Understanding vesicle pH does, however, allow for estimating which enzymes may be more active in digestive cells if they have pH optima near 5.2. Early endosomes are responsible for organizing and transporting molecules to their respective destinations within the cell (Mellman 1996) but the mechanism of digestive cells discriminating between non-nutritive molecules and nutritive plant substances has yet to be observed.

Digestive cells in fed TSSMs appeared stained when observed in the midgut, though this was the effect of plant cell content or cytoplasm being stained rather than vesicles. The method of delivering dyes into fed TSSMs was considered as a factor in affecting the uptake of dyes by early-stage digestive cells. Sandwich micromeshes resulted in more frequent staining of vesicles than the Kimwipe soaking method and microinjections in non-fed TSSMs. However, the lack of stained vesicles despite the presence of dye in the gut lumen could not be explained by possible differences in delivery protocols. Neutral red was

observed to effectively stain digestive cells immediately upon microinjection and regularly

stained vesicles in early-stage cells, but the dye colours were not consistent with the trend

established by bromophenol blue, chlorophenol red and phenol red upon analysis with linear

regression models. Interestingly, dyes that were observed to rapidly penetrate surfaces upon

contact (ex: bromocresol green, phenol red and neutral red) were completely contained within

vesicles, rarely staining the entire digestive cell. This suggests the vesicles retain an effective

mechanism for preventing diffusion of the dyes through the membrane while at the same time

maintaining an acidic internal pH.


## 5.5   Impact of silencing V-ATPase on digestive tract pH in TSSMs

V-ATPase is a membrane-bound protein complex responsible for establishing and

maintaining a pH gradient across organelle membranes and silencing the expression of

*tetur09g004140* was predicted to disrupt that mechanism. The results of my thesis suggest

TSSMs did not effectively demonstrate an RNAi response. The PM in control and F3R3

TSSMs had mean pH ranges of 7.2 (leaf) to 7.3 (artificial) and 7.0 (leaf) to 7.1 (artificial),

respectively. These pH values conflict with the PM pH of 7.4 (leaf) and 7.3 (artificial)

previously observed in fed non-RNAi TSSMs, which may have resulted from uneven staining

in the PM when feeding on phenol red for 24 h. The MC, by contrast, was more consistent in

staining as microinjections ensured a consistent volume of dye whereas the stained PM was

determined by the feeding activity of TSSMs. The MC in VATP TSSMs had the highest

mean pH observed at 7.6 whereas control and F3R3 remained closer to the 7.3-7.5 range with

7.3 and 7.4, respectively. This may indicate that RNAi of *tetur09g04140* expression perturbs

the regulation of pH in the lumen of MC and MV but this cannot be confirmed unless dsRNA

is confirmed to trigger an RNAi response. The ingestion of dsRNA solution was not

monitored as I did not want to risk the pristine pH with tracing agents during the *in vivo*

study. An observable coloured dye (e.g.: blue food colouring) was previously attempted to stain gut lumen but remained in gut compartments beyond 24 h post-feeding, which would interfere with the colours of pH indicator dyes. Fluorescent tracer dyes used by Suzuki et al. (2017a) and Bensoussan et al. (2018) to track the delivery of small molecules into TSSMs were considered but not used as they could have risked influencing the digestive tract pH.

I hypothesized that silencing V-ATPase would disrupt the regulation of pH. The expectation was that organelle and endosomes would demonstrate a comparatively higher effect than in gut lumen as V-ATPase is localized on organelle/endosome membranes. Digestive cell vesicle pH from control TSSMs remained virtually unchanged regardless of non-feeding (pH=5.2) or leaf-feeding (pH=5.1) regimens. However, F3R3 and VATP both had vesicle pH of 4.9, which suggests dsRNA itself had an acidifying effect or RNAi did induce a minor pH response. The influence of dsRNA on pH can be reduced if a shorter time for dsRNA uptake can still trigger an RNAi response. There was also a difference of 24 h between control and knockdown TSSMs which may have also affected vesicle pH. Without vesicle pH data from the non-RNAi feeding regimen, it remains unclear if the leaf diet also played a role in affecting vesicle pH alongside the additional 24 h of feeding on dsRNA solution and/or the dsRNA itself. It is important to note that there was only 1 trial of stained digestive cell vesicles obtained from leaf-fed TSSMs. The single trial was obtained from many dissected TSSMs, which proved impractical to continue for the subsequent feeding regimen experiments as stained vesicles in fed mites were rare.

The results from my thesis did not support my prediction but may hint at a possible effect that can be achieved if dsRNA solution successfully triggers an RNAi response. Suzuki et al. (2017b) observed an increase in mortality of dark body TSSM after *tetur09g04140*

expression was downregulated, which may be attributed to the lack of proper pH maintenance in the digestive tract. Enzymes involved in digestion and detoxification are presumed to reduce or halter performance in response to perturbed pH regulation. Data from my thesis suggest that the change in pH primarily affects processes active in MC and MV lumen rather than in PM or digestive cell vesicles. The dark body phenotype strongly correlated with silencing *tetur09g04140* (Suzuki et al. 2017b) may also support this as midgut lumen became darkened from plant pigment and heavily populated with later-stage digestive cells. This suggests that associated enzymatic activities are negatively impacted by the perturbance of pH regulation as a consequence of silencing V-ATPase.

Previous research examined the impact of perturbed pH regulation in the digestive tract of insects following RNAi of gene expression associated with V-ATPase. Overend et al. (2016) targeted V-ATPase genes such as *vha100-4* in larval *D. melanogaster* after an extensive pH gradient in the midgut was established (**Figure 6**). Wild type and parental controls maintained an acidic region in the midgut (pH = 2) whereas the *vh100-4* knockdown line could not. It was proposed that this strongly acidic region plays a critical role in defending the larvae from pathogenic infections, which was demonstrated when *Pseudomonas* bacteria increased in the gut and affected development and survival of larvae. V-ATPase is a potential target for RNAi pest control for TSSMs as the mechanism for regulating pH is critical for digestion and detoxification. Feeding dsRNA solutions to TSSMs in my thesis was not effective in triggering an RNAi response, however, the increase of gut pH when plant cell contents were ingested indicates TSSMs rely on V-ATPase to generate a slightly alkaline pH environment for proper enzymatic functions. The perturbation of regulating pH could play a key role in increased TSSM mortality following RNAi.

## 5.6 Recommendations for future studies

Selecting the right combination of pH indicator dyes was critical for confidently determining the limits and specific values for pH in TSSMs. Erban and Hubert (2010) recommended that many indicator dyes should be used as they can only provide results in pH with an accuracy of ±1. A total of 13 indicator dyes were applied to TSSMs (**Table 2**) but most were omitted from the statistical analyses for either being redundant or for technical issues. Dyes that required non-water solvents such as ethanol or benzene (not listed) were also attempted by diluting them for safety, but the final solutions were too faint to be seen in TSSMs. All dyes used in this study were either fully or partially soluble in water, which allowed for full saturation to ensure strong colours in TSSMs. For future experiments, indicator dye compounds with a sodium salt cation should be used as it promotes solubility in water and would therefore be safer for the specimen. Such dyes were used in this experiment including thymol blue, phenol red and bromocresol green, with consistently visible staining.

The most challenging aspect of my thesis was developing dye-delivery protocols that reduced the physical and environmental stress on TSSMs as much as possible. It was critical to reduce stress experienced by TSSMs to avoid any physiological reactions that would have influenced pH within the digestive tract. The least stressful method was the sandwich mesh method, which simulated a leaf-like environment where TSSMs were free to move around and could explain why uptake of dyes by digestive cells was greater than the other delivery methods. The Kimwipe soaking method fully immersed TSSMs in liquid, which was stressful due to very limited mobility and lack of oxygen. This method consistently resulted in indicator dyes appearing in PM but rarely penetrating the MC and MV. Microinjections were necessary to bypass the small molecule filtration mechanism in the MV-PM juncture. TSSMs

have evolved this filtration mechanism to eliminate excess fluids during feeding while retaining larger particulates in MV and MC (McEnroe 1969). However, the trade-off with microinjection is the high stress induced by fully restrained mobility and needle penetration. TSSMs rarely survived the trauma of microinjection, so it was not practical to use the indicator dyes for determining pH values in the midgut after 24 h like in Kimwipe or sandwich mesh methods. In this study, the effect of stress experienced by TSSMs on digestive tract pH was not taken into account but is something that merits attention in future experiments. It would be imperative for similar studies to reduce physical and environmental stress as much as possible to preserve the natural pH in the digestive tract of *T. urticae* during *in vivo* studies.

# 6 Conclusion

The internal pH of the digestive tract within *T. urticae* has not been measured directly prior to this study. The identified pH optima of several enzymes extracted from TSSM bodies (Carrillo et al. 2011; Santamaría et al. 2015) provided indirect evidence for pH environments that may exist in the digestive tract. Likewise, the data from previous studies on digestive tract pH in various mite species (Dinsdale 1974; Erban and Hubert 2010, 2012; Nisbet and Billingsley 2000) establish a combined range of pH from 4 to 8 in the digestive tract. The use of pH indicator dyes in TSSMs has for the first time allowed for a visual and statistical approach to determine limits and specific pH within digestive tract compartments. My thesis demonstrated that the ingestion of plant cell contents induces a slight increase in gut pH when compared to non-fed TSSMs. RNAi TSSMs demonstrated changes in digestive tract pH by only ±1 values beyond the established 7.3-7.5 range. It was unclear if this resulted from the intended RNAi response or as a consequence of the dsRNA solution itself influencing pH. My data offer some insight into the underlying condition of pH that facilitates digestive and detoxification processes while TSSMs ingest and process liquified plant cell content. How each enzyme is specifically impacted remains yet to be determined, however, the data suggests that enzymes with acidic pH optima would be more active in digestive cell vesicles whereas neutral or near-neutral alkaline enzymes perform closer to their optima in gut lumen.

# References

Alberti G and Crooker AR. 1985. Internal Anatomy. In: Helle W and Sabelis MW editors. Spider Mites: Their Biology, Natural Enemies and Control. Amsterdam: Elsevier Ltd. p. 29-62.

Ali JA and Agrawal AA. 2012. Specialist versus generalist insect herbivores and plant defense. Trends in Plant Science. 17(5):293-302.

Andre HM and Remacle CI. 1984. Comparative and functional morphology of the ghanthosoma of Tetranychus urticae (Acari: Tetranychidae). Acarologia. 25(2):179-190.

Appel HM and Maines LW. 1995. The Influence of Host Plant on Gut Conditions of Gypsy Moth (*Lymantria dispar*) Caterpillars. 1995. Journal of Insect Physiology. 41(3):241-246.

Attia S, Grissa KL, Lognay G, Bitume E, Hance T and Mailleux AC. 2013. A review of the major biological approaches to control the worldwide pest Tetranychus urticae (Acari: Tetranychidae) with special reference to natural pesticides. Journal of Pest Science. 86(3):361-386.

Barton R. 1966. Fine structure of mesophyll cells in senescing leaves of *Phaseolus*. Planta. 71:314-325.

Bensoussan N, Santamaría ME, Zhurov V, Diaz I, Grbić M and Grbić V. 2016. Plant-Herbivore Interaction: Dissection of the Cellular Pattern of Tetranychus urticae Feeding on the Host Plant. Frontiers in Plant Science. 7:1105.

Bensoussan N, Zhurov V, Yamakawa S, O'Neil C, Suzuki T, Grbić M and Grbić V. 2018. The Digestive System of the Two-Spotted Spider Mite, Tetranychus urticae Koch, in the Context of the Mite-Plant Interaction. Frontiers in Plant Science. Doi: 10.3389/fpls.2018.01206

Berebaum M. 1980. Adaptive significance of midgut pH in larval Lepidoptera. American Naturalist. 115(1):138-146.

Beyenbach KW and Wieczorek H. 2006. The V-type H+ ATPase: molecular structure and function, physiological roles and regulation. Journal of Experimental Biology. 209(Pt 4):577-589.

Boudko DY, Moroz LL, Linser PJ, Trimarchi JR, Smith PJ and Harvey WR. 2001. In situ analysis of pH gradients in mosquito larvae using non-invasive, self-referencing, pH-sensitive microelectrodes. Journal of Experimental Biology. 204(Pt 4):691-699.

Brune A, Emerson D and Breznak JA. 1995. The Termite Gut Microflora as an Oxygen Sink: Microelectrode Determination of Oxygen and pH Gradients in Guts of Lower and Higher Termites. Applied and Environmental Microbiology. 61(7):2681-2687.

Carrillo L, Martinez M, Ramessar K, Cambra I, Castañera P, Ortego F and Díaz I. 2011. Expression of a barley cystatin gene in maize enhances resistance against phytophagous mites by altering their cysteine-proteases. Plant Cell Reports. 30(1): 101-112.

Cazaux M, Navarro M, Bruinsma KA, Zhurov V, Negrave T, Leeuwen TV, Grbić V and Grbić M. 2014. Application of Two-spotted Spider Mite *Tetranychus urticae* for Plant-pest Interaction Studies. JoVE. 89:e51738.

Cristofoletti PT, Ribeiro AF, Deraison C, Rahbe Y and Terra WR. 2003. Midgut adaptation and digestive enzyme distribution in a phloem feeding insect, the pea aphid *Acyrthosiphon pisum*. Journal of Insect Physiology. 49(1):11-24.

Corena MP, VanEkeris L, Salazar MI, Bowers D, Fiedler MM, Silverman D, Tu C and Linser PJ. 2005.f Carbonic anhydrase in the adult mosquito midgut. The Journal of Experimental Biology. 208:3263-3273

Couoh-Cardel S, Milgrom E and Wilkens S. 2015. Affinity Purification and Structural Features of the Yeast Vacuolar ATPase Ѵ Membrane Sector. The Journal of Biological Chemistry. 290(46):27959-27971.

D'Silva NM, Donini A and O'Donnell MJ. 2017. The roles of V-type $H^+$ATPase and $Na^+/K^+$-ATPase in energizing $K^+$ and $H^+$ transport in larval *Drosophila* gut epithelia. Journal of Insect Physiology

Dermauw W, Pym A, Bass C, Leeuwen TV and Feyereisen R. 2018, Does host plant adaptation lead to pesticide resistance in generalist herbivores? Current Opinion in Insect Science. 26:25-33.

Després L, David JP and Gallet C. 2007. The evolutionary ecology of insect resistance to plant chemicals. Trends in Ecology & Evolution. 22(6):298-307.

Dinsdale D. 1974. The digestive activity of a phthiracarid mite mesenteron. Journal of Insect Physiology. 20(11):2247-2259.

Dogan YO, Hazir S, Yildiz A, Butt TM and Cakmak I. 2017. Evaluation of entomopathogenic fungi for the control of Tetranychus urticae (Acari: Tetranychidae) and the effect of Metarhizium brunneum on the predatory mites (Acari: Phytoseiidae). Biological Control. 111:6-12.

Dow JAT. 1992. pH Gradients in Lepidopteran Midgut. Journal of Experimental Biology. 172:355-375.

Dow JAT and Peacock JM. 1989. Microelectrode evidence for the electrical isolation of goblet cell cavities in *Manduca sexta* middle midgut. Journal of Experimental Biology. 143:101-114.

Erban T and Hubert J. 2008. Digestive function of lysozyme in synanthropic acaridid mites enables utilization of bacteria as a food source. Experimental and Applied Acarology. 44(3):199-212.

Erban T and Hubert J. 2010. Determination of pH in Regions of the Midgut of Acaridid. Journal of Insect Science. 10(42):1-12.

Erban T and Hubert J. 2012. Digestive Physiology of Acaridid Mites (Acari: Acaridida). Signpost Open Access Journal of Entomological Studies. 1(2012):1-32.

Febvay G, Delobel B and Rahbe Y. 1987. Influence of the amino acid balance on the improvement of an artificial diet for a biotype of *Acyrthosiphon pisum* (Homoptera: Aphididae). Canadian Journal of Zoology. 66(11):2449-2453.

Felton GW, Donato K, Del Vecchio RJ and Duffey SS. 1989. Activation of plant foliar oxidases by insect feeding reduces the nutritive quality of foliage for noctuid herbivores. Journal of Chemical Ecology. 15:2667-2695.

Felton GW, Workman J and Duffey SS. 1992. Avoidance of antinutritive plant defense: Role of midgut pH in Colorado potato beetle. Journal of Chemical Ecology. 18:561-583.

Finbow ME and Harrison MA. 1997. The Vacuolar H+-ATPase: a Universal Proton Pump of Eukaryotes. Biochemical journal. 324(3):697-712.

Forgac M. 2007. Vacuolar ATPases: rotary proton pumps in physiology and pathophysiology. Nature Reviews Molecular Cell Biology. 8:917-929.

Franzke A, Unsicker SB, Specht J, Köhler G and Weisser WW. 2010. Being a generalist herbivore in a diverse world: how do diets from different grasslands influence food plant selection and fitness of the grasshopper *Chorthippus parallelus*? Ecological Entomology. 35(2):126-138.

Fürstenberg-Hägg J, Zagrobelny M and Bak S. 2013. Plant Defense against Insect Herbivores. International Journal of Molecular Sciences. 14(5):10242-10297.

Giannella RA, Broitman SA and Zamcheck N. 1973. Influence of Gastric Acidity on Bacterial and Parasitic Enteric Infections: a perspective. Annals of Internal Medicine. 78(2):271-276.

Grbić M, Leeuwen VT, Clark RM, Rombauts S, Rouzé, Grbić V, Osborne EJ, Dermauw W, Ngoc PCT, Ortego F et al. 2011. The genome of Tetranychus urticae reveals herbivorous pest adaptations. Nature. 479(7374):487-492.

Grandjean O and Aeschlimann A. (1973). Contribution To the study of digestion in ticks: histology and fine structure of the midgut epithelium of "Ornithodorus moubata", Murray (Ixodoidea, Argasidae). Acta Tropica. 30(4):193–212.

Gross EM, Brune A and Walenciak O. 2008. Gut pH, redox conditions and oxygen levels in an aquatic caterpillar: Potential effects on the fate of ingested tannins. Journal of Insect Physiology. 54(2):462-471.

Harrison JF. 2001. Insect Acid-Base Physiology. Annual Review of Entomology. 46: 221-250.

Huvenne H and Smagghe G. 2010. Mechanisms of dsRNA uptake in insects and potential of RNAi for pest control: a review. Journal of Insect Physiology. 56(3):227-235.

Howe GA and Jander G.2008. Plant Immunity to Insect Herbivores. Annual Review of Plant Biology.

Hughes TE. 1950. The physiology of the alimentary canal of Tyroglyphus farinae. Quarterly Journal of Microscopical Science. 91(1):45-61.

Ikagemi Y, Yano S, Takabayashi J and Takafuji A. 2000. Function of quiescence of *Tetranychus kanzawai* (Acari: Tetranychidae), as a defense mechanism against rain. Applied Entomology and Zoology. 35(3):339-343.

Jongsma MA and Bolter C. 1997. The Adaptation of Insects to Plant Protease Inhibitors. Journal of Insect Physiology. 43(10):885-895.

Jonckheer W, Dermauw W, Zhurov V, Wybouw N, Bulcke JV, Villaroel CA, Greenhalgh R, Grbić M, Schuurink RC, Tirry L et al. 2016. The Salivary Protein Repertoir of the Polyphagous Spider Mite *Tetranychus urticae*: A Quest for Effectors. Molecular & Cellular Proteomics. 15(12):3594-3613.

Joseph ER, Josowicz M, Russel BV and Solntsev KM. 2013. Spectral and Redox Properties of the GFP Synthetic Chromophores as a Function of pH in buffered media. Chemical Communications. 49(71):7788-7790.

Klowden MJ. 1995. Blood, Sex and the Mosquito. American Institute of Biological Sciences. 45(5):326-331

Krantz GW and Lindquist EE. 1979. Evolution of Phytophagous Mites (Acari). Annual Review of Entomology. 24:121-158.

Lara FA, Lins U, Bechara GH and Oliveira PL. 2005. Tracing heme in a living cell: hemoglobin degradation and heme traffic in digest cells of the cattle tick *Boophilus microplus*. Journal of Experimental Biology. 208(16):3093-3101.

Lin YH, Huang JH, Liu Y, Belles X and Lee HJ. 2016. Oral delivery of dsRNA lipoplexes to German cockroach protects dsRNA from degradation and induces RNAi response.

Linser PJ, Smith KE, Seron TJ and Oviedo MN. 2009. Carbonic anhydrases and anion transport in mosquito midgut pH regulation. The Journal of Experimental Biology. 212(11):1662-1671.

Malcom SB and Zalucki MP. 1996. Milkweed latex and cardenolide induction may resolve the lethal plant defense paradox. Entomologia Experimentalis et Applicata. 80(1):193-196

Matos GS, Wybouw N, Martins NE, Zélé F, Riga M et al.. 2017. *Tetranychus urticae* mites do not mount an induced immune response against bacteria. Proceedings of the Royal Society B. 284:20170401.

McEnroe WD. 1969. The Role of the Digestive System in the Water Balance of the Two-spotted Spider Mite. Advances in Acarology. 1:225-231.

Mellman I. 1996. Endocytosis and Molecular Sorting. Annual Review of Cell and Developmental Biology. 12:575-625.

Mello MO and Silva-Filho MC. 2002. Plant-insect interactions: an evolutionary arms race between two distinct defense mechanisms. Brazilian Journal of Plant Physiology. 14(2):71-81.

Memarizadeh N, Ghadamyari M, Sajedi RH and Sendi JJ. 2010. Characterization of esterases from abamectin-resistant and susceptible strains of *Tetranychus urticae* Koch (Acari: Tetranychidae). International Journal of Acarology. 37(4):271-281.

Migeon A and Dorkeld F. 2010. Spider mites web: A comprehensive database for Tetranychidae. In: Sabelis MW and Bruin J editors. Trends in Acarology: Proceedings of the 12th International congress. Amsterdam: Springer. p.557-560.

Mitchell C, Brennan RM, Graham J and Karley AJ. 2016. Plant Defense against Herbivorous Pests: Exploiting Resistance and Tolerance Traits for Sustainable Crop Protection. Frontiers in Plant Science. 7(1132):1-8.

Mothes WU and Seitz KA. 1981. Functional Microscopic Anatomy of The Digestive System of Tetranychus urticae (Acari, Tetranychidae). Acarologia. 22(3):257-270.

Mothes WU. 1985. Fine Structure of The 'Hindgut' of The Two-Spotted Spider Mite Tetranychus urticae, with Special Reference to Origin and Function. Experimental & Applied Acarology. 1(1985):253-272.

Nisbet AJ and Billingsley PF. 2000. A comparative survey of the hydrolytic enzymes of ectoparasitic and free-living mites. International Journal for Parasitology. 30(1):19-27.

Occhipinti A and Maffei ME. 2013. Chlorophyll and its degradation products in the two-spotted spider mite, Tetranychus urticae: observations using epifluorescence and confocal laser scanning microscopy. Experimental and Applied Acarology. 61(2):213-219.

Overend G, Luo Y, Henderson L, Douglas AE, Davies SA and Dow JAT. 2016. Molecular mechanism and functional significance of acid generation in the *Drosophila* midgut. Scientific Reports. 6:27242. Doi: 10.1038/srep27242.

Priya NG, Ojha A, Kajla MK, Raj A and Rajagopal R. 2012. Host Plant Induced Variation in Gut Bacteria of *Helicoverpa armigera*. PLOS One. 7(1):e30768.

Ratlamwala, Huzefa. 2014. Two spotted spider mite (Tetranychus urticae) selection to Arabidopsis thaliana. Electronic Thesis and Dissertation Repository. 2236. https://ir.lib.uwo.ca/etd/2236

Rhodes EM, Liburd OE, Kelts C, Rondon SI and Francis RR. 2006. Comparison of single and combination treatments of *Phytoseiulus persimilis*, *Neoseiulus californicus*, and Acramite (bifenzate) for control of twospotted spider mites in strawberries. Experimental & Applied Acarology. 39:213-225.

Rioja C, Zhurov V, Bruinsma K, Grbić M and Grbić V. 2017. Plant-Herbivore Interactions: A Case of an Extreme Generalist, the Two-Spotted Spider Mite Tetranychus urticae. Molecular Plant-Microbe Interactions Journal. 30(12):935-945.

Sabins RB. 2008. Handbook of Acid-Base Indicators. Boca Raton (FL, USA): Taylor & Francis Group. 398p.

Salehipourshirazi G. 2018. Adaptation Mechanisms of Two-Spotted Spider Mite, Tetranychus urticae, to Arabidopsis Indole Glucosinolates. Electronic Thesis and Dissertation Repository. 5812.

Santamaría ME, Cabrera JG, Martínez M, Grbić V, S Castañera O, Díaz I and Ortego F. 2015. Digestive proteases in bodies and faeces of the two-spotted spider mite, Tetranychus urticae. Journal of Insect Physiology. 78:69-77.

Scott CC, Vacca F and Gruenberg J. 2014. Endosome maturation, transport and functions. Seminars in Cell & Developmental Biology. 31:2-10.

Schultz JC and Lechowicz MJ. 1986. Hostplant, larval age, and feeding behavior influence midgut pH in the gypsy moth (*Lymantria dispar*). Oecologia. 71:133-137.

Shanbhag S and Tripathi S. 2009. Epithelial ultrastructure and cellular mechanisms of acid and base transport in the *Drosophila* midgut. Journal of Experimental Biology. 212(11):1731-1744.

Skibbe U, Christeller JT, Callaghan PT, Eccles CD and Laing WA. 1996. Visualization of pH gradients in the larval midgut of *Spodoptera litura* using P-31-NMR microscopy. Journal of Insect Physiology. 42(8):777-790.

Song H, Fan Y, Zhang J, Cooper AMW, Silver K, Li D, Li T, Ma E, Zhu KY and Zhang J. 2018. Contributions of dsRNases to differential RNAi efficiencies between the injection and oral delivery of dsRNA in *Locusta migratoria*. Pest Management Science. 75(6):1707-1717.

Stahl E, Hilfiker O and Reymond P. 2017. Plant-arthropod interactions: who is the winner? The Plant Journal. 93(4):703-728

Suzuki T, España MU, Nunes MA, Zhurov V, Dermauw W, Osakabe M, Leeuwen TV, Grbić M and Grbić V. 2017a. Protocols for the delivery of small molecules to the two-spotted spider mite, Tetranychus urticae. PLOS One. 12(12):e0190025.

Suzuki T, Kojima T, Takeda M and Sakuma M. 2013. Photo-orientation regulates seasonal habitat selection in the two-spotted spider mite, *Tetranychus urticae*. The Journal of Experimental Biology. 216:977-983.

Suzuki T, Nunes MA, España MU, Namin HN, Jin P, Bensoussan N, Zhurov V, Rahman T, Clercq RD, Hilson P et al. 2017b. RNAi based reverse genetics in the chelicerate model Tetranychus urticae: A comparative analysis of five methods for gene silencing. PLOS One. 12(7):e0180654.

Terra WR and Ferreira C. 1994. Insect digestive enzymes: properties, compartmentalization and function. Comparative Biochemistry and Physiology. 109(1):1-62.

van Leeuwen T and Tirry L. 2007. Esterase-mediated bifenthrin resistance in a multiresistant strain of the two-spotted spider mite, *Tetranychus urticae*. Pest Management Science. 63:150-156.

Wybouw N, Zhurov V, Martel C, Bruinsma KA, Hendrick F, Grbić V and Leeuwen TV. 2015. Adaptation of a polyphagous herbivore to a novel host plant extensively shapes the transcriptome of herbivore and host. Molecular Ecology. 24(18):4647-4663.

Xu X, Smith S, Urban J and Cui Z. 2006. An in line non-invasive optical system to monitor pH in cell and tissue culture. Medical Engineering & Physics. 28(5):468-474.

Zhang Z, Zheng Y, Mazon H, Milgrom E, Kitagawa N, Trier EK, Heck AJR, Kane PM and Wilkens S. 2008. Structure of the Yeast Vacuolar ATPase. Journal of Biological Chemistry. 283(51):35983-35995.

Zhu YX, Song YL, Hoffmann AA, Jin PY, Huo SM and Hong XY. 2018. A change in the bacterial community of spider mites decreases fecundity on multiple plant hosts. Microbiology Open. 8(6). Doi: 10.1002/mbo3.743.

Zhu YX, Song ZR, Zong YL, Zhao DS and Hong XY. 2020. The microbiota in spider mite feces potentially reflects intestinal bacterial communities in the host. Insect Science.27(5):859-868.

Zhurov V, Navarro M, Bruinsma KA, Arbona V, Santamaría ME, Cazaux M, Wybouw N, Osborne EJ, Ens C, Rioja C et al. 2014. Reciprocal Responses in the Interaction between Arabidopsis and the Cell-Content-Feeding Chelicerate Herbivore Spider Mite. Plant Physiology. 164:384-399.

# Appendix

**R Studio information**

R version 3.6.3 (2020-02-29)
Platform: x86_64-w64-mingw32/x64 (64-bit)
Running under: Windows 10 x64 (build 18362)
Matrix products: default

locale:
[1] LC_COLLATE=English_United States.1252  LC_CTYPE=English_United States.1252
LC_MONETARY=English_United States.1252

[4] LC_NUMERIC=C                          LC_TIME=English_United States.1252

attached base packages:
[1] stats    graphics grDevices utils    datasets  methods   base

other attached packages:
[1] ggplot2_3.3.2 gplots_3.0.4 tidyr_1.1.1  dplyr_1.0.1  reshape_0.8.8

loaded via a namespace (and not attached):
 [1] Rcpp_1.0.5      rstudioapi_0.11 magrittr_1.5     munsell_0.5.0     tidyselect_1.1.0
colorspace_1.4-1

 [7] R6_2.4.1        rlang_0.4.7     fansi_0.4.1     plyr_1.8.6      caTools_1.18.0
tools_3.6.3

[13] grid_3.6.3      packrat_0.5.0     gtable_0.3.0      KernSmooth_2.23-16 cli_2.0.2
withr_2.2.0

[19] ellipsis_0.3.1     gtools_3.8.2      assertthat_0.2.1  tibble_3.0.3      lifecycle_0.2.0
crayon_1.3.4

[25] purrr_0.3.4      vctrs_0.3.2      bitops_1.0-6      glue_1.4.1      gdata_2.18.0
compiler_3.6.3

[31] pillar_1.4.6      scales_1.1.1      generics_0.0.2    pkgconfig_2.0.3

# Curriculum Vitae

Zoran Čulo

## Education

Bachelor of Arts, Biology (Honours)**,** 2012 - 2016

  *Wilfrid Laurier University*, Waterloo ON

Master of Science, Biology, 2017 – 2021

  *University of Western Ontario*, London ON

## Scholarships

FOSSA Research Assistant Scholarship

  2016, $1,000

Western Graduate Research Scholarship

  Sept 2017 – Aug 2019, $9,072

## Employment

Teaching Assistant, Sept 2017 – Dec 2019

  *University of Western Ontario*, London ON

General Labourer, May 2016 – August 2017

  *Stonebridge Imports Ltd.*, Kitchener ON